RESEARCH

Keeping Utah Moving

Utah Department of Transportation - Research Division
4501 South 2700 West - P.O. Box 148410 - SLC,UT 84114-8410

Report No. UT-26.12

DURABILITY OF LIGHTWEIGHT CONCRETE BRIDGE DECKS IN UTAH

Prepared For:

Utah Department of Transportation
Research & Innovation Division

Final Report
January 2026

DISCLAIMER

The authors alone are responsible for the preparation and accuracy of the information, data, analysis, discussions, recommendations, and conclusions presented herein. The contents do not necessarily reflect the views, opinions, endorsements, or policies of the Utah Department of Transportation (UDOT) or the U.S. Department of Transportation. UDOT makes no representation or warranty of any kind, and assumes no liability therefore. The authors also make no warranty, express or implied, regarding the suitability of findings documented in this report for a particular purpose and shall not be held liable under any circumstances for any direct, consequential, or other damages with respect to claims by users of any findings documented in this report, including claims based on allegations of errors, omissions, or negligence.

ACKNOWLEDGMENTS

The authors gratefully acknowledge funding for this research through UDOT and the King Husein Professorship within the Department of Civil and Construction Engineering at Brigham Young University (BYU). The patching material used for field work performed in this research was donated by CTS Cement Corporation. Dr. Robert Stevens of Infrastructure Research and Matthew Christensen of BYU assisted with the field and laboratory work.

TECHNICAL REPORT ABSTRACT

1. Report No.	2. Government Accession No.	3. Recipient's Catalog No.
UT-26.12	N/A	N/A

4. Title and Subtitle
Durability of Lightweight Concrete Bridge Decks in Utah

5. Report Date
January 2026

6. Performing Organization Code
N/A

7. Author(s)
W. Spencer Guthrie, Ph.D., Lorenzo Eusebi-Diehr, Steven B. Burdette

8. Performing Organization Report No.
N/A

9. Performing Organization Name and Address
Brigham Young University
Department of Construction and Civil Engineering
368 Clyde Building
Provo, UT 84604

10. Work Unit No.
5H092 38H

11. Contract or Grant No.
23-9019

12. Sponsoring Agency Name and Address
Utah Department of Transportation
4501 South 2700 West
P.O. Box 148410
Salt Lake City, UT 84114-8410

13. Type of Report & Period Covered
Final
March 2023 to January 2026

14. Sponsoring Agency Code
PIC No. UT20.403

15. Supplementary Notes
Prepared in cooperation with the Utah Department of Transportation and the U.S. Department of Transportation, Federal Highway Administration

16. Abstract

The objectives of this research were to document and compare properties of lightweight concrete and normal-weight concrete used for construction of bridge decks and approach slabs in northern Utah. The scope of work included field and laboratory testing to characterize concrete at three lightweight concrete bridge deck sites and the normal-weight concrete approach slabs at one of these sites, as well as laboratory testing to characterize concrete specimens obtained through previous research on lightweight and normal-weight concrete bridge decks. For field testing, a distress survey was performed at each test location, and then cover depth testing, Schmidt rebound hammer testing, resistivity testing, chloride concentration sampling, and coring were performed. For laboratory testing, regarding samples obtained during the current research, modulus of elasticity testing, compressive strength testing, splitting tensile strength testing, rapid chloride permeability and absorption testing, and chloride concentration testing were performed. Regarding samples obtained from previous research, coefficient of thermal expansion testing and freeze-thaw durability testing were performed.

As a basis for discussion, ratios of values for lightweight concrete to values of normal-weight concrete were computed for selected properties, for which the normal-weight concrete approach slabs and the normal-weight concrete cores and cylinders were used as a baseline. The properties include resistivity, modulus of elasticity, compressive strength, splitting tensile strength, chloride permeability, absorption, coefficient of thermal expansion, and stiffness retained after freeze-thaw durability testing. Overall, the data suggest that, compared to normal-weight concrete, lightweight concrete absorbs more water, allows higher rates of chloride ion ingress, is more susceptible to degradation under freeze-thaw cycling, and has lower resistance to cracking. Several recommendations were developed to potentially improve the performance of lightweight concrete.

17. Key Words
Concrete bridge deck, durability, freeze-thaw cycling, lightweight concrete, strength

18. Distribution Statement
Not restricted. Available through:
UDOT Research & Innovation Div.
4501 South 2700 West
P.O. Box 148410
Salt Lake City, UT 84114-8410
www.udot.utah.gov/go/research

23. Registrant's Seal
N/A

19. Security Classification (of this report)	20. Security Classification (of this page)	21. No. of Pages	22. Price
Unclassified	Unclassified	149	N/A

TABLE OF CONTENTS

LIST OF TABLES v
LIST OF FIGURES vi
LIST OF ACRONYMS vii
EXECUTIVE SUMMARY 1
1.0 INTRODUCTION 2
1.1 Problem Statement 2
1.2 Research Objectives and Scope of Work 2
1.3 Outline of Report 4
2.0 BACKGROUND 5
2.1 Overview 5
2.2 Lightweight Aggregate 5
2.3 Lightweight Concrete 6
2.4 Lightweight Concrete Bridge Decks 8
2.5 Summary 10
3.0 PROCEDURES 11
3.1 Overview 11
3.2 Field Testing 11
3.2.1 Distress Surveys 13
3.2.2 Cover Depth Testing 14
3.2.3 Schmidt Rebound Hammer Testing 14
3.2.4 Resistivity Testing 15
3.2.5 Chloride Concentration Sampling 15
3.2.6 Coring 16
3.3 Laboratory Testing 18
3.3.1 Modulus of Elasticity Testing 19
3.3.2 Compressive Strength Testing 20
3.3.3 Splitting Tensile Strength Testing 20
3.3.4 Rapid Chloride Permeability and Absorption Testing 21
3.3.5 Chloride Concentration Testing 22

3.3.6 Coefficient of Thermal Expansion Testing 22
3.3.7 Freeze-Thaw Durability Testing 23
3.4 Summary 24
4.0 RESULTS 26
4.1 Overview 26
4.2 Field Testing 26
4.2.1 Distress Surveys 26
4.2.2 Cover Depth Testing 29
4.2.3 Schmidt Rebound Hammer Testing 30
4.2.4 Resistivity Testing 30
4.3 Laboratory Testing 31
4.3.1 Modulus of Elasticity Testing 33
4.3.2 Compressive Strength Testing 35
4.3.3 Splitting Tensile Testing 36
4.3.4 Rapid Chloride Permeability and Absorption Testing 38
4.3.5 Chloride Concentration Testing 39
4.3.6 Coefficient of Thermal Expansion Testing 40
4.3.7 Freeze-Thaw Durability Testing 42
4.4 Discussion 43
4.5 Summary 45
5.0 CONCLUSION 48
5.1 Summary 48
5.2 Findings 49
5.3 Recommendations 51
REFERENCES 53
APPENDIX A: CONCRETE MIXTURE DESIGNS 57
APPENDIX B: SUPPORTING DATA 59
APPENDIX C: DISTRESS MAPS 70
APPENDIX D: CORE AND CYLINDER PHOTOGRAPHS 90
APPENDIX E: LIGHTWEIGHT COARSE AGGREGATE PHOTOGRAPHS 116

LIST OF TABLES

Table 3.1 Bridge Information 12
Table 4.1 Distresses 27
Table 4.2 Cover Depth 30
Table 4.3 Schmidt Rebound Number and Estimated Compressive Strength 30
Table 4.4 Resistivity 31
Table 4.5 Modulus of Elasticity 34
Table 4.6 Compressive Strength 35
Table 4.7 Splitting Tensile Strength 37
Table 4.8 Chloride Permeability and Absorption 38
Table 4.9 Chloride Concentration 40
Table 4.10 Coefficient of Thermal Expansion 41
Table 4.11 Freeze-Thaw Durability 42
Table 4.12 Comparison of Properties of Lightweight Concrete and Normal-Weight Concrete ...44

LIST OF FIGURES

Figure 3.1 Map of bridge locations. 12
Figure 3.2 Crack comparator card. 13
Figure 3.3 Cover meter. 14
Figure 3.4 Schmidt rebound hammer. 15
Figure 3.5 Resistivity meter. 16
Figure 3.6 Concrete drill. 17
Figure 3.7 Coring machine. 18
Figure 3.8 Stiffness testing. 19
Figure 3.9 Compressive strength testing. 20
Figure 3.10 Splitting tensile strength testing. 21
Figure 3.11 Rapid chloride permeability testing. 22
Figure 3.12 Coefficient of thermal expansion testing. 23
Figure 3.13 Freeze-thaw durability testing. 24
Figure 4.1 Crack density. 27
Figure 4.2 Crack width. 28
Figure 4.3 Scaling. 28
Figure 4.4 Map cracking. 29
Figure 4.5 Delamination. 29
Figure 4.6 Unit weight. 32
Figure 4.7 Typical lightweight coarse aggregate. 32
Figure 4.8 Typical normal-weight coarse aggregate. 33
Figure 4.9 Modulus of elasticity. 34
Figure 4.10 Compressive strength. 35
Figure 4.11 Lightweight concrete fracture face. 36
Figure 4.12 Normal-weight concrete fracture face. 37
Figure 4.13 Splitting tensile strength. 38
Figure 4.14 Chloride permeability. 39
Figure 4.15 Absorption. 39
Figure 4.16 Chloride concentration. 41
Figure 4.17 Lightweight coarse aggregate fractured during freeze-thaw durability testing. 43

LIST OF ACRONYMS

AASHTO	American Association of State Highway and Transportation Officials
ACI	American Concrete Institute
ASTM	American Society for Testing and Materials
EPA	Environmental Protection Agency
ESCSI	Expanded Shale, Clay, and Slate Institute
NRMCA	National Ready Mixed Concrete Association
UDOT	Utah Department of Transportation

EXECUTIVE SUMMARY

The objectives of this research were to document and compare properties of lightweight concrete and normal-weight concrete used for construction of bridge decks and approach slabs in northern Utah. The scope of work included field and laboratory testing to characterize concrete at three lightweight concrete bridge deck sites and the normal-weight concrete approach slabs at one of these sites, which were recommended by the Utah Department of Transportation for evaluation, as well as laboratory testing to characterize concrete specimens obtained through previous research on lightweight and normal-weight concrete bridge decks.

For field testing, a distress survey was performed at each test location, and then cover depth testing, Schmidt rebound hammer testing, resistivity testing, chloride concentration sampling, and coring were performed. For laboratory testing, regarding samples obtained during the current research, modulus of elasticity testing, compressive strength testing, splitting tensile strength testing, rapid chloride permeability and absorption testing, and chloride concentration testing were performed. Regarding samples obtained from previous research, coefficient of thermal expansion testing and freeze-thaw durability testing were performed.

The results are expected to be applicable to lightweight concrete bridge decks with similar construction and service conditions as those evaluated in this research. As a basis for discussion, ratios of values for lightweight concrete to values of normal-weight concrete were computed for selected properties, for which the normal-weight concrete approach slabs and the normal-weight concrete cores and cylinders were used as a baseline. While the selected properties necessarily exclude the results of visual inspection and chloride concentration, which were directly affected by the presence of an epoxy overlay on two of the bridges, they include resistivity, modulus of elasticity, compressive strength, splitting tensile strength, chloride permeability, absorption, coefficient of thermal expansion in the dry and soaked conditions, and stiffness retained after freeze-thaw durability testing. Overall, the data suggest that, compared to normal-weight concrete, lightweight concrete absorbs more water, allows higher rates of chloride ion ingress, is more susceptible to degradation under freeze-thaw cycling, and has lower resistance to cracking. As cracking occurs, the rates of potential degradation from water absorption, chloride ion ingress, and freeze-thaw cycling increase, and localized structural failure can eventually occur. Several recommendations were developed to potentially improve the performance of lightweight concrete.

1.0 INTRODUCTION

1.1 Problem Statement

Structural lightweight aggregate in the United States has been in production for over a century (ESCSI, 1971). This porous aggregate is produced by heating materials such as shale, clay, and slate in a kiln, where they expand into a lightweight structure. For over 80 years, lightweight aggregate has been used to produce concrete specifically for bridge projects (Castrodale, 2021).

Lightweight concrete is often used in the construction of bridges to reduce the overall dead load. A 20 to 30 percent reduction in dead load can be achieved by using lightweight concrete in place of normal-weight concrete (Bender, 1980). A reduced dead load allows for a bridge to have extended span lengths, wider girder spacings, and/or shallower girder sections. The weight reduction can also lower the overall construction cost of a bridge because of the lesser requirements for load-bearing substructure elements and foundations (Castrodale, 2021). These cost savings have led to an increase in construction of lightweight concrete bridge decks during the past several decades (Cui et al., 2012).

Although the results of several previous studies suggest that lightweight concrete has similar or enhanced durability and an extended service life when compared to normal-weight concrete (Delatte et al., 2007; Ramirez et al., 2000; Zhutovsky and Kovler, 2002), Utah Department of Transportation (UDOT) engineers have observed premature degradation of lightweight concrete bridge decks. In some cases, the development of extensive cracking has been followed by localized structural failure, depicted in Figure 1.1, requiring emergency repairs of the deck, depicted in Figure 1.2. UDOT therefore commissioned this study to investigate properties of lightweight concrete typical of bridge decks in northern Utah.

1.2 Research Objectives and Scope of Work

The objectives of this research were to document and compare properties of lightweight concrete and normal-weight concrete used for construction of bridge decks and approach slabs in northern Utah. The scope of work included field and laboratory testing to characterize concrete

Figure 1.1 Localized structural failure of lightweight concrete bridge deck.

Figure 1.2 Emergency repair of lightweight concrete bridge deck.

at three lightweight concrete bridge deck sites and the normal-weight concrete approach slabs at one of these sites, which were recommended by UDOT for evaluation, as well as laboratory testing to characterize concrete specimens obtained through previous research on lightweight and normal-weight concrete bridge decks (Guthrie et al., 2015).

Field testing included distress surveys, cover depth testing, Schmidt rebound hammer testing, resistivity testing, chloride concentration sampling, and coring at each test location. Laboratory testing included modulus of elasticity testing, compressive strength testing, splitting tensile strength testing, rapid chloride permeability and absorption testing, and chloride concentration testing of the specimens obtained from the three field sites, as well as coefficient of thermal expansion testing and freeze-thaw durability testing of the specimens obtained through previous research.

1.3 Outline of Report

This report consists of five chapters. This chapter introduces the research, defines the problem statement, and states the research objective and scope of work. Chapter 2 provides background information based on a literature review of the research topic. Chapter 3 describes the field and laboratory testing procedures, and Chapter 4 discusses the results. Chapter 5 offers conclusions and recommendations resulting from the research.

2.0 BACKGROUND

2.1 Overview

This chapter presents background information obtained from a literature review related to the objective of this research. The following sections describe lightweight aggregate, lightweight concrete, and lightweight concrete bridge decks.

2.2 Lightweight Aggregate

Development of the rotary kiln process for manufacturing lightweight aggregate is attributed to a ceramic engineer, Stephen J. Hayde, who observed the expansion of clay during hot weather in his brickmaking practice (ESCSI, 1971). An investigation into the viability and production of lightweight aggregate began in 1908, and the process was commercialized a decade later when a patent was issued in 1918 (Holm and Ries, 2007). Numerous manufactured lightweight aggregates are now available and used in construction (Sims et al., 2019).

Manufactured lightweight aggregate that is used for construction is produced primarily from materials such as clay, shale, and slate. These raw materials are primarily mined or quarried for manufacturing at a lightweight aggregate production plant, where the raw material is crushed. The crushed material is screened before being fed into a rotary kiln that reaches temperatures of 2200°F, causing primarily carbon dioxide gas to form and expand in the particles (Holm and Ries, 2007). The volume of the particles increases with the expansion of the gas, and, upon cooling, the particles retain the expanded form, being approximately twice the volume of the original material (Castrodale, 2021; EPA, 1993). The expansion of the material results in a product that is porous, low-density, and highly absorptive (Mindess et al., 2003), having properties comparable to those of natural aggregates (EPA, 1993) but more consistent (Castrodale, 2021).

Several engineering properties of lightweight aggregates have been reported. Lightweight aggregates have low specific gravities, reduced from about 2.65 for the raw material to less than 1.55 for the expanded aggregate (Castrodale, 2021; Ramirez et al, 2000), compared to normal-weight aggregates, for which specific gravities are typically in the range of 2.5 to 2.8 (Mindess et al., 2003). The thermal processing that occurs during production causes the solid material in the manufactured aggregate to have a hardness similar to that of quartz (Holm and Ries, 2000). The particle shapes of lightweight aggregate can vary by source and processing method, ranging from rounded and smooth to angular and irregular. The surface textures can also vary from fairly smooth with few exposed pores to very irregular and angular with many exposed pores (Castrodale, 2021). Lightweight aggregate absorption, ranging from 5 to 25 percent, is significantly greater than that of normal-weight aggregate, which is usually less than 2 percent by dry weight of aggregate (Ramirez et al., 2000).

2.3 Lightweight Concrete

The most common approach for lightweight concrete mixture design involves use of normal-weight fine aggregate and lightweight coarse aggregate, which is typically referred to as "sand-lightweight" concrete. Unless otherwise specified in this research, "lightweight concrete" denotes concrete with normal-weight sand and lightweight coarse aggregate. Lightweight aggregate characteristics, such as the pore volume and gradation, affect workability, pumpability, fine-to-coarse aggregate ratio, binder content, and water content (ACI, 2003; Kim and Lee, 2010). Regarding water, the high absorption of lightweight aggregate requires that it be pre-wetted in the batching process to prevent undesirable impacts on the properties of the resulting concrete (Castrodale, 2021; Ramirez et al., 2000). When the lightweight aggregate is not pre-wetted, it can absorb water from the concrete mixture, causing slump loss during transit; in this case, if insufficient water was added to account for the water absorption, the slump can be restored by adding water (Hoff, 2002), but excess water can cause segregation of the lightweight aggregate from the mortar (NRMCA, 2016) and/or a reduction in concrete strength (Mindess et al., 2003). The governing material specification for lightweight aggregate for use in structural concrete is American Association of State Highway and Transportation Officials (AASHTO) M 195 (Standard Specification for Lightweight Aggregates for Structural Concrete), which is also designated as American Society for Testing and Materials (ASTM) C330 (Standard Specification for Lightweight Aggregates for Structural Concrete).

In a typical lightweight concrete mixture, the normal-weight coarse aggregate is completely replaced with lightweight coarse aggregate, which occupies a total concrete volume fraction of 30 to 50 percent (Cui et al., 2012). Substitution of normal-weight coarse aggregate for lightweight coarse aggregate achieves a concrete that is 20 to 30 percent lighter, on average (ESCSI, 1971). Typical unit weight values for lightweight concrete range from 110 to 125 pcf, while unit weight values for normal-weight concrete range from 140 to 155 pcf (Castrodale, 2021). Because of the reduced aggregate weight, lightweight concrete typically exhibits a slump that is 1 to 2 in. less than that of normal-weight concrete having the same overall workability (Kosmatka and Wilson, 2016).

The modulus of elasticity ranges from 2500 to 4000 ksi for lightweight concrete and from 3000 to 6000 ksi for normal-weight concrete (Holm and Ries, 2000; Holm and Ries, 2007); therefore, the modulus of elasticity of lightweight concrete is approximately 50 to 75 percent of the value of normal-weight concrete (Lopez et al., 2003). The 28-day compressive strength ranges from 2500 to 6000 psi for lightweight concrete and from 5000 to 15,000 psi for normal-weight concrete (Castrodale, 2021). Regarding splitting tensile strength, for similar curing and/or compressive strength, lightweight concrete typically reaches a value that is approximately 70 to 85 percent (ACI, 2003; Holm and Ries, 2006) of the value of normal-weight concrete; a minimum splitting tensile strength of 290 psi is required by ASTM C330 for lightweight concrete (Holm and Ries, 2007). Finally, the coefficient of thermal expansion of lightweight concrete is assumed to be less than that of normal-weight concrete (Castrodale, 2021), with typical values reported as $4x10^{-6}$/°F and $6x10^{-6}$/°F, respectively (Byard and Schindler,, 2010), although the same overall range of approximately $3x10^{-6}$/°F to $7x10^{-6}$/°F has been reported for both lightweight and normal-weight concrete (Castrodale, 2021; Kosmatka and Wilson, 2016; Russell et al., 2006). The coefficient of thermal expansion of lightweight concrete can be affected by its moisture content (Russell et al., 2006).

While normal-weight concrete generally fractures through the paste around the aggregate particles, lightweight concrete often fractures through the lightweight aggregate particles because the aggregate-paste bonding is better and the stiffness of the aggregate is more similar to that of the paste (Holm and Ries, 2000; Lopez et al., 2003; Ramirez et al., 2000). Indeed, lightweight aggregates can comprise the weakest component within lightweight concrete (Short and Kinniburgh, 1978), where greater aggregate strength yields greater concrete strength (Lo et al., 2007; Lo et al., 2008). The strength of lightweight concrete can also be improved through the use of smaller lightweight aggregate particles (Ramirez et al., 2000).

Perhaps because the surface texture of lightweight aggregate is rougher, depending on the pore sizes (Lo et al., 2007), than the surface texture of a typical normal-weight aggregate, more free water and/or paste can be required in lightweight concrete than in normal-weight concrete to achieve a similar workability. Providing an adequate paste volume is important to coat each aggregate particle sufficiently so that the coarse aggregate particles will not separate from the mortar (Kosmatka and Wilson, 2016). For a given water-cement ratio, the amount of cement in lightweight concrete is therefore typically higher than the amount of cement in normal-weight concrete (Castrodale, 2021; Holm and Ries, 2007). At high strengths, the additional cement required for lightweight concrete can exceed 50 percent of the cement required for normal-weight concrete having a similar strength (Ramirez et al., 2000).

Although the durability of lightweight concrete may potentially benefit from internal curing (Ozyildirim, 2009), which can occur as pre-soaked lightweight aggregate particles release water into the surrounding paste as it cures, the extent to which the in-service degree of saturation remains high can be a concern. When lightweight concrete is critically saturated, its resistance to damage from freeze-thaw cycling may be reduced (Ozyildirim, 2009).

2.4 Lightweight Concrete Bridge Decks

A limited number of laboratory and/or field studies have been performed in conjunction with lightweight concrete bridge deck projects (Cavalline et al., 2013; Delatte et al., 2007; Guthrie et al., 2015; Ozyildirim, 2009; Ramirez et al., 2000; Wagner, 2015; Zhutovsky and Kovler, 2002). With only one exception, in all of these studies for which concrete material properties were measured, the tests were performed on specimens that were cast by the researchers, either in the laboratory or in the field, rather than on cores removed from in-service bridge decks.

In one laboratory study, evaluations of a sand-lightweight concrete comprising 30 percent normal-weight aggregate, a sand-lightweight concrete including fly ash, and a sand-lightweight concrete including slag were performed on specimens cast in the field in conjunction with bridge deck construction. The testing procedures included modulus of elasticity, compressive strength, splitting tensile strength, rapid chloride permeability, freeze-thaw cycling, drying shrinkage, and creep (Ozyildirim, 2009). Another laboratory study involved development of several sand-lightweight concrete mixtures, comprising a variety of cementitious materials such as Type I Portland cement, Type III Portland cement, fly ash, and silica fume and different aggregate sources, for lightweight concrete bridge decks and girders (Ramirez et al., 2000); however, use of the mixtures on actual bridge decks was not reported.

Regarding field studies of in-service lightweight bridge decks, one was focused on comparing the results of laboratory-measured and field-measured shrinkage cracking for six newly constructed bridge decks (Delatte et al., 2007). While examining a correlation between rapid chloride permeability and surface resistivity in the laboratory, another study also evaluated in-service lightweight concrete bridge decks; this study concluded that improperly wetted lightweight coarse aggregate can float to the surface of lightweight concrete deck placements and proposed that decks comprising lightweight concrete should therefore not be subject to surface grinding for the purposes of meeting profile requirements because the lightweight aggregate exposed by grinding may then allow accelerated chloride ion ingress through aggregate pore connectivity (Wagner, 2015). In another study, which was conducted in Utah, sensors that could measure volumetric moisture content were embedded in both lightweight and normal-weight concrete bridge decks at the time of construction, and the sensor readings showed that the lightweight concrete bridge decks were 33, 18, 33, and 19 percent wetter, on average, than the normal-weight concrete bridge decks at 28 days, 6 months, 1 year, and 2 years, respectively (Guthrie et al., 2015). Finally, a regional field study of nine lightweight and nine normal-weight concrete bridge decks performed in the southeast U.S. included visual inspection, Schmidt rebound hammer testing, surface resistivity testing, permeability testing, coring, and concrete powder sampling in the field, as well as unit weight, moisture content, dynamic modulus, compressive strength, rapid chloride permeability, sorptivity, chloride concentration testing, and petrography in the laboratory (Cavalline et al., 2013). The average age of both the lightweight and normal-weight concrete bridge decks evaluated in this study was 15 years. Overall, although no consistent differences in cracking, compressive strength, or rapid chloride permeability were observed, the lightweight concrete decks exhibited lower Schmidt rebound numbers, lower resistivity values, higher permeability values, lower modulus values, higher sorptivity, and more secondary deposits, including ettringite and salts that were reported to have partially infilled entrained air voids and other voids in the paste and coarse aggregate, than the normal-weight concrete decks (Cavalline et al., 2013).

2.5 Summary

Development of the rotary kiln process for manufacturing lightweight aggregate is attributed to a ceramic engineer, Stephen J. Hayde, who observed the expansion of clay during hot weather in his brickmaking practice. Manufactured lightweight aggregate that is used for construction is produced primarily from materials such as clay, shale, and slate. Several engineering properties of lightweight aggregates have been reported.

The most common approach for lightweight concrete mixture design involves use of normal-weight fine aggregate and lightweight coarse aggregate, which is typically referred to as "sand-lightweight" concrete. Lightweight aggregate characteristics, such as the pore volume and gradation, affect workability, pumpability, fine-to-coarse aggregate ratio, binder content, and water content. The governing material specification for lightweight aggregate for use in structural concrete is AASHTO M 195, which is also designated as ASTM C330.

A limited number of laboratory and/or field studies have been performed in conjunction with lightweight concrete bridge deck projects. With only one exception, in all of these studies for which concrete material properties were measured, the tests were performed on specimens that were cast by the researchers, either in the laboratory or in the field, rather than on cores removed from in-service bridge decks.

3.0 PROCEDURES

3.1 Overview

This chapter describes the procedures used for this research, which involved field and laboratory testing of lightweight and normal-weight concrete. Field testing included three bridge decks constructed using lightweight concrete and one of the adjacent normal-weight concrete approach slabs. The subsequent laboratory testing included concrete samples obtained from the field work performed during the current research and samples obtained from previous research (Guthrie et al., 2015).

Bridges C-989, C-1011, and F-792 were selected by UDOT personnel for evaluation in this research, and concrete samples from bridges C-993 and F-818, which were the focus of previous research, were also included. All five of these bridges are located in northern Utah, as shown in Figure 3.1, and specific bridge information is provided in Table 3.1 and Appendix A. Bridges C-989 and F-792 received thin-bonded epoxy overlays at the time of construction, and the overlay on bridge F-792 was replaced in 2023 just prior to this research. Field testing of bridges C-1011, F-792, and C-989 occurred in September 2023, September 2023, and October 2023, respectively. Cylinders obtained from bridges C-993 and F-818 were cast during construction of those decks, stored for several years in a fog room and then on open shelves in the Highway Materials Laboratory at Brigham Young University, and then tested for this research during the period from December 2024 to February 2025. Therefore, the bridges had similar ages of 13 to 15 years at the time of testing in this research. Sand-lightweight concrete was utilized for all of the lightweight concrete bridges. The following sections describe the field and laboratory testing performed in this research.

3.2 Field Testing

To facilitate this research, a portion of each bridge, typically the right or left lane and the adjacent shoulder, was closed to traffic. Specifically, the right lane, right lane, and left lane, as well as the adjacent shoulders, were closed for testing of bridges C-989, C-1011, and F-792, respectively. At each site, five test locations were then selected for evaluation using a formal random sampling procedure to eliminate potential bias. A distress survey was performed at each

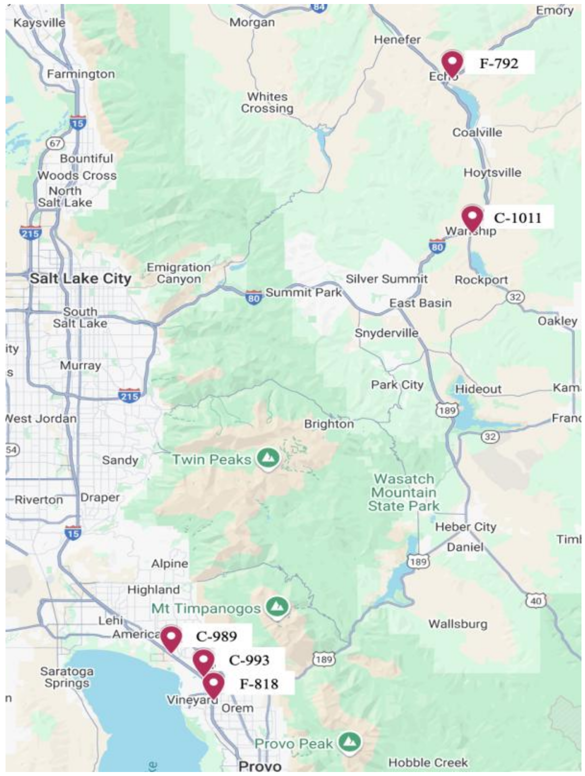

Figure 3.1 Map of bridge locations.

Table 3.1 Bridge Information

Bridge Identifier	Roadway Carried	Feature Crossed	Length (ft)	Construction Date	Scope of Testing
C-989	Sam White	I-15	357	May 2011	Lightweight deck and normal-weight approach slabs
C-993	I-15	Geneva Road	195	April 2011	Lightweight deck
C-1011	I-80 Wanship Interchange	SR-32	90	May 2012	Lightweight deck
F-792	I-80	Echo Dam Road	82	September 2009	Lightweight deck
F-818	I-15	400 N, Orem	103	April 2011	Normal-weight deck

test location, and then cover depth testing, Schmidt rebound hammer testing, resistivity testing, chloride concentration sampling, and coring were performed as described in the following sections. At all of the bridge sites, the concrete surfaces were observed to be dry at the time of testing.

3.2.1 Distress Surveys

Distress surveys were performed to quantify the degree of cracking, scaling, and delamination experienced at each test site; distresses that were presumed to be the result of construction-related issues were also noted. A 12-ft by 12-ft area approximately centered around each test location was inspected and mapped in general accordance with Federal Highway Administration guidelines for performing distress surveys of concrete pavements (Miller and Bellinger, 2014). All sites were inspected visually to identify cracking and scaling, and cracks having a width greater than 0.15 mm were recorded using a crack comparator card as shown in Figure 3.2. Delamination was identified using chain dragging. Bridges C-989 and F-792 were previously treated with an epoxy overlay, preventing an inspection of the underlying decks.

Figure 3.2 Crack comparator card.

3.2.2 Cover Depth Testing

Cover depth testing was performed to document the depth of the steel reinforcing bars as well as to determine locations for chloride concentration sampling and coring, which were necessarily performed between bars. A No. 5 bar size was assumed at all test sites for cover depth testing. The cover depth over both longitudinal and transverse bars was recorded. Use of the cover meter is illustrated in Figure 3.3.

3.2.3 Schmidt Rebound Hammer Testing

Schmidt rebound hammer testing was performed in general accordance with ASTM C805 (Standard Test Method for Rebound Number of Hardened Concrete) to estimate the stiffness of the concrete at each test location. Because of the presence of the epoxy overlays at bridges C-989 and F-792, use of the Schmidt rebound hammer, depicted in Figure 3.4, was limited to Bridge C-

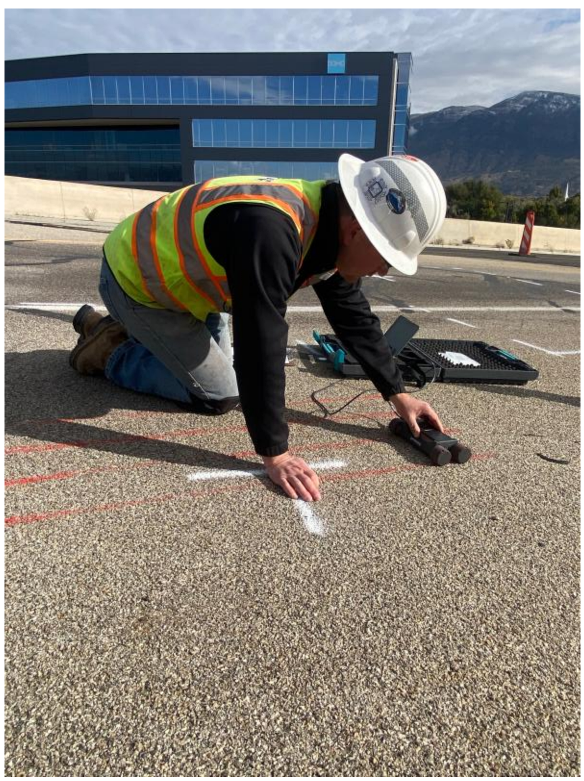

Figure 3.3 Cover meter.

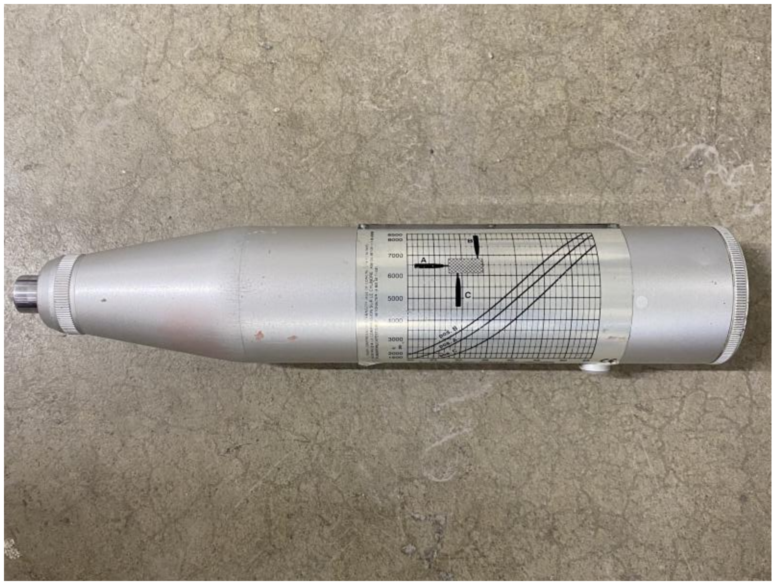

Figure 3.4 Schmidt rebound hammer.

1011. An angle grinder was used to smooth the concrete surface prior to testing. Five rebound numbers were recorded at each test location, and the average of the middle three numbers was reported as the Schmidt rebound number for the given location.

3.2.4 Resistivity Testing

Resistivity testing was performed to evaluate the potential for corrosion of reinforcing steel embedded in the concrete. For this test, two 0.25-in.-diameter holes were drilled to a depth of approximately 0.5 in. into the concrete, and a few drops of a conductive solution were placed into each hole. As shown in Figure 3.5, a two-prong resistivity probe was then inserted into the holes, and the resistivity was recorded. The probe was removed, rotated end for end, and then re-inserted into the holes to obtain a second measurement.

3.2.5 Chloride Concentration Sampling

Chloride concentration sampling was performed at each bridge to evaluate the susceptibility of the concrete to chloride ion ingress. Sampling was performed by obtaining concrete powder samples in 1-in. depth intervals to a total depth of 4 in. at each test location. When an epoxy overlay was present, the overlay was removed using drilling to expose the

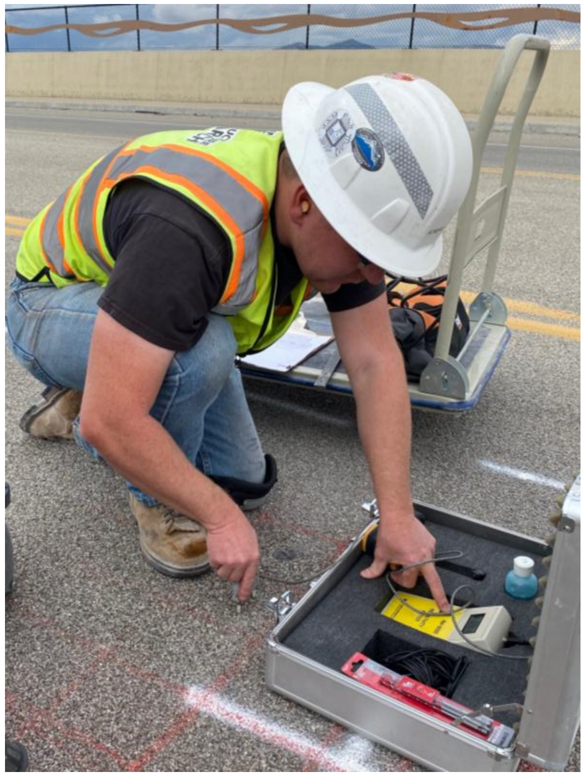

Figure 3.5 Resistivity meter.

surface of the underlying concrete before sampling was performed. A rotary hammer equipped with drill bits having diameters of 1.75 in., 1.5 in., 1.375 in., and 1.25 in. was used to pulverize the concrete, as shown in Figure 3.6. Use of smaller drill bits with increasing depth prevented the inadvertent scraping of near-surface concrete and potential contamination of deeper samples. The concrete powder obtained from each depth interval was sealed in a bag and transported to the laboratory for testing. A rapid-setting, air-entrained concrete mixture was used to patch the holes.

3.2.6 Coring

A coring machine was used, as shown in Figure 3.7, to remove approximately 4-in.-diameter concrete cores from all test locations for further laboratory testing. Cracked and delaminated areas were avoided to ensure that intact cores would be obtained. Maximum coring depths of 6 in. and 8 in. were achieved on the decks and approach slabs, respectively. After each core was extracted, it was wrapped in plastic and placed in a padded container for transport to the

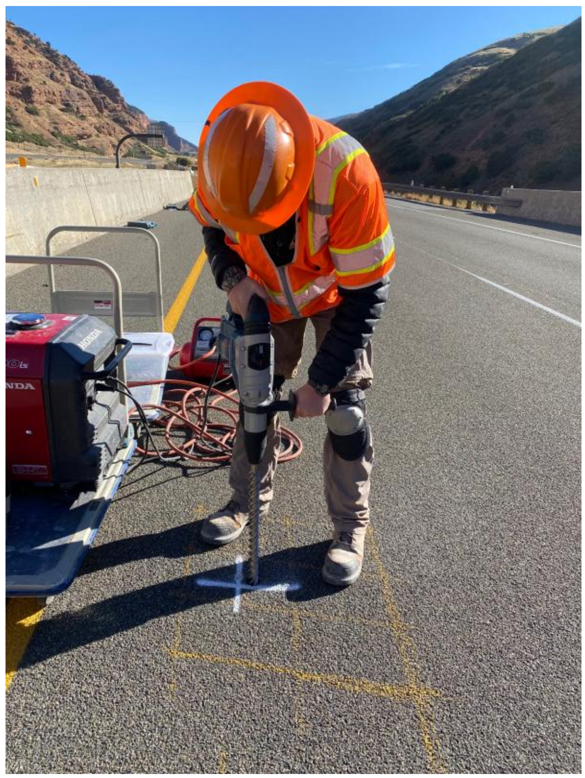

Figure 3.6 Concrete drill.

Figure 3.7 Coring machine.

laboratory for testing. A rapid-setting, air-entrained concrete mixture was again used to patch the holes.

3.3 Laboratory Testing

For this research, laboratory testing was performed on concrete samples obtained from the field work performed during the current research and samples obtained from previous research (Guthrie et al., 2015). Regarding samples obtained during the current research, modulus of elasticity testing, compressive strength testing, splitting tensile strength testing, rapid chloride permeability and absorption testing, and chloride concentration testing were performed. Regarding samples obtained from previous research, coefficient of thermal expansion testing and freeze-thaw durability testing were performed. In total, 20 concrete cores and 80 concrete powder samples were obtained from the field work performed during the current research, and six concrete cylinders were obtained from previous research. The unit weight of each concrete core or cylinder was measured prior to testing.

3.3.1 Modulus of Elasticity Testing

Modulus of elasticity testing was performed on all of the cores in general accordance with ASTM C215 (Standard Test Method for Fundamental Transverse, Longitudinal, and Torsional Resonant Frequencies of Concrete Specimens) to evaluate the stiffness of each core. As shown in Figure 3.8, the cores were oriented vertically on two open-cell foam blocks to isolate them from the laboratory bench. An accelerometer was fastened to the top of each core using modeling clay, and a hammer instrumented with a load cell was used to strike the bottom of the core. The data were analyzed using software, which computed the resonant frequency of the core. Together with the unit weight and length of the core, the resonant frequency was used to calculate the modulus of elasticity.

Figure 3.8 Stiffness testing.

3.3.2 Compressive Strength Testing

Compressive strength testing was performed in general accordance with ASTM C39 (Standard Test Methods for Compressive Strength of Cylindrical Concrete Specimens), as shown in Figure 3.9. For each of the four sites, two cores were tested after modulus of elasticity testing was performed. The cores were capped with neoprene pads and tested at a target strain rate of 0.05 in./minute. The peak load was recorded, and a compressive strength was calculated.

3.3.3 Splitting Tensile Strength Testing

Splitting tensile strength tests were performed in general accordance with ASTM C496 (Standard Test Method for Splitting Tensile Strength of Cylindrical Concrete Specimens), as shown in Figure 3.10. For each of the four sites, portions of two cores were tested after specimens required for rapid chloride permeability testing were first removed using a concrete

Figure 3.9 Compressive strength testing.

Figure 3.10 Splitting tensile strength testing.

saw. For splitting tensile strength testing, thin softwood loading strips were placed on opposite sides of the core where the fewest number of defects were apparent, and the load was applied diametrically at a target strain rate of 0.05 in./minute. The peak load was recorded, and a tensile strength was calculated.

3.3.4 Rapid Chloride Permeability and Absorption Testing

Rapid chloride permeability tests were performed in general accordance with ASTM C1202 (Standard Test Method for Electrical Indication of Concrete's Ability to Resist Chloride Ion Penetration), as shown in Figure 3.11. For each of the four sites, lower portions of two cores, each cut to a height of approximately 2.0 in., were vacuum-saturated, weighed in a soaked but surface-dry condition, loaded in a test cell, and then tested for 6 hours. The total current passing through the specimen during the test was computed in coulombs, and a corresponding permeability class was reported.

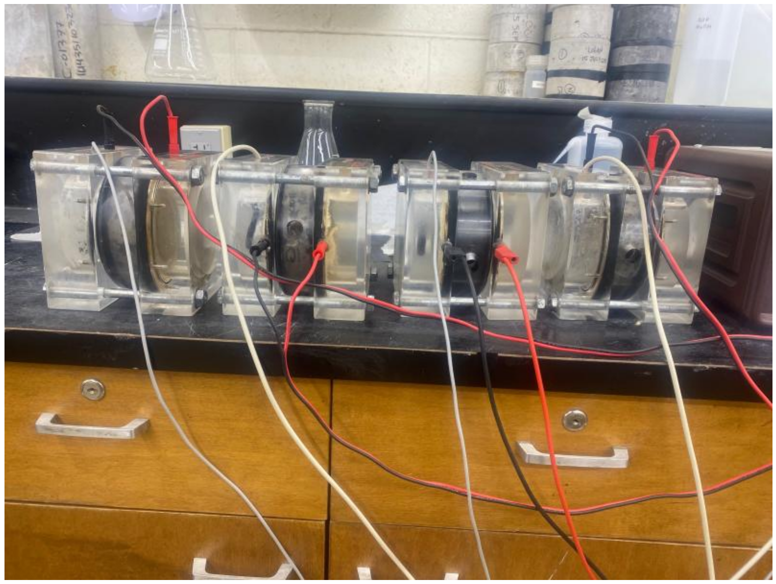

Figure 3.11 Rapid chloride permeability testing.

After the rapid chloride permeability testing was complete, the specimens were dried to constant weight in an oven at 230°F and weighed, and the soaked weight and dry weight were used to estimate an absorption value for each specimen.

3.3.5 Chloride Concentration Testing

Chloride concentration tests were performed in general accordance with ASTM C1152 (Standard Test Method for Acid-Soluble Chloride in Mortar and Concrete). Following a digestion process, titration using silver nitrate was performed. Chloride concentrations were reported in units of pounds of chloride per cubic yard of concrete using the average concrete unit weight determined from cores removed from the given site. From the resulting chloride concentration profiles and the measured concrete cover depths, the corrosion activity of the reinforcing steel was assessed with respect to a threshold of 2.0 lb Cl^{-}/yd^{3} of concrete at which corrosion of exposed steel is expected to be initiated (Waters Emery et al., 2020).

3.3.6 Coefficient of Thermal Expansion Testing

Testing to evaluate the coefficient of thermal expansion of cylinders obtained from previous research was performed in general accordance with ASTM E831 (Standard Test

Method for Linear Thermal Expansion of Solid Materials by Thermomechanical Analysis), as shown in Figure 3.12. Prior to testing, an angle grinder was used to flatten the surface of one end of each cylinder to ensure stable height measurements. The other end of each cylinder was marked in three locations near the center of the circular face, at which height measurements were obtained. The cylinders were tested at temperatures of 0°F, 72.5°F, and 140°F before and after being soaked in water for 72 hours. Specimens were equilibrated at each temperature for at least 12 hours before height measurements were obtained.

3.3.7 Freeze-Thaw Durability Testing

Freeze-thaw durability testing of cylinders obtained from previous research was performed in general accordance with ASTM C666 (Standard Test Method for Resistance of Concrete to Rapid Freezing and Thawing), as shown in Figure 3.13, using two computer-controlled chest freezers. Prior to testing, the cylinders were soaked in water for a period of 48 hours. Consistent with Procedure B of ASTM C666, the cylinders were then placed on a wire

Figure 3.12 Coefficient of thermal expansion testing.

Figure 3.13 Freeze-thaw durability testing.

rack in the bottom of a chest freezer, where they were subjected to freezing conditions for a period of 3 hours to achieve a target internal temperature of 0±3°F. The cylinders were then moved to buckets of water in another chest freezer, where they were subjected to thawing conditions for a period of 1 hour to achieve a target internal temperature of 40±3°F. Testing proceeded at a rate of four cycles per day, with the cylinders being held in freezing conditions overnight, until 300 cycles were accomplished. At the conclusion of the thawing period on a 20-cycle interval, the surface of each cylinder was dried with a towel, the cylinders were weighed, and modulus of elasticity testing was performed as previously described.

3.4 Summary

The procedures used for this research involved field and laboratory testing of lightweight and normal-weight concrete. Field testing included three bridge decks constructed using lightweight concrete and one of the adjacent normal-weight concrete approach slabs. Bridges C-989, C-1011, and F-792 were selected by UDOT personnel for evaluation in this research, and concrete samples from bridges C-993 and F-818, which were the focus of previous research, were also included.

For field testing, a portion of each bridge, typically the right or left lane and the adjacent shoulder, was closed to traffic, and five test locations were then selected for evaluation using a formal random sampling procedure to eliminate potential bias. A distress survey was performed at each test location, and then cover depth testing, Schmidt rebound hammer testing, resistivity testing, chloride concentration sampling, and coring were performed.

For laboratory testing, regarding samples obtained during the current research, modulus of elasticity testing, compressive strength testing, splitting tensile strength testing, rapid chloride permeability and absorption testing, and chloride concentration testing were performed. Regarding samples obtained from previous research, coefficient of thermal expansion testing and freeze-thaw durability testing were performed. In total, 20 concrete cores and 80 concrete powder samples were obtained from the field work performed during the current research, and six concrete cylinders were obtained from previous research. The unit weight of each concrete core or cylinder was measured prior to testing.

4.0 RESULTS

4.1 Overview

The results obtained from both field and laboratory testing are presented in this chapter, and supporting data are provided in Appendix B. The results are expected to be applicable to lightweight concrete bridge decks with similar construction and service conditions as those evaluated in this research.

4.2 Field Testing

The results of distress surveys, cover depth testing, Schmidt rebound hammer testing, and resistivity testing are presented in the following sections for the lightweight concrete bridge decks and adjacent normal-weight concrete approach slabs that were evaluated in this research.

4.2.1 Distress Surveys

Based on the distress surveys performed on the three bridge decks and approach slabs evaluated in this research, distress maps were prepared for all locations where distress was observed and are presented in Appendix C. Distress calculations were performed for each site, as shown in Table 4.1, and average values and ranges for crack density, crack width, scaling, map cracking, and delamination for each site are depicted in Figure 4.1, Figure 4.2, Figure 4.3, Figure 4.4, and Figure 4.5, respectively; a small amount of localized damage, presumed to be the result of a construction-related issue that occurred during placement of the epoxy overlay on the deck, was observed on bridge C-989 but not analyzed. Because an epoxy overlay was present at bridges C-989 and F-792, the crack density data for C-989 is based on cracks observed in the epoxy overlay; no cracks were visible in the new epoxy overlay at bridge F-792. The average crack density and crack width for all of the lightweight concrete bridges evaluated in this research were calculated as 0.021 ft/ft^2 and 4 mils, respectively, while corresponding values for normal-weight concrete were calculated as 0.005 ft/ft^2 and 10 mils. Given the absence of an epoxy overlay, bridge C-1011 was the only deck that exhibited scaling and map cracking, which affected an average of 20.4 percent and 28.1 percent, respectively, of the inspected deck area.

Table 4.1 Distresses

Bridge Identifier	Concrete Type	Test Location	Total Crack Length (ft)	Crack Density (ft/ft^2)	Average Crack Width (mils)	Scaling (ft^2/ft^2)	Map Cracking (ft^2/ft^2)	Delamination (ft^2/ft^2)
C-989	Lightweight with 12-Year-Old Epoxy Overlay	1	0	0.000	0	0.000	0.000	0.000
		2	5	0.003	10	0.000	0.000	0.000
		3	0	0.000	0	0.000	0.000	0.000
		4	11	0.007	9	0.000	0.000	0.000
		5	19	0.011	8	0.000	0.000	0.000
C-1011	Lightweight with No Overlay	1	64	0.037	15	0.193	0.485	0.000
		2	77	0.044	2	0.372	0.354	0.000
		3	85	0.049	1	0.244	0.120	0.000
		4	148	0.086	3	0.045	0.000	0.000
		5	134	0.078	7	0.167	0.445	0.000
F-792	Lightweight with New Epoxy Overlay	1	0	0.000	0	0.000	0.000	0.000
		2	0	0.000	0	0.000	0.000	0.000
		3	0	0.000	0	0.000	0.000	0.000
		4	0	0.000	0	0.000	0.000	0.007
		5	0	0.000	0	0.000	0.000	0.010
C-989	Normal-Weight with 12-Year-Old Epoxy Overlay	1	8	0.005	11	0.000	0.000	0.000
		2	4	0.002	11	0.000	0.000	0.000
		3	2	0.001	8	0.000	0.000	0.002
		4	18	0.011	13	0.000	0.000	0.000
		5	7	0.004	9	0.000	0.000	0.000

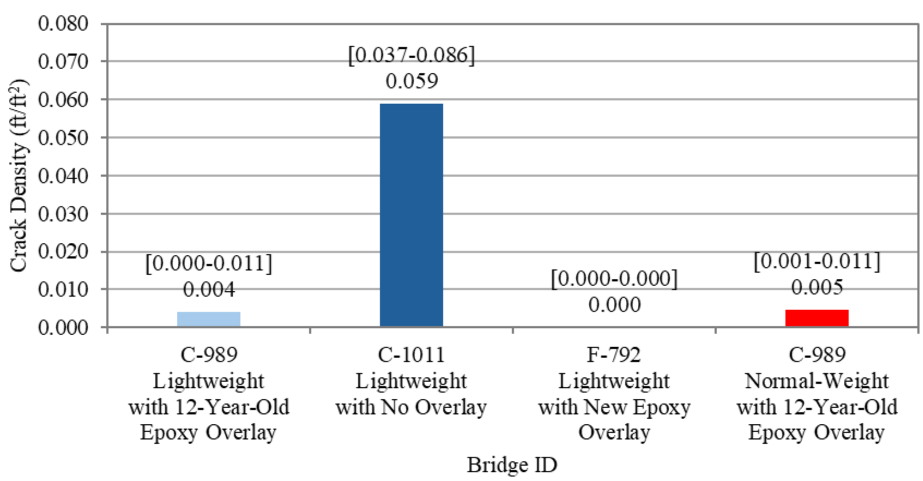

Figure 4.1 Crack density.

Delamination, which was measured only at bridge F-792 and the approach slabs of bridge C-989, affected an average of 0.3 percent and 0.1 percent of the inspected deck area for lightweight concrete and normal-weight concrete bridges, respectively; the cause of the delamination, which

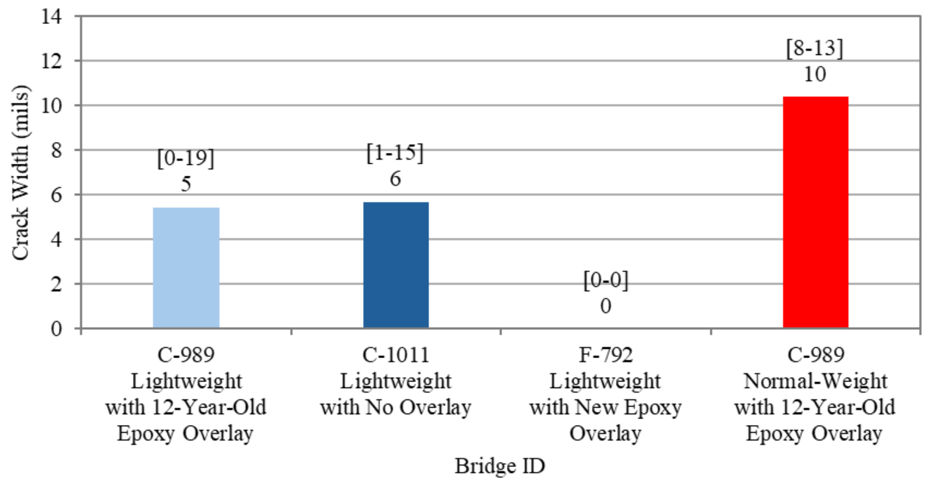

Figure 4.2 Crack width.

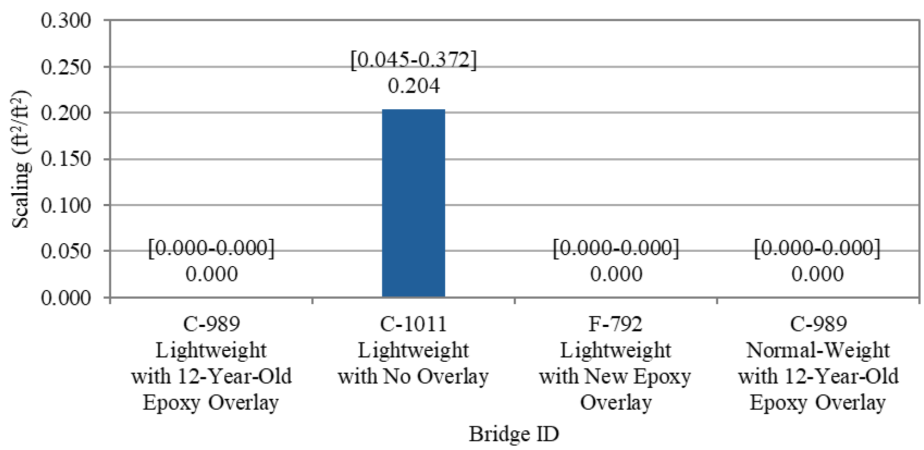

Figure 4.3 Scaling.

may have been debonding of the overlay or corrosion-induced delamination of the underlying concrete (Waters Emery et al., 2020), was not investigated in this research. While the values of crack density and crack width are relatively low compared to those measured in previous studies of concrete bridge decks having similar ages and service conditions, the percentages of scaling, map cracking, and delamination are typical (Cavalline et al., 2017; Guthrie and Tuttle, 2006; Guthrie et al., 2006).

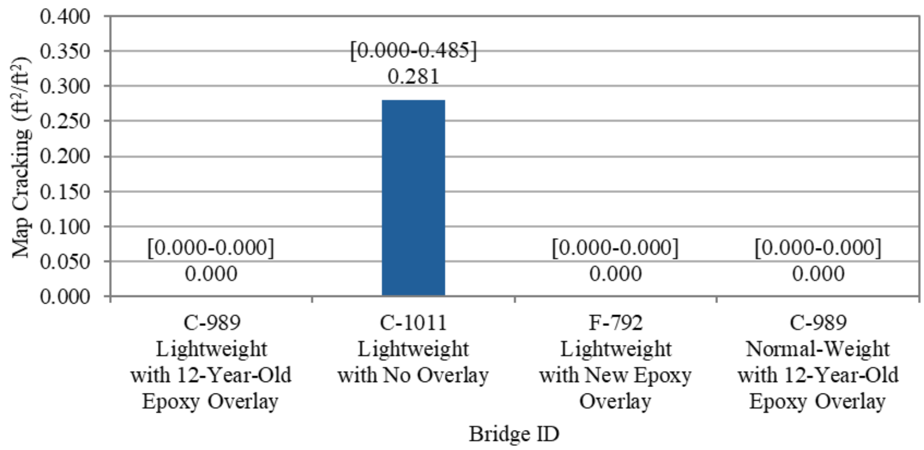

Figure 4.4 Map cracking.

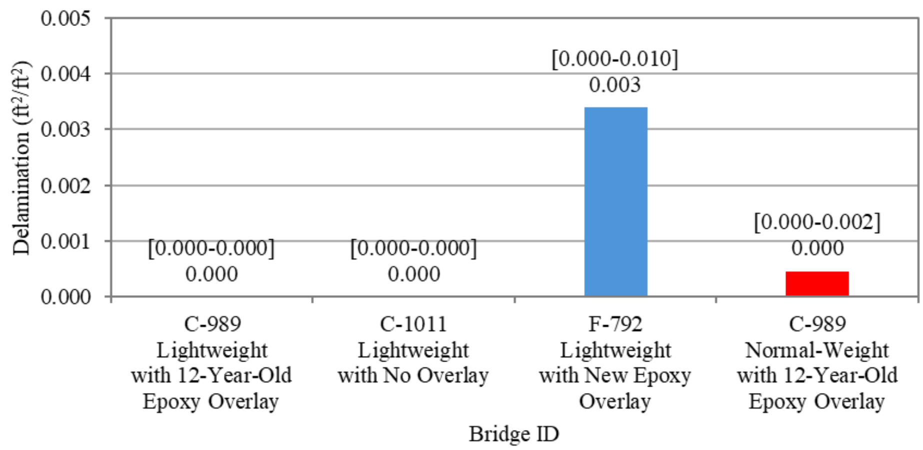

Figure 4.5 Delamination.

4.2.2 Cover Depth Testing

The results of cover depth testing are presented in Table 4.2, which includes averages for both longitudinal and transverse bars at each location. Average cover depths for the lightweight concrete bridge decks were calculated as 2.73 in. and 2.61 in. for the longitudinal and transverse reinforcement depths, respectively, and corresponding values for the normal-weight concrete were 3.20 in. and 3.37 in. Although lower cover depths of 2.39 in. and 2.35 in. were calculated for bridge C-1011 for the longitudinal and transverse reinforcement depths, respectively, the average cover depth for all lightweight concrete bridges and the average cover depth for the

Table 4.2 Cover Depth

Bridge Identifier	Concrete Type	Cover Depth (in.)				
		Location 1	Location 2	Location 3	Location 4	Location 5
Longitudinal Reinforcement						
C-989	Lightweight	2.11	2.95	2.69	3.63	2.71
C-1011		2.36	2.37	2.30	2.38	2.56
F-792		3.02	2.86	2.99	3.25	2.82
C-989	Normal-Weight	2.52	3.78	3.21	3.42	3.07
Transverse Reinforcement						
C-989	Lightweight	1.90	2.85	2.42	3.32	2.60
C-1011		2.36	2.30	2.25	2.41	2.46
F-792		2.87	2.73	2.80	3.17	2.67
C-989	Normal-Weight	2.59	3.68	3.76	3.56	3.27

normal-weight concrete approach slabs exceed the minimum cover depth of 2.5 in. required by UDOT.

4.2.3 Schmidt Rebound Hammer Testing

The results of Schmidt rebound hammer testing are shown in Table 4.3. Based on the average Schmidt rebound number measured at each test location at bridge C-1011, which was the only tested bridge that did not have an epoxy overlay, a concrete compressive strength was estimated. The average Schmidt rebound number and estimated compressive strength for bridge C-1011 were calculated as 51 and 7840 psi, respectively.

4.2.4 Resistivity Testing

Average resistivity values and surface temperatures measured at the time of resistivity testing are shown in Table 4.4. The average resistivity values for lightweight concrete and

Table 4.3 Schmidt Rebound Number and Estimated Compressive Strength

Bridge Identifier	Concrete Type	Test Location	Average Schmidt Rebound Number	Estimated Compressive Strength (psi)
C-1011	Lightweight	1	49	7500
		2	51	7900
		3	50	7800
		4	52	8100
		5	51	7900

Table 4.4 Resistivity

Bridge Identifier	Concrete Type	Test Location	Average Resistivity (kohm-in.)	Surface Temperature (^oF)
C-989	Lightweight	1	33.9	78
		2	37.4	72
		3	37.6	70
		4	28.0	69
		5	37.5	74
C-1011	Lightweight	1	24.7	62
		2	29.7	65
		3	20.9	74
		4	22.2	68
		5	32.0	72
F-792	Lightweight	1	29.8	69
		2	33.7	69
		3	37.4	71
		4	14.0	75
		5	11.1	77
C-989	Normal-Weight	1	37.2	91
		2	37.9	87
		3	38.9	90
		4	37.2	84
		5	38.7	86

normal-weight concrete were calculated as 28.7 and 38.0, respectively, which both correspond to a corrosion potential classification of "low" (Barrus, 2012).

4.3 Laboratory Testing

The results of modulus of elasticity, compressive strength, splitting tensile strength, rapid chloride permeability and absorption, chloride concentration, coefficient of thermal expansion, and freeze-thaw durability testing are presented in the following sections. Where applicable, the unit weight of the concrete is reported for each tested sample, and average values and ranges for each site are depicted in Figure 4.6. Regarding samples obtained during the current research, the average unit weights were 116.8 pcf for lightweight concrete and 136.1 pcf for normal-weight concrete. Regarding samples obtained from previous research, the average unit weights were 122.0 pcf for lightweight concrete and 145.3 pcf for normal-weight concrete.

Photographs of the cores and cylinders obtained during the current research are provided in Appendix D, and Figures 4.7 and 4.8 present representative photographs of the lightweight coarse aggregate and normal-weight coarse aggregate observed on the outside surfaces of the

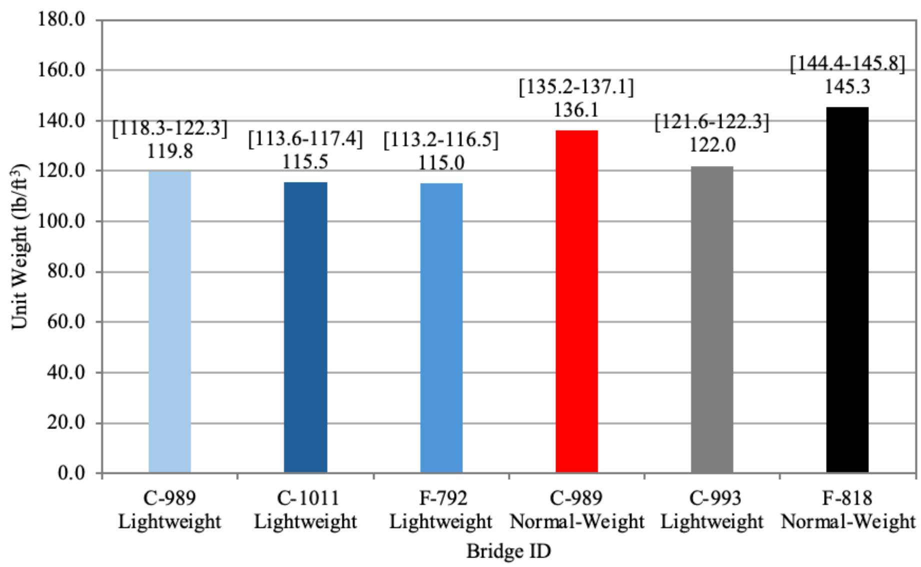

Figure 4.6 Unit weight.

Figure 4.7 Typical lightweight coarse aggregate.

Figure 4.8 Typical normal-weight coarse aggregate.

cores removed from the lightweight concrete bridge decks and normal-weight concrete approach slabs before any testing was performed. While the normal-weight coarse aggregate appears to be intact, the lightweight coarse aggregate exhibits internal cracking and the possible occurrence of secondary deposits. Additional pictures showing porosity and cracking of the lightweight coarse aggregate observed on the outside surfaces of the cores, prior to any testing, are provided in Appendix E.

4.3.1 Modulus of Elasticity Testing

The results of modulus of elasticity testing are shown in Table 4.5, and average values and ranges for each site are depicted in Figure 4.9. The average modulus of elasticity values for lightweight concrete and normal-weight concrete were calculated as 1928 ksi and 5650 ksi, respectively.

Table 4.5 Modulus of Elasticity

Bridge Identifier	Concrete Type	Test Location	Unit Weight (lb/ft^3)	Modulus of Elasticity (ksi)
C-989	Lightweight	1	119.5	2015
		2	118.3	2171
		3	119.4	1811
		4	122.3	2180
		5	119.6	1877
C-1011	Lightweight	1	115.4	1949
		2	113.6	1786
		3	115.3	2052
		4	117.4	1750
		5	115.9	1688
F-792	Lightweight	1	114.7	2146
		2	116.2	2173
		3	113.2	1846
		4	116.5	1863
		5	114.4	1612
C-989	Normal-Weight	1	137.1	5856
		2	136.5	5705
		3	135.3	5525
		4	136.6	5657
		5	135.2	5510

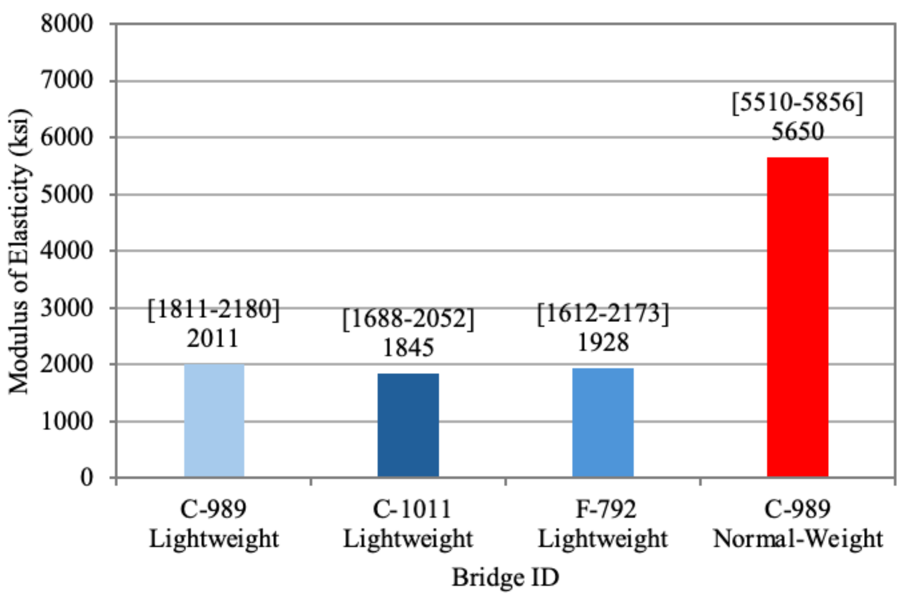

Figure 4.9 Modulus of elasticity.

4.3.2 Compressive Strength Testing

The results of compressive strength testing are shown in Table 4.6, and average values and ranges for each site are depicted in Figure 4.10. The average compressive strengths for lightweight concrete and normal-weight concrete were calculated as 7355 psi and 10,199 psi, respectively. All lightweight concrete cores therefore met the minimum compressive strength requirement specified according to their unit weight, as outlined in ASTM C330. Regarding bridge C-1011, in particular, the measured average compressive strength of 7010 psi was approximately 11 percent less than the compressive strength of 7840 psi estimated from Schmidt

Table 4.6 Compressive Strength

Bridge Identifier	Concrete Type	Test Location	Unit Weight (lb/ft^3)	Compressive Strength (psi)
C-989	Lightweight	3	116.0	7407
		5	124.7	7628
C-1011	Lightweight	1	111.3	6895
		2	111.8	7124
F-792	Lightweight	3	109.1	7040
		4	112.3	8038
C-989	Normal-Weight	2	132.8	10193
		4	135.2	10206

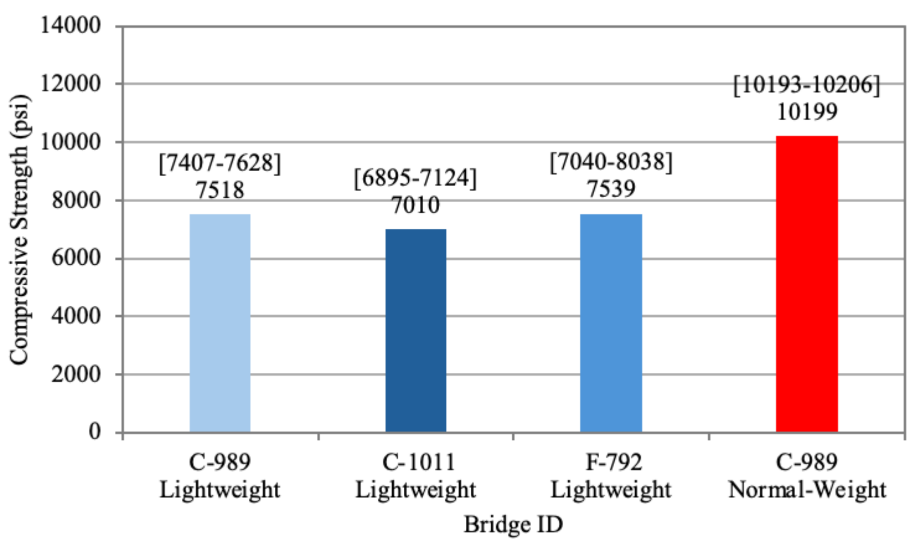

Figure 4.10 Compressive strength.

rebound hammer testing. As previously explained, while normal-weight concrete generally fractures through the paste around the aggregate particles, lightweight concrete often fractures through the lightweight aggregate particles (Holm and Ries, 2000; Lopez et al., 2003; Ramirez et al., 2000); as evidenced in Figures 4.11 and 4.12 for samples of lightweight concrete and normal-weight concrete, respectively, the lightweight coarse aggregate particles were observed to be completely fractured, while many of the normal-weight coarse aggregate particles remained intact.

4.3.3 Splitting Tensile Testing

The results of splitting tensile strength testing are shown in Table 4.7, and average values and ranges for each site are depicted in Figure 4.13. The average splitting tensile strengths for lightweight concrete and normal-weight concrete were calculated as 610 psi and 753 psi, respectively. All lightweight concrete cores therefore met the minimum tensile strength

Figure 4.11 Lightweight concrete fracture face.

Figure 4.12 Normal-weight concrete fracture face.

Table 4.7 Splitting Tensile Strength

Bridge Identifier	Concrete Type	Test Location	Unit Weight (lb/ft^3)	Splitting Tensile Strength (psi)
C-989	Lightweight	2	114.7	629
		4	114.6	489
C-1011	Lightweight	3	108.6	505
		5	113.4	796
F-792	Lightweight	1	111.4	615
		5	108.8	625
C-989	Normal-Weight	1	134.5	826
		2	134.2	680

requirement specified according to their unit weight, as outlined in ASTM C330. Consistent with the results of compressive strength testing, the lightweight coarse aggregate particles were again observed to be completely fractured, while many of the normal-weight coarse aggregate particles remained intact.

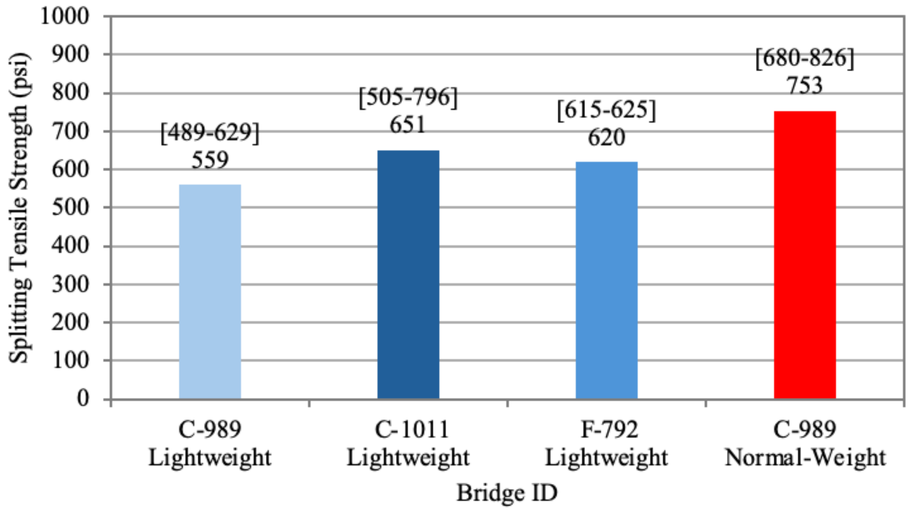

Figure 4.13 Splitting tensile strength.

4.3.4 Rapid Chloride Permeability and Absorption Testing

The results of rapid chloride permeability and absorption testing are shown in Table 4.8, and average values and ranges for each site are depicted in Figures 4.14 and 4.15. The average rapid chloride permeability values for lightweight concrete and normal-weight concrete were calculated as 550 C and 75 C, respectively, which correspond to chloride permeability classifications of "very low" and "negligible" (Hema et al., 2004). The average absorption values for lightweight concrete and normal-weight concrete were calculated as 12.7 percent and 4.7 percent, respectively.

Table 4.8 Chloride Permeability and Absorption

Bridge Identifier	Concrete Type	Test Location	Unit Weight (lb/ft^3)		Chloride Permeability (C)	Absorption (%)
			Dry	Wet		
C-989	Lightweight	1	108.9	122.1	499	12.1
		4	109.1	124.5	1083	14.1
C-1011	Lightweight	3	104.8	118.2	421	12.9
		4	106.6	120.7	805	13.2
F-792	Lightweight	1	103.0	115.2	239	11.8
		2	104.4	116.8	255	11.9
C-989	Normal-Weight	1	129.6	135.5	67	4.6
		2	129.4	135.5	82	4.7

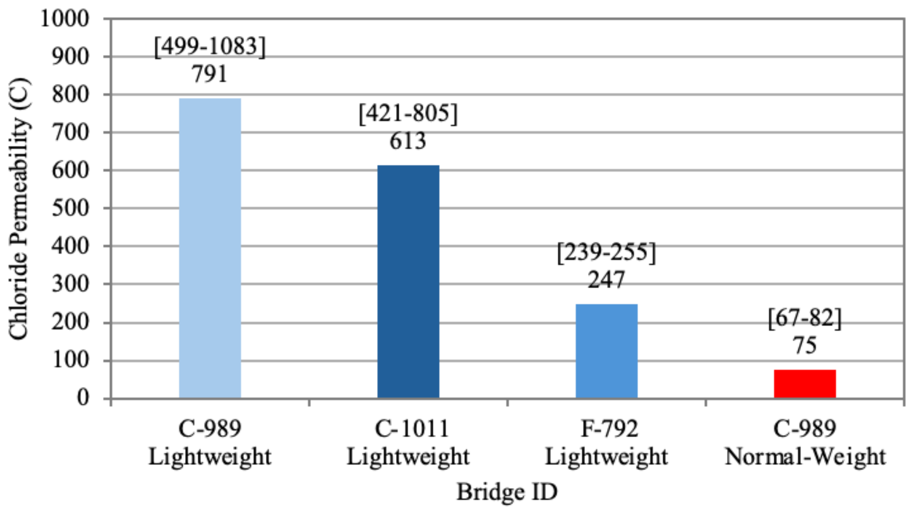

Figure 4.14 Chloride permeability.

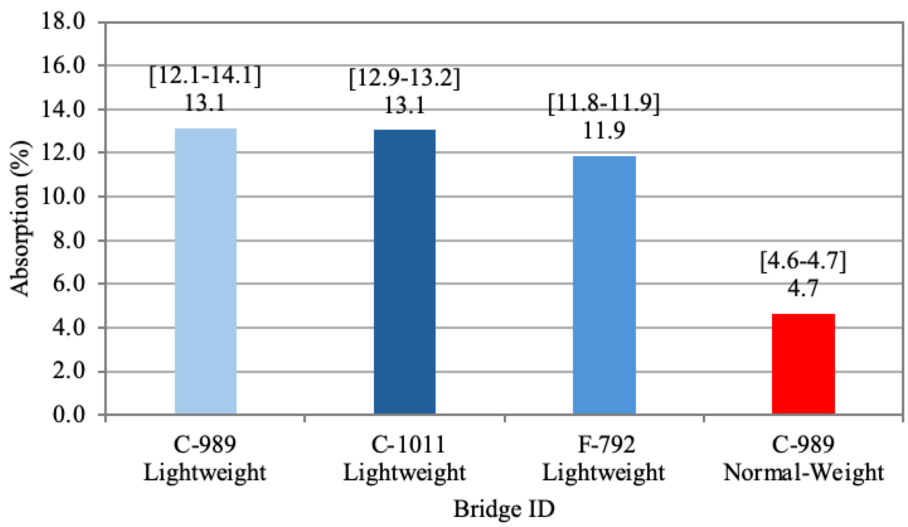

Figure 4.15 Absorption.

4.3.5 Chloride Concentration Testing

The results of chloride concentration testing are shown in Table 4.9 for a depth range of 0 to 4 in. The average chloride concentrations for lightweight concrete and normal-weight concrete to which an epoxy overlay had been applied, including bridges C-989 and F-792, were calculated as 5.5, 0.8, 0.4, and 0.4 lb Cl^-/yd^3 of concrete and 0.4, 0.4, 0.3, and 0.4 lb Cl^-/yd^3 of concrete,

Table 4.9 Chloride Concentration

Bridge Identifier	Concrete Type	Test Location	Average Unit Weight (lb/ft^3)	Chloride Concentration (lb Cl^-/yd^3 Concrete) at Indicated Depth Interval (in.)			
				0-1	1-2	2-3	3-4
C-989	Lightweight	1	119.8	2.0	0.4	0.5	0.6
		2		1.9	0.5	0.5	0.5
		3		0.6	0.5	0.5	0.4
		4		0.8	0.3	0.0	0.1
		5		1.3	0.3	0.4	0.3
C-1011	Lightweight	1	115.0	24.8	2.9	0.6	0.4
		2		26.5	6.4	0.7	0.5
		3		26.8	8.3	0.6	0.5
		4		32.9	10.5	0.7	0.6
		5		27.3	5.3	0.4	0.3
F-792	Lightweight	1	115.5	9.8	0.6	0.3	0.4
		2		4.7	0.4	0.4	0.5
		3		7.1	0.5	0.3	0.1
		4		16.4	3.1	0.5	0.4
		5		11.0	1.0	0.5	0.5
C-989	Normal-Weight	1	136.1	0.5	0.5	0.3	0.4
		2		0.4	0.4	0.4	0.4
		3		0.4	0.4	0.4	0.4
		4		0.4	0.4	0.3	0.4
		5		0.2	0.2	0.3	0.4

respectively, for depth intervals ending at 1, 2, 3, and 4 in. The average chloride concentrations for bridge C-1011, which did not have an epoxy overlay, were 27.7, 6.7, 0.6, and 0.4 lb Cl^-/yd^3 of concrete. While the efficacy of the epoxy overlay in preventing chloride ion ingress at bridge C-989 is apparent, the epoxy overlay originally placed at bridge F-792 had become compromised, allowing chloride ion ingress, and was replaced in 2023 just prior to this research. Average chloride concentration values and ranges at each depth interval for each site are depicted in Figure 4.16. Given that the average cover depths were all greater than 2.5 in., at which depth the chloride concentrations are less than the threshold of 2.0 lb Cl^-/yd^3, widespread corrosion of the reinforcing steel on these decks would not yet be expected.

4.3.6 Coefficient of Thermal Expansion Testing

The results of coefficient of thermal expansion testing are shown in Table 4.10. The average coefficients of thermal expansion for lightweight concrete in the dry and soaked conditions were calculated as 9.8×10^{-6}/°F and 9.6×10^{-6}/°F, respectively, while corresponding

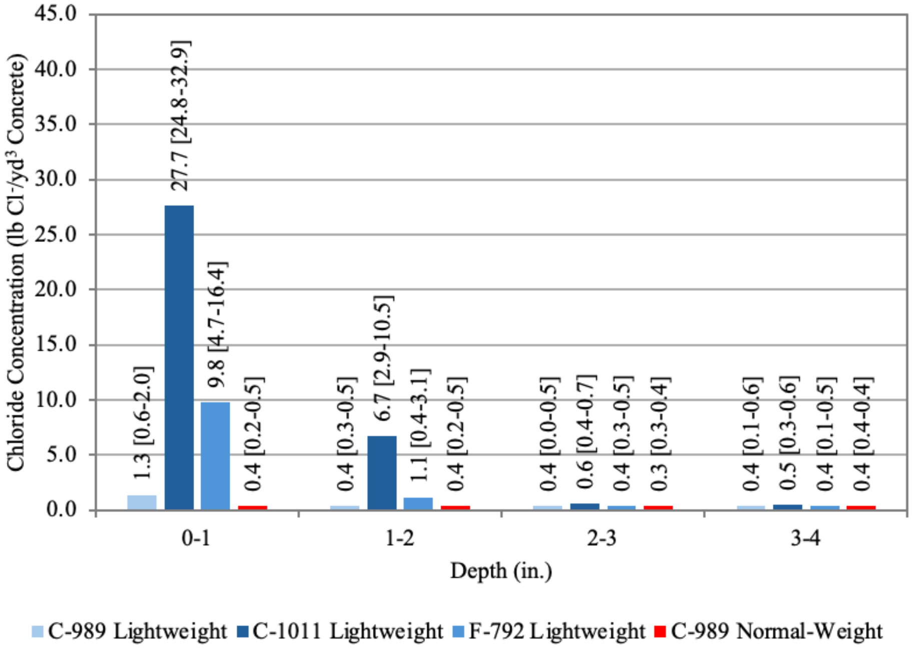

Figure 4.16 Chloride concentration.

Table 4.10 Coefficient of Thermal Expansion

Bridge Identifier	Concrete Type	Sample	Unit Weight (lb/ft^3)		Coefficient of Thermal Expansion (/°F)	
			Dry	Soaked	Dry	Soaked
C-993	Lightweight	1	112.8	121.6	$11.2x10^{-6}$	$9.6x10^{-6}$
		2	115.0	122.3	$10.9x10^{-6}$	$7.5x10^{-6}$
		3	113.8	122.0	$7.4x10^{-6}$	$9.4x10^{-6}$
F-818	Normal-Weight	1	141.4	145.8	$9.8x10^{-6}$	$7.6x10^{-6}$
		2	141.7	145.6	$8.5x10^{-6}$	$8.5x10^{-6}$
		3	140.5	144.4	$10.3x10^{-6}$	$6.6x10^{-6}$

values for normal-weight concrete were calculated as $8.9x10^{-6}$/°F and $7.5x10^{-6}$/°F. These values are consistently higher than the typical range of $3x10^{-6}$/°F to $7x10^{-6}$/°F reported in the literature for lightweight concrete (Castrodale, 2021; Kosmatka and Wilson, 2016; Russell et al., 2006), indicating that more thermal expansion and contraction would be expected to occur during heating and cooling, respectively.

4.3.7 Freeze-Thaw Durability Testing

The results of freeze-thaw durability testing are shown in Table 4.11. The average values of stiffness retained for lightweight concrete and normal-weight concrete were calculated as 74.6 percent and 100 percent, respectively. While all three lightweight concrete cylinders exhibited degradation in this test, lightweight concrete sample 1 reached the failure condition, defined as less than 60 percent stiffness retained in ASTM C666, between cycles 260 and 280. Figure 4.17 shows a fractured coarse aggregate at the base of an approximately 1-in.-diameter popout that occurred in lightweight concrete sample 3 between cycles 160 and 180. None of the normal-weight concrete cylinders exhibited degradation.

To the extent that the lightweight concrete mixtures, some of which are presented in Appendix A, are similar for all of the bridges evaluated in this research, the initial modulus of elasticity values computed before freeze-thaw durability testing, corresponding to cycle 0 in Table 4.11, can be compared to the modulus of elasticity values computed in Table 4.5 for the lightweight concrete cores. Although the concrete bridges from which the cores were removed had a lower unit weight and may not have been cured as well as the cylinders that were subjected

Table 4.11 Freeze-Thaw Durability

Cycle	Modulus (ksi) for Indicated Bridge Identifier, Concrete Type, and Sample at Indicated Freeze-Thaw Cycle					
	C-993 Lightweight			F-818 Normal-Weight		
	1	2	3	1	2	3
0	3259	3542	3359	6208	6267	6130
20	3170	3496	3269	6141	6132	6130
40	3170	3496	3269	6141	6199	6130
60	3170	3496	3269	6141	6178	6130
80	3170	3496	3269	6141	6199	6130
100	3214	3496	3269	6208	6199	6130
120	3082	3496	3269	6141	6199	6130
140	3082	3496	3269	6208	6199	6196
160	2995	3450	3224	6208	6199	6196
180	2867	3450	3180	6208	6199	6196
200	2783	3404	3180	6208	6199	6196
220	2660	3358	3136	6208	6199	6196
240	2620	3313	3092	6208	6267	6196
260	2307	3268	3048	6208	6267	6196
280	1910	3179	2963	6208	6267	6196
300	1742	3048	2836	6208	6267	6196
Stiffness Retained (%)	53.4	86.0	84.4	100.0	100.0	100.0

Figure 4.17 Lightweight coarse aggregate fractured during freeze-thaw durability testing.

to coefficient of thermal expansion and freeze-thaw durability testing in this research, such that the cores may have had a lower initial modulus than the cylinders, the comparatively low average value of 1928 ksi for the cores compared to the average initial value of 3387 ksi for the cylinders suggests that the lightweight concrete bridges had sustained a degree of degradation from freeze-thaw cycling in the field prior to testing. Indeed, the photograph presented in Figure 4.7 clearly shows cracking of the lightweight coarse aggregate that may have occurred from freeze-thaw cycling in the field.

4.4 Discussion

As a basis for discussion of the test results, ratios of values for lightweight concrete to values of normal-weight concrete were computed for selected properties shown in Table 4.12, for which the normal-weight concrete approach slabs and the normal-weight concrete cores and cylinders were used as a baseline. While the selected properties necessarily exclude the results of visual inspection and chloride concentration, which were directly affected by the presence of an

Table 4.12 Comparison of Properties of Lightweight Concrete and Normal-Weight Concrete

Property	Ratio of Value for Lightweight Concrete to Value of Normal-Weight Concrete
Resistivity	0.75
Modulus of Elasticity	0.34
Compressive Strength	0.72
Splitting Tensile Strength	0.81
Chloride Permeability	7.39
Absorption	2.73
Dry Coefficient of Thermal Expansion	1.03
Soaked Coefficient of Thermal Expansion	1.17
Stiffness Retained after Freeze-Thaw Durability	0.75

epoxy overlay on two of the bridges, they include resistivity, modulus of elasticity, compressive strength, splitting tensile strength, chloride permeability, absorption, coefficient of thermal expansion in the dry and soaked conditions, and stiffness retained after freeze-thaw durability testing.

The resistivity of lightweight concrete is 75 percent of the corresponding value of normal-weight concrete, which indicates a higher corrosion potential. The modulus of elasticity of lightweight concrete is 34 percent of the corresponding value of normal-weight concrete, which indicates that a higher strain will occur for a given stress within the elastic region. The compressive strength and splitting tensile strength of lightweight concrete are 72 percent and 81 percent of the corresponding values of normal-weight concrete, which indicate lower resistance to compressive and tensile stresses and therefore a higher cracking potential. The chloride permeability and absorption of lightweight concrete are 739 percent and 273 percent of the corresponding values of normal-weight concrete, which indicate higher rates of chloride ion ingress and higher water retention. The coefficients of thermal expansion of lightweight concrete in the dry and soaked conditions are 103 and 117 percent of the corresponding values of normal-weight concrete, which indicate that more thermal expansion and contraction would be expected to occur during heating and cooling, respectively; the greater increase in the coefficient of thermal expansion in the soaked condition is likely attributable to the greater absorption of lightweight concrete. The stiffness retained after freeze-thaw durability testing of lightweight concrete is 75 percent of the corresponding value of normal-weight concrete, indicating a greater susceptibility to degradation under freeze-thaw cycling.

Overall, these data suggest that, compared to normal-weight concrete, lightweight concrete absorbs more water, allows higher rates of chloride ion ingress, is more susceptible to degradation under freeze-thaw cycling, and has lower resistance to cracking. As cracking occurs, the rates of potential degradation from water absorption, chloride ion ingress, and freeze-thaw cycling increase, and localized structural failure, as depicted in Figure 1.1, can eventually occur.

4.5 Summary

Results were obtained from both field and laboratory testing. The results are expected to be applicable to lightweight concrete bridge decks with similar construction and service conditions as those evaluated in this research. From field testing, the results of distress surveys, cover depth testing, Schmidt rebound hammer testing, and resistivity testing are presented for the lightweight concrete bridge decks and adjacent normal-weight concrete approach slabs that were evaluated in this research. The average crack density and crack width for all of the lightweight concrete bridges evaluated in this research were calculated as 0.0210 ft/ft^2 and 4 mils, respectively, while corresponding values for normal-weight concrete were calculated as 0.0046 ft/ft^2 and 10 mils. Given that an epoxy overlay was present at bridges C-989 and F-792, the values of crack density and crack width are relatively low compared to those measured in previous studies of concrete bridge decks having similar ages and service conditions; however, the percentages of scaling, map cracking, and delamination are typical. Average cover depths for the lightweight concrete bridge decks were calculated as 2.73 in. and 2.61 in. for the longitudinal and transverse reinforcement depths, respectively, and corresponding values for the normal-weight concrete were 3.20 in. and 3.37 in. For bridge C-1011, which was the only tested bridge that did not have an epoxy overlay, the average Schmidt rebound number and estimated compressive strength were calculated as 51 and 7840 psi, respectively. The average resistivity values for lightweight concrete and normal-weight concrete were calculated as 28.7 and 38.0, respectively, which both correspond to a corrosion potential classification of "low."

From laboratory testing, the results of modulus of elasticity, compressive strength, splitting tensile strength, rapid chloride permeability and absorption, chloride concentration, coefficient of thermal expansion, and freeze-thaw durability testing are presented. Regarding samples obtained during the current research, the average unit weights were 116.8 pcf for lightweight concrete and 136.1 pcf for normal-weight concrete. Regarding samples obtained from previous research, the average unit weights were 122.0 pcf for lightweight concrete and 145.3 pcf for normal-weight concrete. The average modulus of elasticity values for lightweight concrete and normal-weight concrete were calculated as 1928 ksi and 5651 ksi, respectively. The average compressive strengths for lightweight concrete and normal-weight concrete were calculated as 7355 psi and 10,199 psi, respectively. The average splitting tensile strengths for lightweight concrete and normal-weight concrete were calculated as 610 psi and 753 psi, respectively. The average rapid chloride permeability values for lightweight concrete and normal-weight concrete were calculated as 550 C and 75 C, respectively, which correspond to chloride permeability classifications of "very low" and "negligible." The average absorption values for lightweight concrete and normal-weight concrete were calculated as 12.7 percent and 4.7 percent, respectively. The average chloride concentrations for lightweight concrete and normal-weight concrete to which an epoxy overlay had been applied, including bridges C-989 and F-792, were calculated as 5.5, 0.8, 0.4, and 0.4 lb Cl^-/yd^3 of concrete and 0.4, 0.4, 0.3, and 0.4 lb Cl^-/yd^3 of concrete, respectively, for depth intervals ending at 1, 2, 3, and 4 in. The average chloride concentrations for bridge C-1011, which did not have an epoxy overlay, were 27.7, 6.7, 0.6, and 0.4 lb Cl^-/yd^3 of concrete. While the efficacy of the epoxy overlay in preventing chloride ion ingress at bridge C-989 is apparent, the epoxy overlay originally placed at bridge F-792 had become compromised, allowing chloride ion ingress, and was replaced in 2023 just prior to this research. The average coefficients of thermal expansion for lightweight concrete in the dry and soaked conditions were calculated as $9.8x10^{-6}/°F$ and $9.6x10^{-6}/°F$, respectively, while corresponding values for normal-weight concrete were calculated as $8.9x10^{-6}/°F$ and $7.5x10^{-6}/°F$. While all three lightweight concrete cylinders exhibited degradation in freeze-thaw durability testing, one of the lightweight concrete samples reached the failure condition, defined as less than 60 percent stiffness retained in ASTM C666, between cycles 260 and 280. None of the normal-weight concrete cylinders exhibited degradation.

As a basis for discussion of the test results, ratios of values for lightweight concrete to values of normal-weight concrete were computed for selected properties, for which the normal-weight concrete approach slabs and the normal-weight concrete cores and cylinders were used as a baseline. While the selected properties necessarily exclude the results of visual inspection and chloride concentration, which were directly affected by the presence of an epoxy overlay on two of the bridges, they include resistivity, modulus of elasticity, compressive strength, splitting tensile strength, chloride permeability, absorption, coefficient of thermal expansion in the dry and soaked conditions, and stiffness retained after freeze-thaw durability testing. Overall, these data suggest that, compared to normal-weight concrete, lightweight concrete absorbs more water, allows higher rates of chloride ion ingress, is more susceptible to degradation under freeze-thaw cycling, and has lower resistance to cracking. As cracking occurs, the rates of potential degradation from water absorption, chloride ion ingress, and freeze-thaw cycling increase, and localized structural failure can eventually occur.

5.0 CONCLUSION

5.1 Summary

The objectives of this research were to document and compare properties of lightweight concrete and normal-weight concrete used for construction of bridge decks and approach slabs in northern Utah. The scope of work included field and laboratory testing to characterize concrete at three lightweight concrete bridge deck sites and the normal-weight concrete approach slabs at one of these sites, which were recommended by UDOT for evaluation, as well as laboratory testing to characterize concrete specimens obtained through previous research on lightweight and normal-weight concrete bridge decks.

The procedures for this research involved field and laboratory testing of lightweight and normal-weight concrete. Field testing included three bridge decks constructed using lightweight concrete and one of the adjacent normal-weight concrete approach slabs. Bridges C-989, C-1011, and F-792 were selected by UDOT personnel for evaluation in this research, and concrete samples from bridges C-993 and F-818, which were the focus of previous research, were also included.

For field testing, a portion of each bridge, typically the right or left lane and the adjacent shoulder, was closed to traffic, and five test locations were then selected for evaluation using a formal random sampling procedure to eliminate potential bias. A distress survey was performed at each test location, and then cover depth testing, Schmidt rebound hammer testing, resistivity testing, chloride concentration sampling, and coring were performed.

For laboratory testing, regarding samples obtained during the current research, modulus of elasticity testing, compressive strength testing, splitting tensile strength testing, rapid chloride permeability and absorption testing, and chloride concentration testing were performed. Regarding samples obtained from previous research, coefficient of thermal expansion testing and freeze-thaw durability testing were performed. In total, 20 concrete cores and 80 concrete powder samples were obtained from the field work performed during the current research, and six concrete cylinders were obtained from previous research. The unit weight of each concrete core or cylinder was measured prior to testing.

5.2 Findings

Results were obtained from both field and laboratory testing. The results are expected to be applicable to lightweight concrete bridge decks with similar construction and service conditions as those evaluated in this research. From field testing, the results of distress surveys, cover depth testing, Schmidt rebound hammer testing, and resistivity testing are presented for the lightweight concrete bridge decks and adjacent normal-weight concrete approach slabs that were evaluated in this research. The average crack density and crack width for all of the lightweight concrete bridges evaluated in this research were calculated as 0.0210 ft/ft^2 and 4 mils, respectively, while corresponding values for normal-weight concrete were calculated as 0.0046 ft/ft^2 and 10 mils. Given that an epoxy overlay was present at bridges C-989 and F-792, the values of crack density and crack width are relatively low compared to those measured in previous studies of concrete bridge decks having similar ages and service conditions; however, the percentages of scaling, map cracking, and delamination are typical. Average cover depths for the lightweight concrete bridge decks were calculated as 2.73 in. and 2.61 in. for the longitudinal and transverse reinforcement depths, respectively, and corresponding values for the normal-weight concrete were 3.20 in. and 3.37 in. For bridge C-1011, which was the only tested bridge that did not have an epoxy overlay, the average Schmidt rebound number and estimated compressive strength were calculated as 51 and 7840 psi, respectively. The average resistivity values for lightweight concrete and normal-weight concrete were calculated as 28.7 and 38.0, respectively, which both correspond to a corrosion potential classification of "low."

From laboratory testing, the results of modulus of elasticity, compressive strength, splitting tensile strength, rapid chloride permeability and absorption, chloride concentration, coefficient of thermal expansion, and freeze-thaw durability testing are presented. Regarding samples obtained during the current research, the average unit weights were 116.8 pcf for lightweight concrete and 136.1 pcf for normal-weight concrete. Regarding samples obtained from previous research, the average unit weights were 122.0 pcf for lightweight concrete and 145.3 pcf for normal-weight concrete. The average modulus of elasticity values for lightweight concrete and normal-weight concrete were calculated as 1928 ksi and 5651 ksi, respectively. The average compressive strengths for lightweight concrete and normal-weight concrete were calculated as 7355 psi and 10,199 psi, respectively. The average splitting tensile strengths for lightweight concrete and normal-weight concrete were calculated as 610 psi and 753 psi, respectively. The average rapid chloride permeability values for lightweight concrete and normal-weight concrete were calculated as 550 C and 75 C, respectively, which correspond to chloride permeability classifications of "very low" and "negligible." The average absorption values for lightweight concrete and normal-weight concrete were calculated as 12.7 percent and 4.7 percent, respectively. The average chloride concentrations for lightweight concrete and normal-weight concrete to which an epoxy overlay had been applied, including bridges C-989 and F-792, were calculated as 5.5, 0.8, 0.4, and 0.4 lb Cl^-/yd^3 of concrete and 0.4, 0.4, 0.3, and 0.4 lb Cl^-/yd^3 of concrete, respectively, for depth intervals ending at 1, 2, 3, and 4 in. The average chloride concentrations for bridge C-1011, which did not have an epoxy overlay, were 27.7, 6.7, 0.6, and 0.4 lb Cl^-/yd^3 of concrete. While the efficacy of the epoxy overlay in preventing chloride ion ingress at bridge C-989 is apparent, the epoxy overlay originally placed at bridge F-792 had become compromised, allowing chloride ion ingress, and was replaced in 2023 just prior to this research. The average coefficients of thermal expansion for lightweight concrete in the dry and soaked conditions were calculated as $9.8 \times 10^{-6}/°F$ and $9.6 \times 10^{-6}/°F$, respectively, while corresponding values for normal-weight concrete were calculated as $8.9 \times 10^{-6}/°F$ and $7.5 \times 10^{-6}/°F$. While all three lightweight concrete cylinders exhibited degradation in freeze-thaw durability testing, one of the lightweight concrete samples reached the failure condition, defined as less than 60 percent stiffness retained in ASTM C666, between cycles 260 and 280. None of the normal-weight concrete cylinders exhibited degradation.

As a basis for discussion of the test results, ratios of values for lightweight concrete to values of normal-weight concrete were computed for selected properties, for which the normal-weight concrete approach slabs and the normal-weight concrete cores and cylinders were used as a baseline. While the selected properties necessarily exclude the results of visual inspection and chloride concentration, which were directly affected by the presence of an epoxy overlay on two of the bridges, they include resistivity, modulus of elasticity, compressive strength, splitting tensile strength, chloride permeability, absorption, coefficient of thermal expansion in the dry and soaked conditions, and stiffness retained after freeze-thaw durability testing. Overall, these data suggest that, compared to normal-weight concrete, lightweight concrete absorbs more water, allows higher rates of chloride ion ingress, is more susceptible to degradation under freeze-thaw cycling, and has lower resistance to cracking. As cracking occurs, the rates of potential degradation from water absorption, chloride ion ingress, and freeze-thaw cycling increase, and localized structural failure can eventually occur.

5.3 Recommendations

Several recommendations based on the results of this research and information obtained from the literature were developed. To potentially improve the performance of sand-lightweight concrete, use of smaller lightweight coarse aggregate particles may be appropriate to increase concrete strength and reduce the occurrence of degradation under freeze-thaw cycling (Ramirez et al., 2000). In addition, as long as the resulting unit weight is sufficiently low, use of a blend of lightweight coarse aggregate and normal-weight coarse aggregate may improve the performance of lightweight concrete (Ozyildirim, 2009). If permitted, rather than sand-lightweight concrete, lightweight fine aggregate and normal-weight coarse aggregate could also be considered. Another approach could be to increase the quality and/or volume of paste in lightweight concrete mixtures to compensate for the comparatively low strength of the lightweight coarse aggregate particles (Kosmatka and Wilson, 2016). Use of fibers in lightweight concrete mixtures to inhibit widening of cracks may further reduce the occurrence of localized structural failures when cracking occurs (Mindess et al., 2003). Applying a thin-bonded epoxy overlay or similar product to seal the surface of the deck against water and chloride ion ingress is recommended as soon as possible after construction of lightweight concrete bridge decks and approach slabs, and the overlay should be replaced before it is compromised (Waters Emery et al., 2020). During construction of lightweight concrete bridge decks and approach slabs, a high level of quality control should be implemented to avoid surface grinding for the purposes of meeting profile requirements because the lightweight aggregate exposed by grinding may then allow accelerated chloride ion ingress through aggregate pore connectivity in the absence of an overlay (Wagner, 2015). Use of lightweight concrete mixtures may also be restricted to regions that do not experience freezing conditions.

Further research is recommended to evaluate the freeze-thaw durability and other relevant properties of lightweight concrete mixtures involving smaller coarse aggregate particles, a blend of lightweight coarse aggregate and normal-weight coarse aggregate, use of lightweight fine aggregate and normal-weight coarse aggregate, improved paste quality and/or volume, fibers, and/or other improvements. Furthermore, petrographic analyses of samples of lightweight concrete bridge decks that exhibit premature degradation may be appropriate to examine the possibility of secondary deposits, including ettringite and salts that may partially infill entrained air voids and other voids in the paste and coarse aggregate. Finally, performing structural analyses of a typical lightweight concrete bridge deck section to evaluate critical compressive and tensile stresses is recommended.

REFERENCES

ACI (American Concrete Institute). 2003. *Guide for structural lightweight aggregate concrete*. ACI 213R-03. ACI, Farmington Hills, MI.

Barrus, N. C. 2012. *Sensitivity of resistivity measurements on concrete bridge decks to operator-controlled and concrete material variables*. M.S. thesis. Provo, UT: Brigham Young University.

Bender, B. F. 1980. "Economics and use of lightweight concrete in prestressed structures." *Prestressed Concrete Institute (PCI)*, 25 (6), 62–67.

Byard, B. E., and A. K. Schindler. 2010. *Cracking tendency of lightweight concrete*. Research report. Herbert Engineering Center, Auburn University, Auburn, AL.

Castrodale, R. 2021. *Lightweight concrete bridge design primer*. FHWA-HIF-19-067. U.S. Dept. of Transportation, Federal Highway Administration, Washington, DC.

Cavalline, T. L., A. M. Kitts, and J. T. Calamusa. 2013. *Durability of lightweight concrete bridge decks – Field evaluation*. Rep. No. FHWA/NC/2011-06. North Carolina Department of Transportation, Raleigh, NC.

Cavalline, T. L., A. M. Kitts, J. T. Calamusa, and B. Q. Tempest. 2017. "Field-observed cracking of paired lightweight and normalweight concrete bridge decks." *Int. J. Concr. Struct. Mater.*, 11, 85–97.

Cui, H. Z., T. Y. Lo, S. A. Memon, and W. Xu. 2012. "Effect of lightweight aggregates on the mechanical properties and brittleness of lightweight aggregate concrete." *Constr. Build. Mater.*, 35, 149–158.

Delatte, N., D. Crowl, and E. Mack. 2007. “Reducing cracking of high performance concrete bridge decks.” Proceedings of Transportation Research Board 86th Annual Meeting. Washington, DC: TRB.

EPA (Environmental Protection Agency). 1993. “Lightweight aggregate manufacturing.” *Emission Factor Documentation for AP-42*, 5th ed., Vol.1, Sec. 11.20. EPA, Washington, DC, 1–39. EPA. https://www.epa.gov/sites/default/files/2020-10/documents/b11s20.pdf.

ESCSI (Expanded Shale, Clay, and Slate Institute). 1971. *Lightweight concrete: History, applications, economics*. ESCSI, Chicago, IL.

Guthrie, W. S., and R. S. Tuttle. 2006. *Condition analysis of concrete bridge decks in Utah*. Rep. UT-06-01. Utah Department of Transportation, Salt Lake City, UT.

Guthrie, W. S., S. L. Frost, A. W. Birdsall, E. T. Linford, L. A. Ross, R. A. Crane, and D. L. Eggett. 2006. “Effect of stay-in-place metal forms on performance of concrete bridge decks.” *Transp. Res. Rec*., 1958, 33–41.

Guthrie, W. S., T. Waters, and G. B. Reese. 2015. “Comparison of moisture content and electrical conductivity of lightweight and normal-weight concrete bridge decks: Instrumentation and monitoring.” *Proc., 16th International Conference on Cold Regions Engineering*, American Society of Civil Engineers, July 19–22, 2015, Salt Lake City, UT, 346–357.

Hema, J., W. S. Guthrie, and F. S. Fonseca. 2004. *Concrete bridge deck condition assessment and improvement strategies*. Report UT-04-16. Utah Department of Transportation, Salt Lake City, UT.

Hoff, G. C. 2002. *Guide for the use of low-density concrete in civil works projects*. ERDC/GSL TR-02-13 (TR INP-02-7). U.S. Army Corp of Engineers, Washington, DC.

Holm, T. A., and J. P. Ries. 2000. *Specified density concrete: A transition for the concrete industry*. ESCSI, Chicago, IL.

Holm, T. A., and J. P. Ries. 2006. “Chapter 46: Lightweight concrete and aggregates.” *Significance of tests and properties of concrete and concrete-making materials*, STP169D-EB, American Society for Testing and Materials, Philadelphia, PA.

Holm, T. A., and J. P. Ries. 2007. *Reference manual for the properties and applications of expanded shale, clay and slate lightweight aggregate*. ESCSI, Chicago, IL.

Kim, H. K., and H. K. Lee. 2010. “Acoustic absorption modeling of porous concrete considering the gradation and shape of aggregates and void ratio.” *Journal of Sound and Vibration*, 329 (7), 866–879.

Kosmatka, S. H., and M. L. Wilson. 2016. *Design and control of concrete mixtures*. 16th ed. Portland Cement Association, Skokie, IL.

Lo, T. Y., W. C. Tang, and H. Z. Cui. 2007. “The effects of aggregate properties on lightweight concrete.” *Building and Environment*, 42 (8), 3025–3029.

Lo, T. Y., W. C. Tang, H. Z. Cui, and C. E. Leung. 2008. “The effect of aggregate absorption on pore area at interfacial zone of lightweight concrete.” *Constr. Build. Mater.*, 22 (4), 623-628.

Lopez, M., L. F. Kahn, K. E. Kurtis, and J. S. Lai. 2003. *Creep, shrinkage, and prestress losses of high-performance lightweight concrete*. Rep. No. 03-11. Office of Materials and Research, Georgia Department of Transportation, Atlanta, GA.

Miller, J. S., and W. Y. Bellinger. 2014. *Distress identification manual for the long-term pavement performance program.* Rep. FHWA-HRT-13-092. Office of Infrastructure Research and Development, Federal Highway Administration, McLean, VA.

Mindess, S., J. Young, and D. Darwin. 2003. *Concrete*. 2nd ed. Pearson Education, Upper Saddle River, NJ.

NRMCA (National Ready Mixed Concrete Association). 2016. *What, why, and how? Structural lightweight concrete*. CIP 36. Concrete in Practice, NRMCA, Silver Spring, MD.

Ozyildirim, H. C. 2009. *Evaluation of lightweight high performance concrete in bulb-T beams and decks in two bridges on Route 33 in Virginia*. Rep. 09-R22. Virginia Transportation Research Council,
Charlottesville, VA.

Ramirez, J., J. Olek, E. Rolle, and B. Malone. 2000. Performance of bridge decks and girders with lightweight aggregate concrete. Rep. FHWA/IN/JTRP-98/17. West Lafayette, IN: Joint Transportation Research Program, Purdue University.

Russell, H. G., R. A. Miller, H. C. Ozyildirim, and M. K. Tadros. 2006. *Compilation and evaluation of results from high-performance concrete bridge projects, Vol. 1: Final Report*. Rep. No. FHWA-HRT-05-056. Federal Highway Administration, McLean, VA.

Short, A., and W. Kinniburgh. 1978. *Lightweight concrete*. Applied Science Publishers, London, UK.

Sims, I., J. Lay, and J. Ferrari. 2019. "15–Concrete aggregates." Lea's Chemistry of Cement and Concrete, 5th Ed., P. C. Hewlett, and M. Liska, Eds. Amsterdam, Netherlands: Butterworth-Heinemann, Elsevier.

Wagner, A. M. 2015. *Durability of lightweight concrete for bridge decks*. M.S. thesis. Knoxville, TN: University of Tennessee.

Waters Emery, T., H. Polanco, and W. S. Guthrie. 2020. *Development of a management guide for concrete bridge decks in Utah*. Rep. UT-20.28. UDOT, Salt Lake City, UT.

Zhutovsky, S., and K. Kovler. 2002. "Efficiency of lightweight aggregates for internal curing of high strength concrete to eliminate autogenous shrinkage." *Mat. Struct*., 35, 97–101.

APPENDIX A: CONCRETE MIXTURE DESIGNS

Table A.1 Mixture Design for Lightweight Concrete Deck at Bridge C-989

Materials	Weight (lb)	Specific Gravity
Cement	544	3.15
Class F Fly Ash	136	2.30
Water	284	1.00
Lightweight Coarse Aggregate	1152	1.78
Fine Aggregate	1119	2.58
Percent Air (Design)	6.00	0.00
Total	3235	-
Unit Weight (lb/ft^3)	119.9	
Slump (in.)	9.00	
Percent Air (Actual)	5.75	
Design Water-Cementitious Materials Ratio	0.42	
Maximum Aggregate Size (in.)	0.75	

Table A.2 Mixture Design for Lightweight Concrete Deck at Bridge C-1011

Materials	Weight (lb)	Specific Gravity
Cement	544	3.15
Class F Fly Ash	136	2.30
Water	275	1.00
Lightweight Coarse Aggregate	1080	1.79
Fine Aggregate	1220	2.53
Percent Air (Design)	6.00	0.00
Total	3255	-
Unit Weight (lb/ft^3)	119.5	
Slump (in.)	8.00	
Percent Air (Actual)	6.25	
Design Water-Cementitious Materials Ratio	0.40	
Maximum Aggregate Size (in.)	0.75	

Table A.3 Mixture Design for Lightweight Concrete Deck at Bridge F-792

Materials	Weight (lb)	Specific Gravity
Cement	564	3.15
Class F Fly Ash	141	2.30
Water	310	1.00
Lightweight Coarse Aggregate	1092	1.77
Fine Aggregate	1069	2.60
Percent Air (Design)	6.30	0.00
Total	3176	-
Unit Weight (lb/ft^3)	117.2	
Slump (in.)	2.50	
Percent Air (Actual)	5.75	
Design Water-Cementitious Materials Ratio	0.44	
Maximum Aggregate Size (in.)	-	

Table A.4 Mixture Design for Normal-Weight Concrete Approach Slabs at Bridge C-989

Materials	Weight (lb)	Specific Gravity
Cement	526	3.15
Class F Fly Ash	132	2.30
Water	263	1.00
Coarse Aggregate	1508	2.59
Medium Aggregate	150	2.59
Fine Aggregate	1179	2.58
Percent Air (Design)	6.00	0.00
Total	3758	-
Unit Weight (lb/ft^3)	138.5	
Slump (in.)	9.00	
Percent Air (Actual)	7.30	
Design Water-Cementitious Materials Ratio	0.40	
Maximum Aggregate Size (in.)	1.00	

APPENDIX B: SUPPORTING DATA

In the distress surveys, crack widths are indicated in mm (1 mm = 39.4 mils).

Table B.1 Distress Data

Bridge Identifier	Concrete Type	Distress Type	Location 1	Location 2	Location 3	Location 4	Location 5
C-989	Lightweight	0.15-mm Cracking (ft)	0.0	0.0	0.0	4.9	10.8
		0.20-mm Cracking (ft)	0.0	1.1	0.0	0.0	3.2
		0.25-mm Cracking (ft)	0.0	2.9	0.0	0.0	0.4
		0.30-mm Cracking (ft)	0.0	0.0	0.0	6.5	4.3
		0.33-mm Cracking (ft)	0.0	0.0	0.0	0.0	0.0
		0.40-mm Cracking (ft)	0.0	0.7	0.0	0.0	0.0
		0.50-mm Cracking (ft)	0.0	0.0	0.0	0.0	0.0
		0.60-mm Cracking (ft)	0.0	0.0	0.0	0.0	0.0
		0.80-mm Cracking (ft)	0.0	0.0	0.0	0.0	0.0
		Scaling (ft^2)	0.0	0.0	0.0	0.0	0.0
		Map Cracking (ft^2)	0.0	0.0	0.0	0.0	0.0
		Delamination (ft^2)	0.0	0.0	0.0	0.0	0.0
		Construction Issues (ft^2)	0.3	0.0	0.0	0.0	0.0
C-1011	Lightweight	0.15-mm Cracking (ft)	0.8	10.6	6.5	12.6	14.9
		0.20-mm Cracking (ft)	6.2	12.4	7.7	6.4	38.7
		0.25-mm Cracking (ft)	6.5	0.0	2.9	11.3	14.0
		0.30-mm Cracking (ft)	14.4	0.0	0.0	2.3	10.1
		0.33-mm Cracking (ft)	4.9	0.0	0.0	0.0	6.9
		0.40-mm Cracking (ft)	14.8	0.0	0.0	0.0	7.4
		0.50-mm Cracking (ft)	9.5	0.0	0.0	0.0	1.2
		0.60-mm Cracking (ft)	5.6	0.0	0.0	0.0	0.0
		0.80-mm Cracking (ft)	1.7	0.0	0.0	0.0	1.4
		Scaling (ft^2)	27.8	53.6	35.1	6.5	24.1
		Map Cracking (ft^2)	69.8	51.0	0.0	17.2	64.1
		Delamination (ft^2)	0.0	0.0	0.0	0.0	0.0
		Construction Issues (ft^2)	0.0	0.0	0.0	0.0	0.0
F-792	Lightweight	0.15-mm Cracking (ft)	0.0	0.0	0.0	0.0	0.0
		0.20-mm Cracking (ft)	0.0	0.0	0.0	0.0	0.0
		0.25-mm Cracking (ft)	0.0	0.0	0.0	0.0	0.0
		0.30-mm Cracking (ft)	0.0	0.0	0.0	0.0	0.0
		0.33-mm Cracking (ft)	0.0	0.0	0.0	0.0	0.0
		0.40-mm Cracking (ft)	0.0	0.0	0.0	0.0	0.0
		0.50-mm Cracking (ft)	0.0	0.0	0.0	0.0	0.0
		0.60-mm Cracking (ft)	0.0	0.0	0.0	0.0	0.0
		0.80-mm Cracking (ft)	0.0	0.0	0.0	0.0	0.0
		Scaling (ft^2)	0.0	0.0	0.0	0.0	0.0
		Map Cracking (ft^2)	0.0	0.0	0.0	0.0	0.0
		Delamination (ft^2)	0.0	0.0	0.0	0.9	1.5
		Construction Issues (ft^2)	0.0	0.0	0.0	0.0	0.0
C-989	Normal-Weight	0.15-mm Cracking (ft)	0.0	0.0	0.0	2.8	1.7
		0.20-mm Cracking (ft)	3.0	1.1	2.0	0.0	2.2
		0.25-mm Cracking (ft)	0.0	0.0	0.0	2.4	2.1
		0.30-mm Cracking (ft)	3.6	2.8	0.0	1.6	1.1
		0.33-mm Cracking (ft)	0.0	0.0	0.0	0.0	0.0
		0.40-mm Cracking (ft)	1.2	0.0	0.0	11.3	0.0
		0.50-mm Cracking (ft)	0.0	0.0	0.0	0.0	0.5
		0.60-mm Cracking (ft)	0.0	0.0	0.0	0.0	0.0
		0.80-mm Cracking (ft)	0.0	0.0	0.0	0.0	0.0
		Scaling (ft^2)	0.0	0.0	0.0	0.0	0.0
		Map Cracking (ft^2)	0.0	0.0	0.0	0.0	0.0
		Delamination (ft^2)	0.0	0.0	0.3	0.0	0.0
		Construction Issues (ft^2)	0.0	0.0	0.0	0.0	0.0

Table B.2 Cover Depth Data

Bridge Identifier	Concrete Type	Cover Depth (in.)				
		Location 1	Location 2	Location 3	Location 4	Location 5
Longitudinal Reinforcement						
C-989	Lightweight	2.21	3.06	2.83	3.55	2.84
		2.06	3.01	2.57	3.75	2.48
		1.92	2.85	2.55	3.69	2.59
		2.12	2.78	2.81	3.53	2.95
		2.20	3.02	2.81	3.54	2.84
		2.13	2.96	2.55	3.71	2.55
C-1011	Lightweight	2.33	2.22	2.27	2.36	2.41
		2.33	2.46	2.45	2.41	2.47
		2.45	2.38	2.37	2.43	2.45
		2.43	2.41	2.31	2.34	2.55
		2.29	2.37	2.18	2.35	2.72
		2.35	2.37	2.23	2.41	2.74
F-792	Lightweight	2.98	2.89	3.02	3.39	2.60
		2.97	3.06	3.13	3.17	3.00
		2.88	2.98	3.02	3.12	3.16
		3.02	2.85	2.84	3.30	2.62
		3.10	2.64	2.84	3.27	2.57
		3.15	2.71	3.11	3.22	2.98
C-989	Normal-Weight	3.24	4.19	3.24	3.05	2.74
		3.04	4.33	3.48	3.03	2.61
		2.25	3.60	3.08	4.05	2.81
		2.15	3.48	2.98	3.93	2.80
		2.28	3.55	3.22	3.16	3.75
		2.14	3.55	3.28	3.31	3.69
Transverse Reinforcement						
C-989	Lightweight	1.69	2.75	2.30	3.29	2.90
		1.67	2.84	2.31	3.32	2.83
		1.67	2.81	2.60	3.28	2.52
		1.60	2.93	2.62	3.24	2.48
		2.39	2.85	2.33	3.41	2.41
		2.39	2.94	2.34	3.35	2.46
C-1011	Lightweight	2.37	2.36	2.21	2.39	2.48
		2.37	2.22	2.23	2.38	2.50
		2.37	2.32	2.26	2.41	2.46
		2.36	2.28	2.30	2.38	2.36
		2.33	2.32	2.28	2.41	2.44
		2.34	2.30	2.22	2.48	2.51
F-792	Lightweight	2.91	2.67	2.72	3.20	2.62
		2.82	2.61	2.87	3.18	2.60
		2.92	2.75	2.70	3.20	2.66
		2.85	2.70	2.74	3.15	2.72
		2.85	2.80	2.87	3.15	2.65
		2.88	2.84	2.87	3.13	2.74
C-989	Normal-Weight	2.88	3.48	3.54	3.52	3.32
		2.86	3.60	3.48	3.49	3.48
		2.83	3.63	3.65	3.57	3.31
		2.92	3.81	3.85	3.62	3.34
		2.07	3.69	4.09	3.53	3.00
		1.97	3.85	3.93	3.62	3.15

Table B.3 Schmidt Rebound Number and Estimated Compressive Strength Data

Bridge Identifier	Concrete Type	Test Location	Schmidt Rebound Number 1	2	3	Average	Estimated Compressive Strength (psi)
C-1011	Lightweight	1	50	49	49	49	7500
		2	49	54	51	51	7900
		3	50	50	49	50	7800
		4	54	51	50	52	8100
		5	48	55	49	51	7900

Table B.4 Resistivity Data

Bridge Identifier	Concrete Type	Test Location	Resistivity (kohm-in.) for Indicated Location 1	2	Average	1	2	Average	Average Resistivity (kohm-in.)	Surface Temperature (°F)
C-989	Lightweight	1	31.4	31.2	31.3	36.4	36.5	36.4	33.9	78
		2	37.2	37.2	37.2	37.6	37.5	37.5	37.4	72
		3	37.6	37.6	37.6	37.7	37.7	37.7	37.6	70
		4	29.4	29.0	29.2	26.8	26.8	26.8	28.0	69
		5	37.3	37.3	37.3	37.6	37.6	37.6	37.5	74
C-1011	Lightweight	1	19.6	19.6	19.6	29.8	29.8	29.8	24.7	62
		2	30.9	30.6	30.8	28.6	28.5	28.6	29.7	65
		3	19.3	19.2	19.2	22.7	22.4	22.6	20.9	74
		4	21.1	20.9	21.0	23.5	23.3	23.4	22.2	68
		5	28.3	28.0	28.1	35.9	35.8	35.9	32.0	72
F-792	Lightweight	1	28.0	27.9	27.9	31.8	31.7	31.8	29.8	69
		2	36.0	35.9	36.0	31.5	31.4	31.5	33.7	69
		3	37.6	37.5	37.5	37.3	37.3	37.3	37.4	71
		4	12.8	12.8	12.8	15.3	15.1	15.2	14.0	75
		5	11.1	11.1	11.1	11.2	11.2	11.2	11.1	77
C-989	Normal-Weight	1	37.4	37.4	37.4	37.0	37.0	37.0	37.2	91
		2	38.1	38.2	38.2	37.7	37.6	37.7	37.9	87
		3	38.7	38.7	38.7	39.1	39.1	39.1	38.9	90
		4	37.6	37.7	37.7	36.8	36.8	36.8	37.2	84
		5	38.1	38.1	38.1	39.3	39.3	39.3	38.7	86

Table B.5 Modulus of Elasticity Data

Bridge Identifier	Concrete Type	Sample	Length (in.)					Diameter (in.)					Weight (lb)	Unit Weight (lb/ft^3)	Frequency (Hz)	Modulus of Elasticity (ksi)
			1	2	3	4	Average	1	2	3	4	Average				
C-989	Lightweight	1	5.235	5.236	5.292	5.261	5.256	4.028	4.033	4.030	4.031	4.031	4.637	119.5	10094.8	2015
		2	3.901	3.882	3.933	3.918	3.909	4.027	4.025	4.028	4.027	4.027	3.408	118.3	14161.6	2171
		3	5.801	5.796	5.822	5.793	5.803	4.031	4.028	4.028	4.035	4.031	5.114	119.4	8671.7	1811
		4	4.621	4.603	4.621	4.616	4.615	4.024	4.027	4.023	4.030	4.026	4.158	122.3	11818.9	2180
		5	5.395	5.319	5.371	5.356	5.360	4.027	4.027	4.026	4.027	4.027	4.724	119.6	9550.5	1877
C-1011	Lightweight	1	5.043	5.000	5.017	5.035	5.024	4.015	4.015	4.020	4.014	4.016	3.682	115.4	10569.9	1949
		2	5.212	5.225	5.238	5.220	5.224	4.031	4.034	4.030	4.029	4.031	3.637	113.6	9809.9	1786
		3	4.826	4.849	4.882	4.886	4.861	4.023	4.025	4.021	4.023	4.023	4.339	115.3	11215.0	2052
		4	2.716	2.728	2.722	2.713	2.720	4.004	4.009	4.007	4.006	4.007	4.717	117.4	18342.4	1750
		5	2.596	2.595	2.584	2.561	2.584	4.016	4.018	4.016	4.019	4.017	2.091	115.9	19085.3	1688
F-792	Lightweight	1	4.379	4.317	4.340	4.367	4.351	4.028	4.033	4.028	4.027	4.029	4.249	114.7	12843.9	2146
		2	4.222	4.219	4.249	4.283	4.243	4.029	4.029	4.026	4.027	4.028	4.381	116.2	13165.9	2173
		3	5.230	5.213	5.179	5.182	5.201	4.027	4.029	4.029	4.024	4.027	4.122	113.2	10032.0	1846
		4	5.465	5.473	5.504	5.523	5.491	4.028	4.026	4.031	4.027	4.028	2.329	116.5	9408.6	1863
		5	2.541	2.480	2.444	2.467	2.483	4.022	4.025	4.023	4.025	4.024	2.196	114.4	19531.3	1612
C-989	Normal-Weight	1	6.635	6.634	6.635	6.653	6.639	4.022	4.023	4.028	4.021	4.024	6.696	137.1	12719.6	5856
		2	6.875	6.837	6.892	6.850	6.864	4.021	4.020	4.022	4.023	4.022	6.887	136.5	12169.2	5705
		3	7.246	7.227	7.251	7.275	7.250	4.015	4.017	4.022	4.021	4.019	7.200	135.3	11387.9	5525
		4	7.215	7.219	7.227	7.240	7.225	4.030	4.029	4.030	4.028	4.029	7.282	136.6	11507.8	5657
		5	5.931	5.896	5.872	5.891	5.898	4.030	4.031	4.028	4.028	4.025	5.872	135.2	13984.4	5510

Table B.6 Compressive Strength Data

Bridge Identifier	Concrete Type	Test Location	Length (in.)			Diameter (in.)			Weight (lb)	Unit Weight (lb/ft^3)	Force (lb)	Compressive Strength (psi)
			1	2	Average	1	2	Average				
C-989	Lightweight	3	5.794	5.802	5.798	4.027	4.027	4.027	4.955	116.0	94320	7407
		5	5.377	5.367	5.372	4.030	4.028	4.029	4.942	124.7	97230	7628
C-1011	Lightweight	1	5.019	5.008	5.013	4.025	4.020	4.022	4.102	111.3	87610	6895
		2	5.223	5.219	5.221	4.000	4.017	4.008	4.261	111.8	89895	7124
F-792	Lightweight	3	5.194	5.225	5.209	4.026	4.022	4.024	4.182	109.1	89515	7040
		4	5.507	5.495	5.501	4.024	4.026	4.025	4.547	112.3	102265	8038
C-989	Normal-Weight	2	7.274	7.276	7.275	4.035	4.015	4.025	7.113	132.8	129675	10193
		4	7.233	7.222	7.227	4.027	4.026	4.027	7.200	135.2	129960	10206

Table B.7 Splitting Tensile Strength Data

Bridge Identifier	Concrete Type	Test Location	Length (in.)			Diameter (in.)			Weight (lb)	Unit Weight (lb/ft^3)	Force (lb)	Splitting Tensile Strength (psi)
			1	2	Average	1	2	Average				
C-989	Lightweight	2	3.888	3.911	3.899	4.024	4.024	4.024	3.292	114.7	15505	629
		4	2.317	2.312	2.315	4.027	4.027	4.027	1.955	114.6	7165	489
C-1011	Lightweight	3	2.560	2.502	2.531	4.035	4.024	4.029	2.028	108.6	8090	505
		5	2.545	2.520	2.532	4.014	4.007	4.010	2.098	113.4	12700	796
F-792	Lightweight	1	2.045	2.029	2.037	4.007	4.015	4.011	1.659	111.4	7895	615
		5	2.457	2.510	2.483	4.026	4.025	4.025	1.990	108.8	9805	625
C-989	Normal-Weight	1	4.348	4.337	4.342	4.038	4.009	4.023	4.298	134.5	22680	826
		2	4.579	4.513	4.546	4.029	4.022	4.025	4.492	134.2	19540	680

Table B.8 Chloride Permeability and Absorption Data

Bridge Identifier	Concrete Type	Test Location	Length (in.)			Diameter (in.)			Dry Weight (lb)	Soaked Weight (lb)	Unit Weight (lb/ft^3)	Chloride Permeability (C)	Absorption (%)
			1	2	Average	1	2	Average					
C-989	Lightweight	1	2.125	2.141	2.133	4.028	4.032	4.030	1.714	1.922	108.9	499	12.1
		4	2.071	2.088	2.079	4.027	4.028	4.027	1.672	1.908	109.1	1083	14.1
C-1011	Lightweight	3	2.077	2.071	2.074	4.021	4.024	4.023	1.598	1.803	104.8	421	12.9
		4	2.064	2.089	2.076	4.006	4.005	4.005	1.613	1.827	106.6	805	13.2
F-792	Lightweight	1	2.094	2.065	2.079	4.026	4.026	4.026	1.578	1.764	103.0	239	11.8
		2	2.008	2.067	2.037	4.026	4.032	4.029	1.569	1.756	104.4	255	11.9
C-989	Normal-Weight	1	2.070	2.081	2.075	4.022	4.019	4.021	1.976	2.067	129.6	67	4.6
		2	2.008	2.084	2.046	4.023	4.019	4.021	1.946	2.038	129.4	82	4.7

Table B.9 Chloride Concentration Data

Bridge Identifier	Concrete Type	Test Location	Chloride Percent (%) at Indicated Depth Interval (in.)				Average Unit Weight (lb/ft^3)	Chloride Concentration ($lb\ Cl^-/yd^3$ Concrete) at Indicated Depth Interval (in.)			
			0-1	1-2	2-3	3-4		0-1	1-2	2-3	3-4
C-989	Lightweight	1	0.061	0.013	0.015	0.017	119.8	2.0	0.4	0.5	0.6
		2	0.059	0.015	0.015	0.016		1.9	0.5	0.5	0.5
		3	0.018	0.016	0.015	0.011		0.6	0.5	0.5	0.4
		4	0.024	0.009	0.001	0.003		0.8	0.3	0.0	0.1
		5	0.041	0.009	0.011	0.009		1.3	0.3	0.4	0.3
C-1011	Lightweight	1	0.799	0.094	0.018	0.013	115.0	24.8	2.9	0.6	0.4
		2	0.853	0.206	0.021	0.016		26.5	6.4	0.7	0.5
		3	0.863	0.268	0.021	0.018		26.8	8.3	0.6	0.5
		4	1.061	0.337	0.023	0.018		32.9	10.5	0.7	0.6
		5	0.880	0.171	0.013	0.010		27.3	5.3	0.4	0.3
F-792	Lightweight	1	0.315	0.020	0.011	0.013	115.5	9.8	0.6	0.3	0.4
		2	0.150	0.013	0.013	0.015		4.7	0.4	0.4	0.5
		3	0.227	0.015	0.011	0.003		7.1	0.5	0.3	0.1
		4	0.524	0.100	0.017	0.012		16.4	3.1	0.5	0.4
		5	0.353	0.031	0.017	0.016		11.0	1.0	0.5	0.5
C-989	Normal-Weight	1	0.012	0.012	0.009	0.010	136.1	0.5	0.5	0.3	0.4
		2	0.010	0.010	0.010	0.010		0.4	0.4	0.4	0.4
		3	0.011	0.011	0.010	0.010		0.4	0.4	0.4	0.4
		4	0.011	0.011	0.009	0.012		0.4	0.4	0.3	0.4
		5	0.007	0.007	0.008	0.012		0.2	0.2	0.3	0.4

Table B.10 Dry Coefficient of Thermal Expansion Data

Bridge Identifier	Concrete Type	Sample	Length at 0°F (in.)				Length at 72.5°F (in.)				Length at 140°F (in.)				Dry Coefficient of Thermal Expansion (/°F)		
			1	2	3	Average	1	2	3	Average	1	2	3	Average	0°F to 72.5°F	72.5°F to 140°F	Average
C-993	Lightweight	1	7.982	7.995	7.997	7.991	7.984	7.999	7.999	7.994	7.988	8.004	8.003	7.998	$8.0x10^{-6}$	$14.3x10^{-6}$	$11.2x10^{-6}$
		2	7.932	7.928	7.917	7.926	7.935	7.930	7.921	7.929	7.938	7.924	7.935	7.932	$9.6x10^{-6}$	$12.2x10^{-6}$	$10.9x10^{-6}$
		3	7.944	7.926	7.934	7.935	7.948	7.937	7.928	7.938	7.939	7.929	7.950	7.939	$9.0x10^{-6}$	$5.9x10^{-6}$	$7.4x10^{-6}$
F-818	Normal-Weight	1	7.879	7.902	7.895	7.892	7.884	7.905	7.901	7.896	7.885	7.903	7.906	7.898	$14.2x10^{-6}$	$5.6x10^{-6}$	$7.6x10^{-6}$
		2	7.930	7.930	7.944	7.934	7.933	7.935	7.947	7.938	7.936	7.948	7.935	7.940	$11.9x10^{-6}$	$5.3x10^{-6}$	$8.5x10^{-6}$
		3	7.854	7.825	7.835	7.838	7.857	7.830	7.839	7.842	7.860	7.842	7.830	7.844	$12.3x10^{-6}$	$8.3x10^{-6}$	$10.3x10^{-6}$

Table B.11 Soaked Coefficient of Thermal Expansion Data

Bridge Identifier	Concrete Type	Sample	Length at 0°F (in.)				Length at 72.5°F (in.)				Length at 140°F (in.)				Soaked Coefficient of Thermal Expansion (/°F)		
			1	2	3	Average	1	2	3	Average	1	2	3	Average	0°F to 72.5°F	72.5°F to 140°F	Average
C-993	Lightweight	1	7.986	7.998	7.999	7.995	7.989	8.004	8.005	7.999	7.992	8.004	8.006	8.001	$13.8x10^{-6}$	$5.4x10^{-6}$	$9.6x10^{-6}$
		2	7.937	7.930	7.920	7.929	7.939	7.932	7.923	7.931	7.941	7.936	7.925	7.934	$6.5x10^{-6}$	$8.5x10^{-6}$	$7.5x10^{-6}$
		3	7.947	7.928	7.937	7.937	7.951	7.930	7.940	7.940	7.953	7.933	7.943	7.943	$7.9x10^{-6}$	$11.0x10^{-6}$	$9.4x10^{-6}$
F-818	Normal-Weight	1	7.884	7.902	7.898	7.895	7.885	7.907	7.903	7.899	7.888	7.906	7.904	7.899	$12.2x10^{-6}$	$2.9x10^{-6}$	$7.6x10^{-6}$
		2	7.931	7.932	7.945	7.936	7.935	7.935	7.949	7.940	7.937	7.936	7.950	7.941	$13.1x10^{-6}$	$3.9x10^{-6}$	$8.5x10^{-6}$
		3	7.857	7.828	7.836	7.840	7.859	7.830	7.840	7.843	7.860	7.831	7.842	7.844	$8.0x10^{-6}$	$5.2x10^{-6}$	$6.6x10^{-6}$

APPENDIX C: DISTRESS MAPS

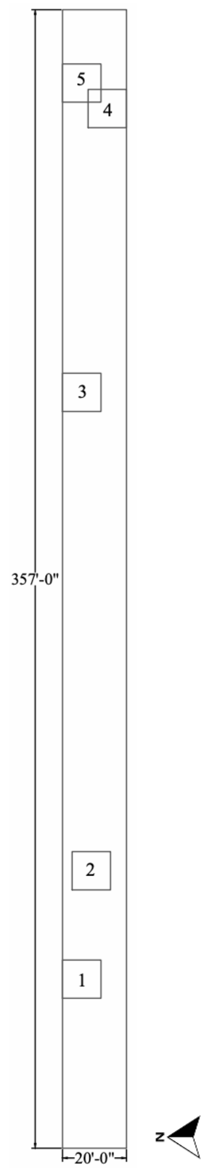

Figure C.1 Lightweight concrete deck at bridge C-989.

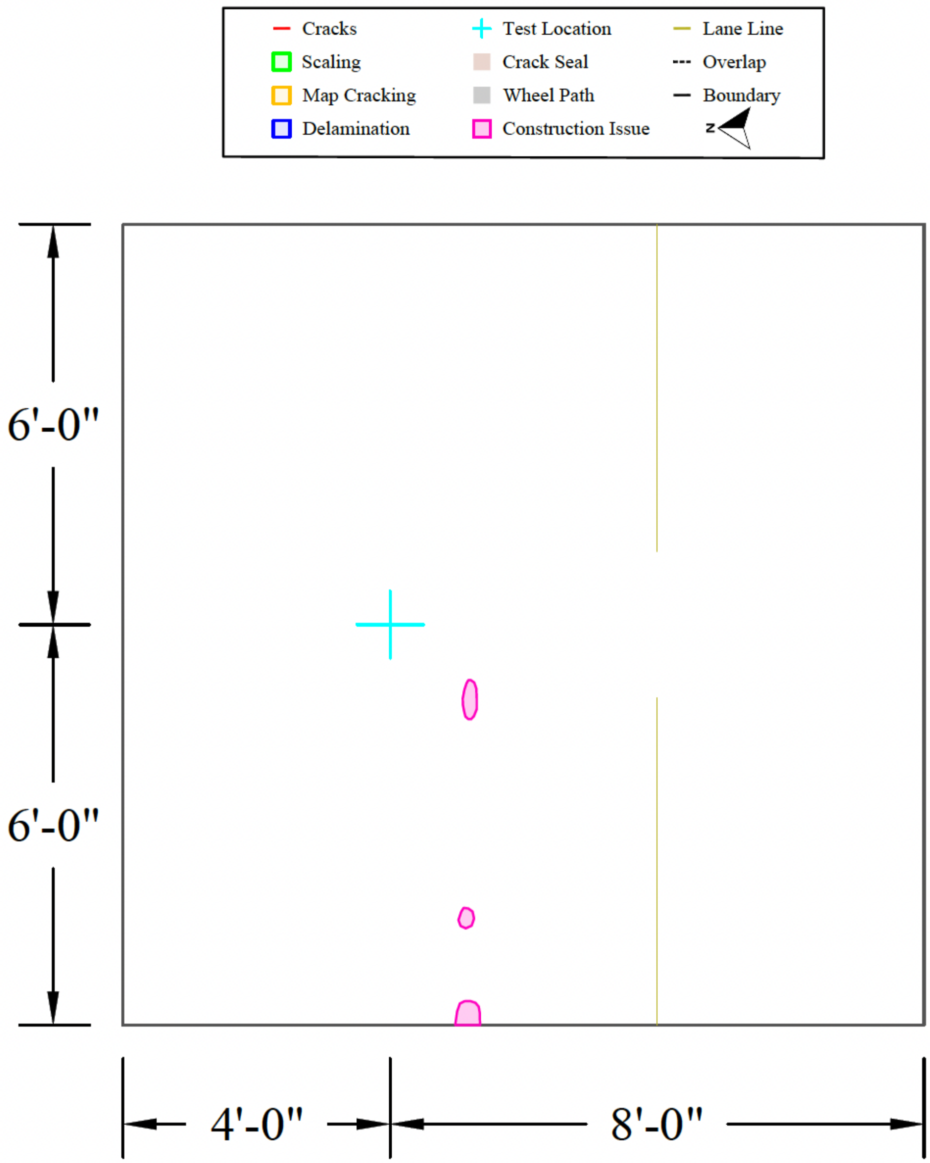

Figure C.2 Test location 1 of lightweight concrete deck at bridge C-989.

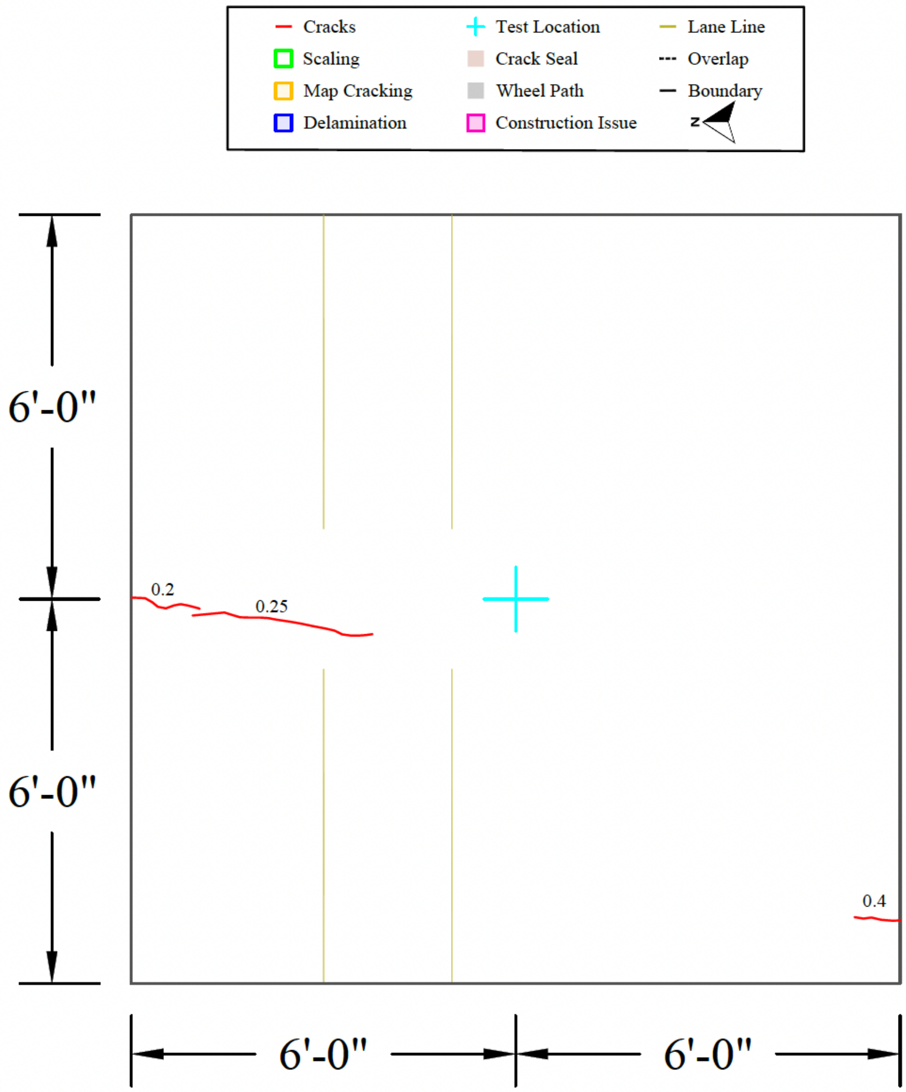

Figure C.3 Test location 2 of lightweight concrete deck at bridge C-989.

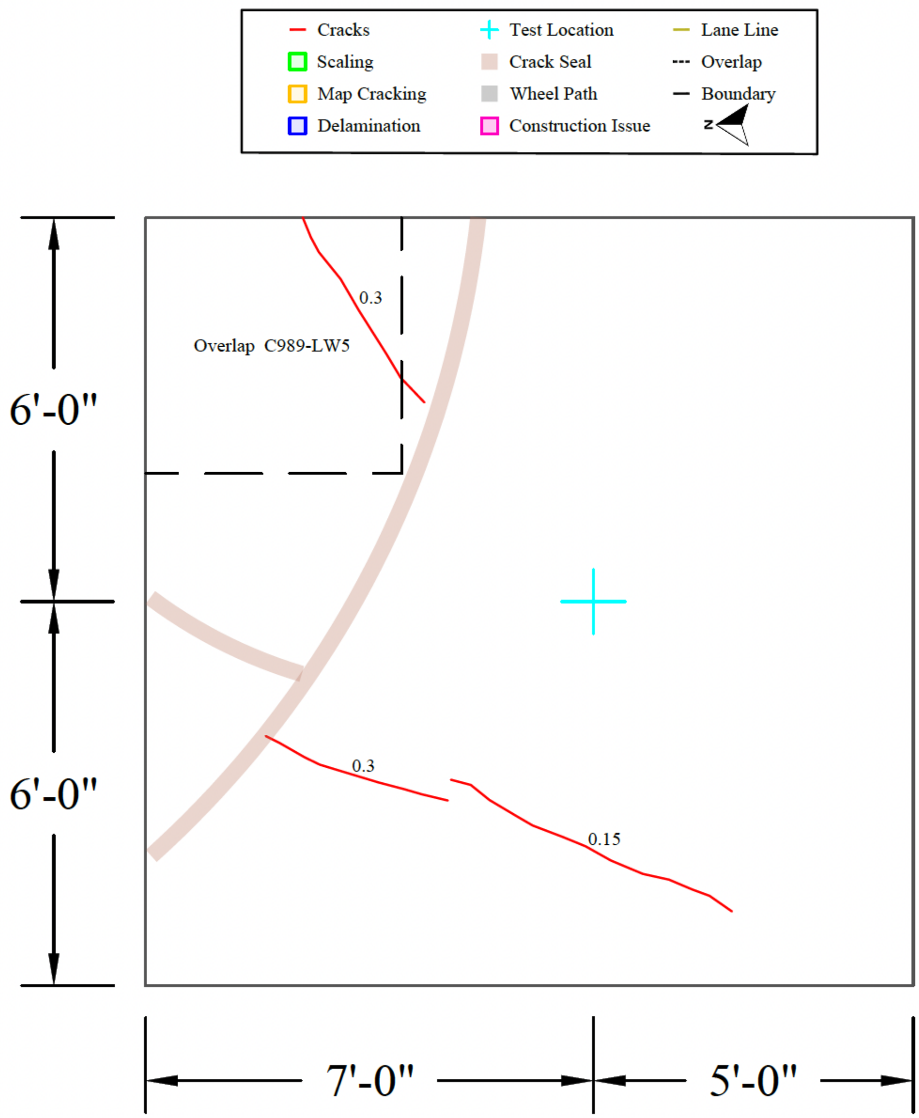

Figure C.4 Test location 4 of lightweight concrete deck at bridge C-989.

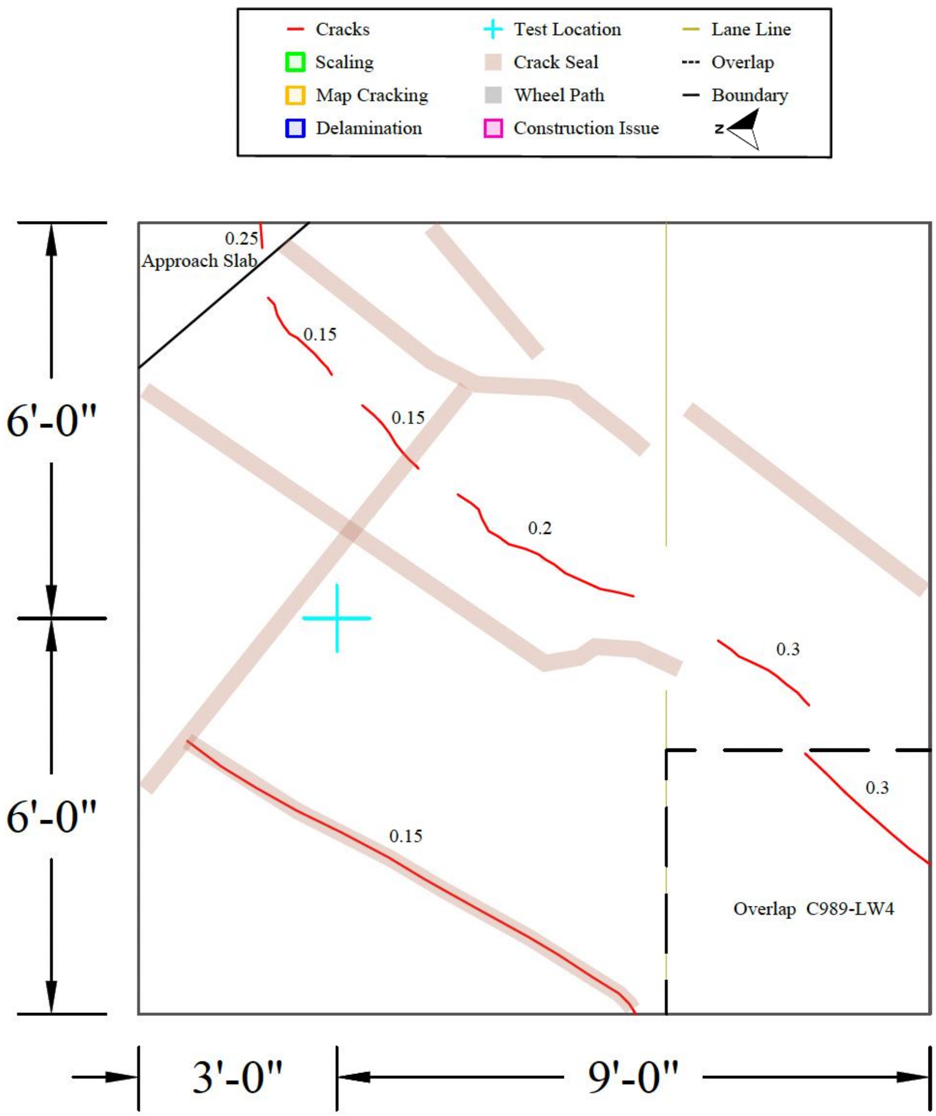

Figure C.5 Test location 5 of lightweight concrete deck at bridge C-989.

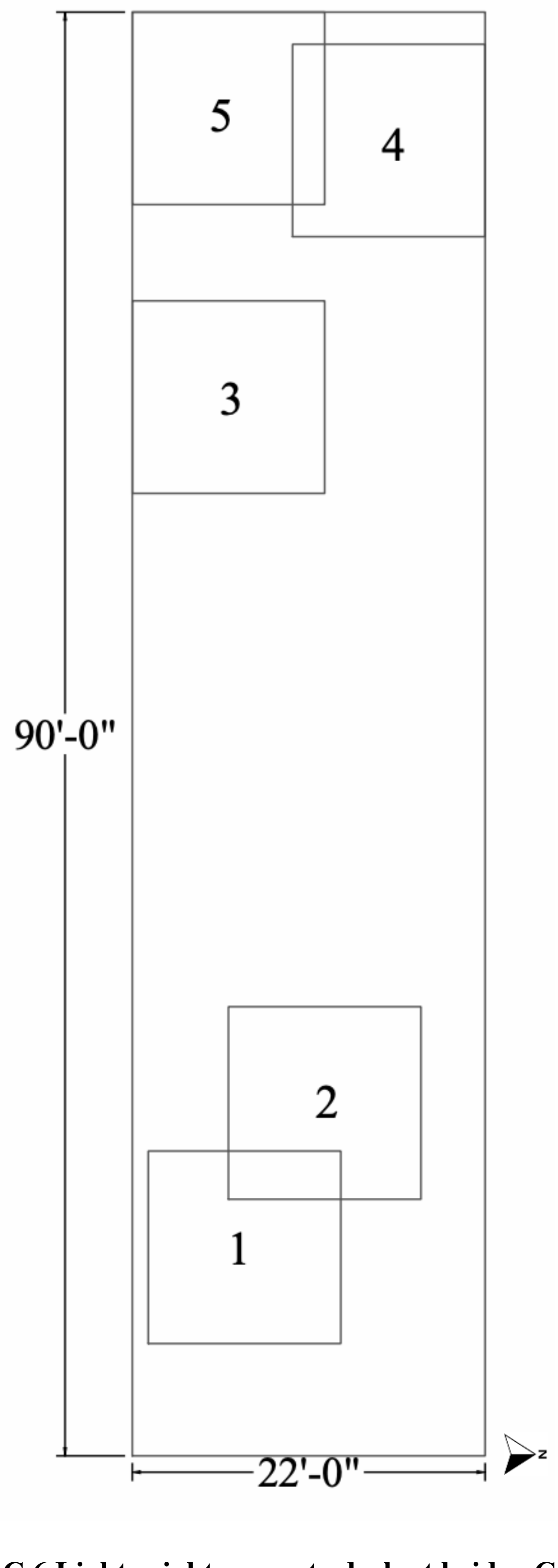

Figure C.6 Lightweight concrete deck at bridge C-1011.

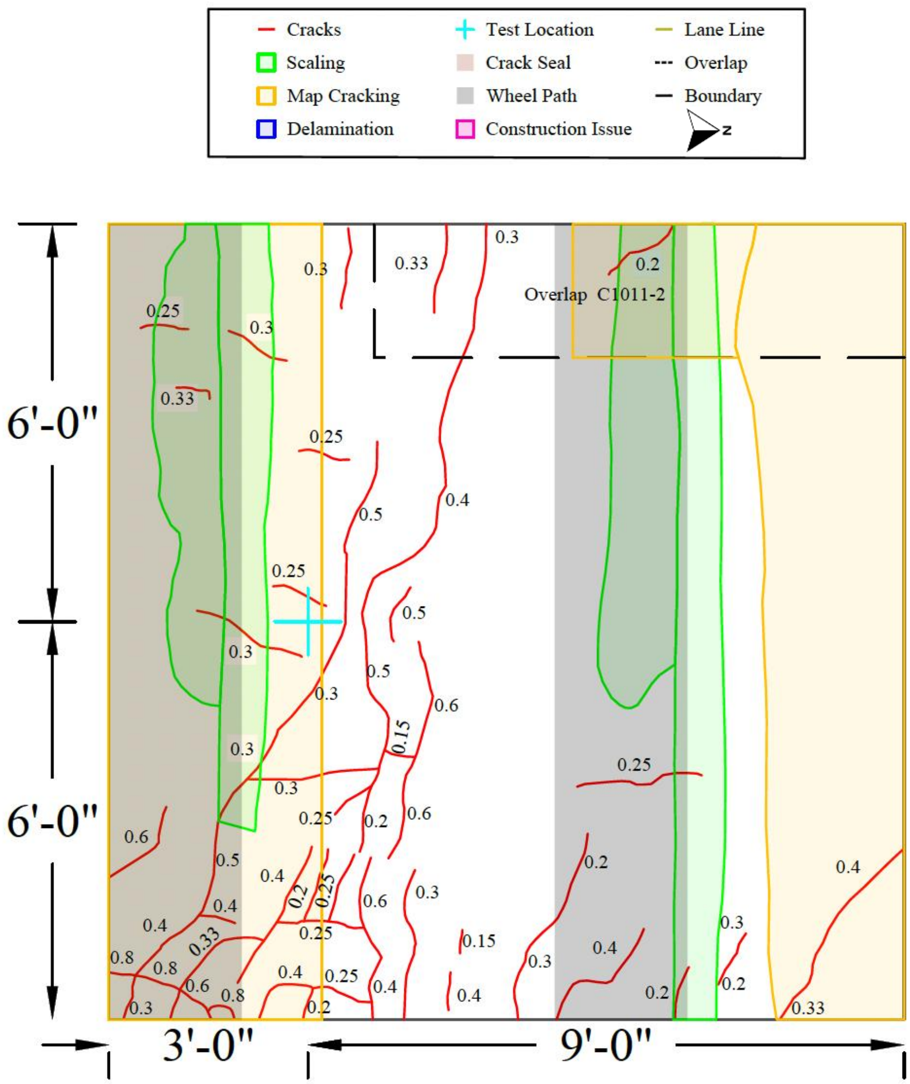

Figure C.7 Test location 1 of lightweight concrete deck at bridge C-1011.

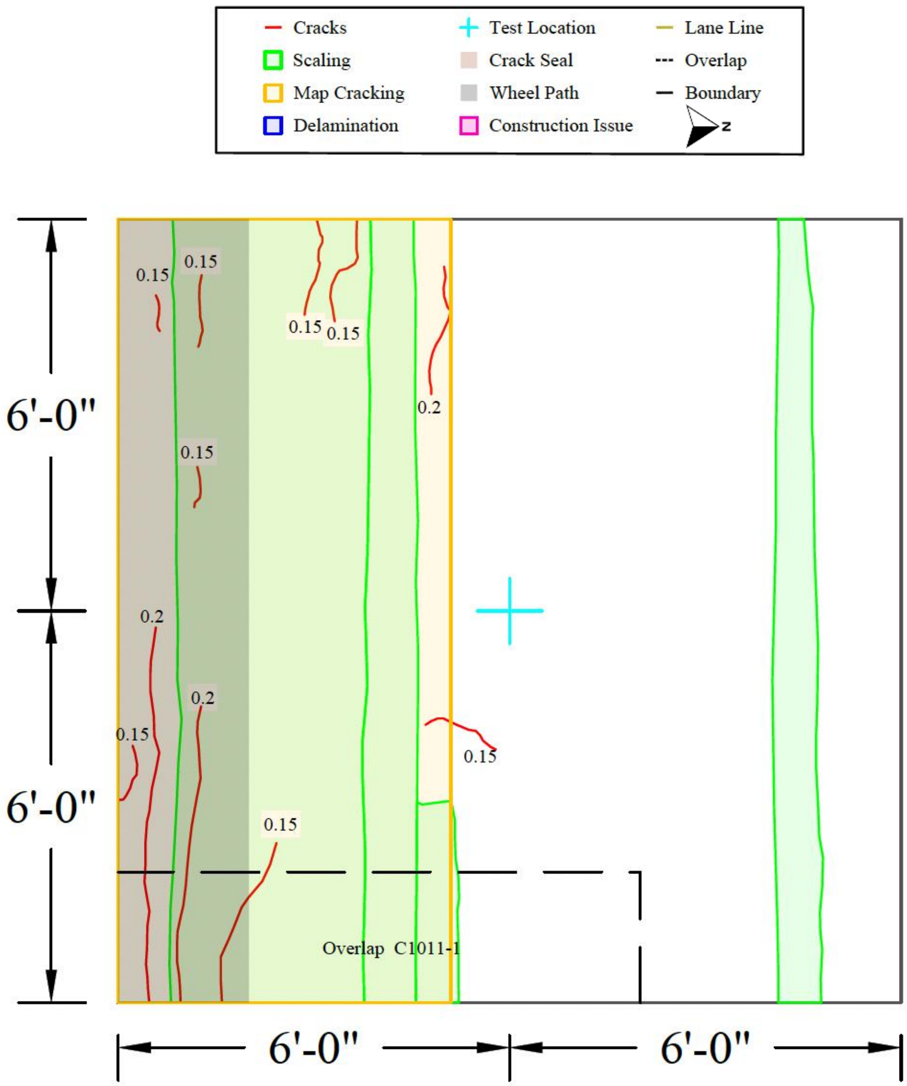

Figure C.8 Test location 2 of lightweight concrete deck at bridge C-1011.

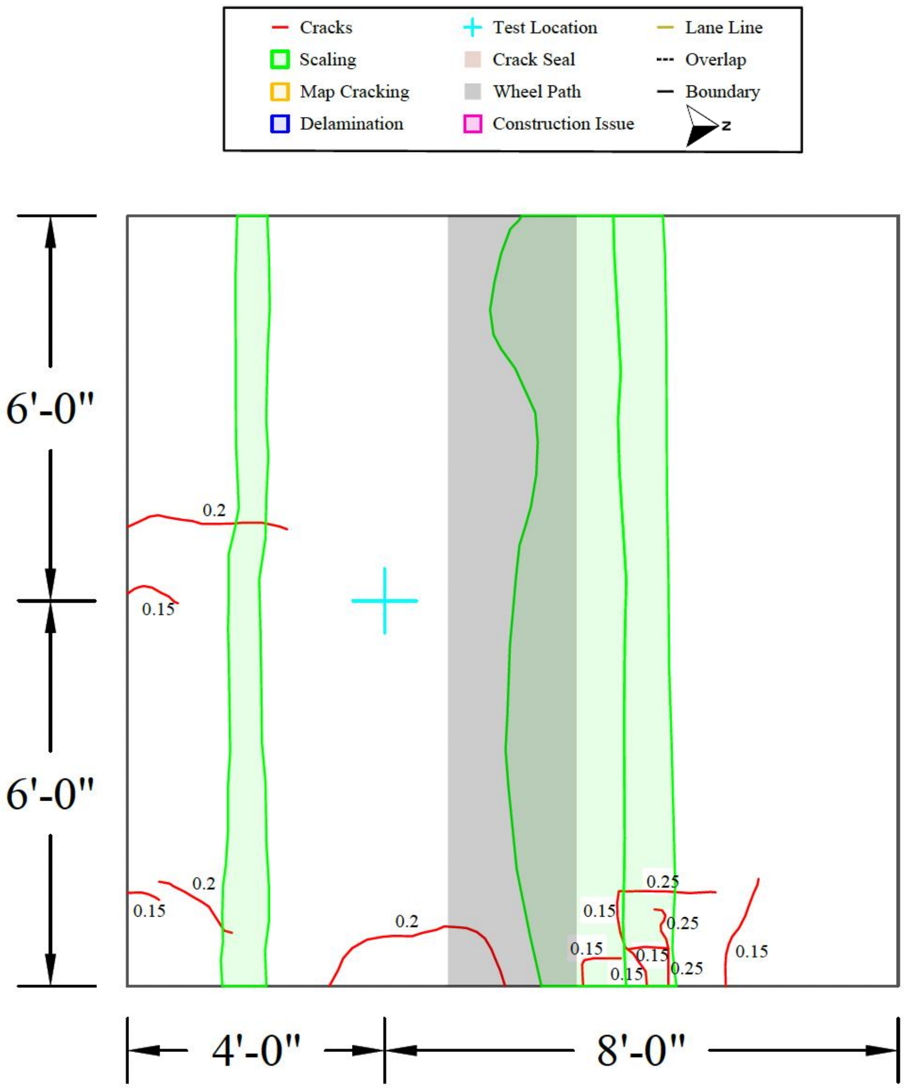

Figure C.9 Test location 3 of lightweight concrete deck at bridge C-1011.

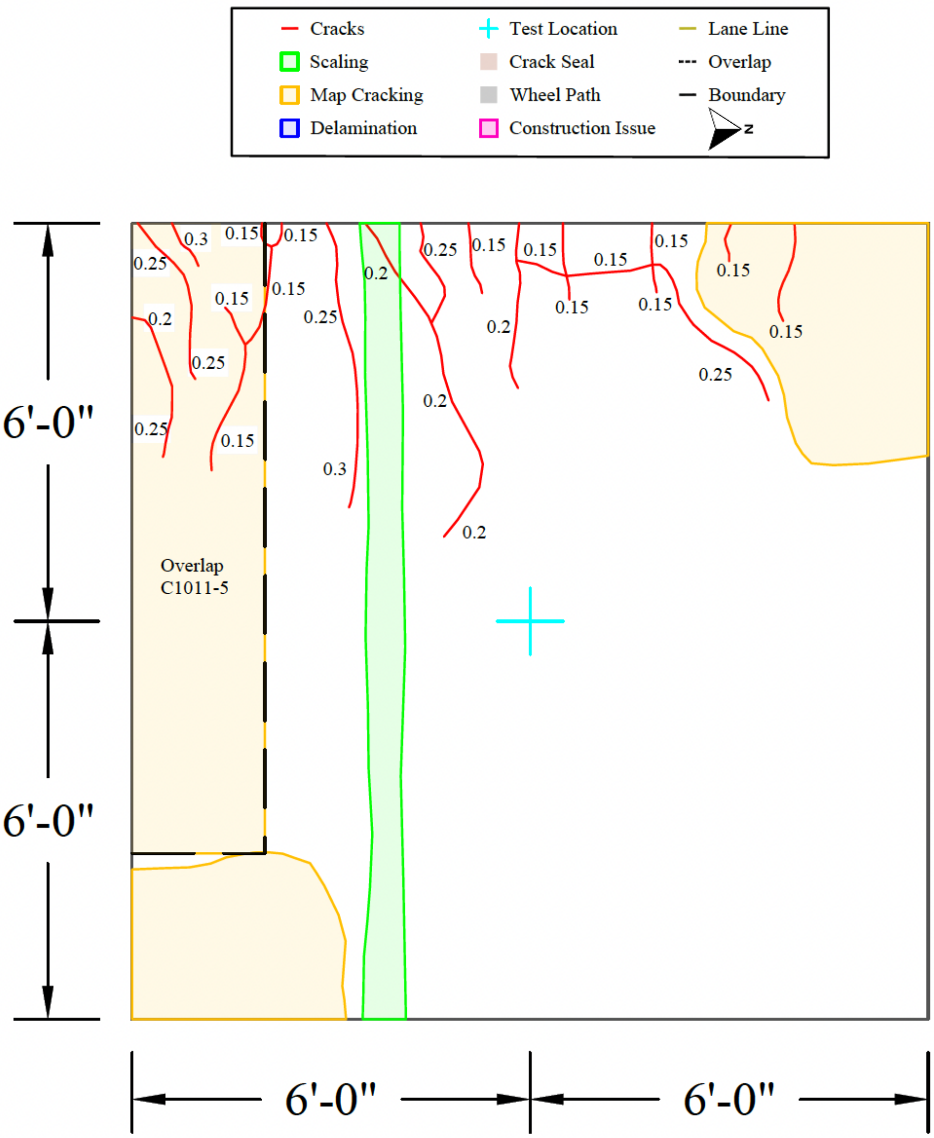

Figure C.10 Test location 4 of lightweight concrete deck at bridge C-1011.

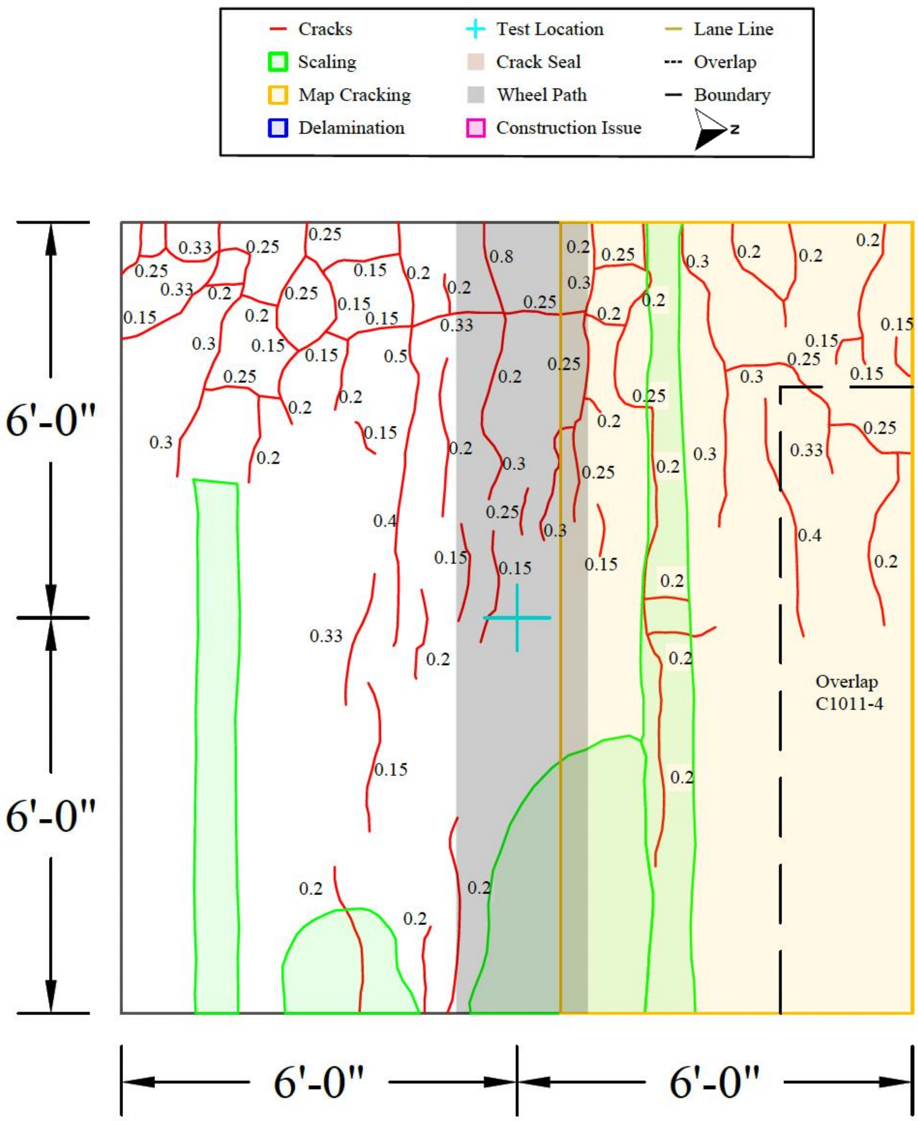

Figure C.11 Test location 5 of lightweight concrete deck at bridge C-1011.

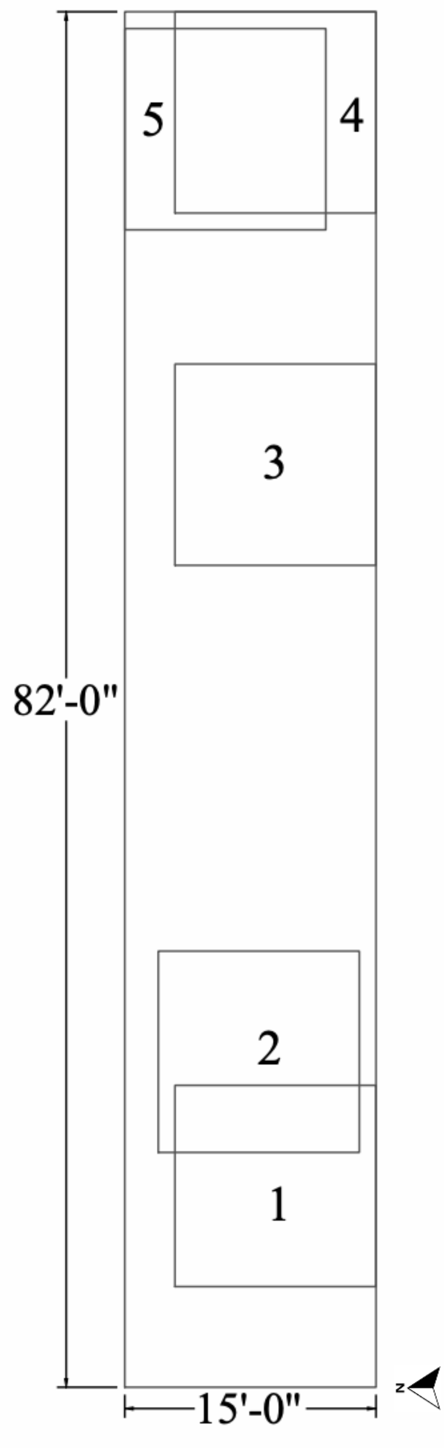

Figure C.12 Lightweight concrete deck at bridge F-792.

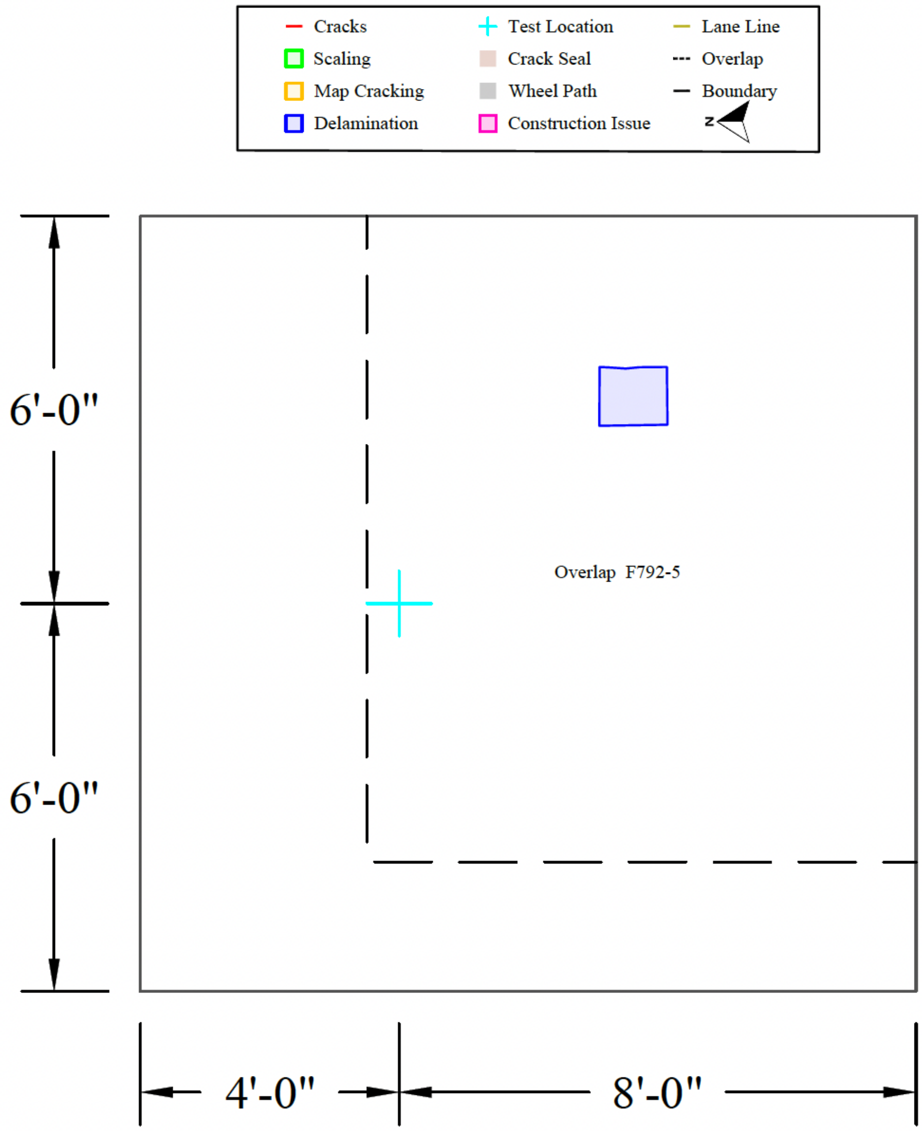

Figure C.13 Test location 4 of lightweight concrete deck at bridge F-792.

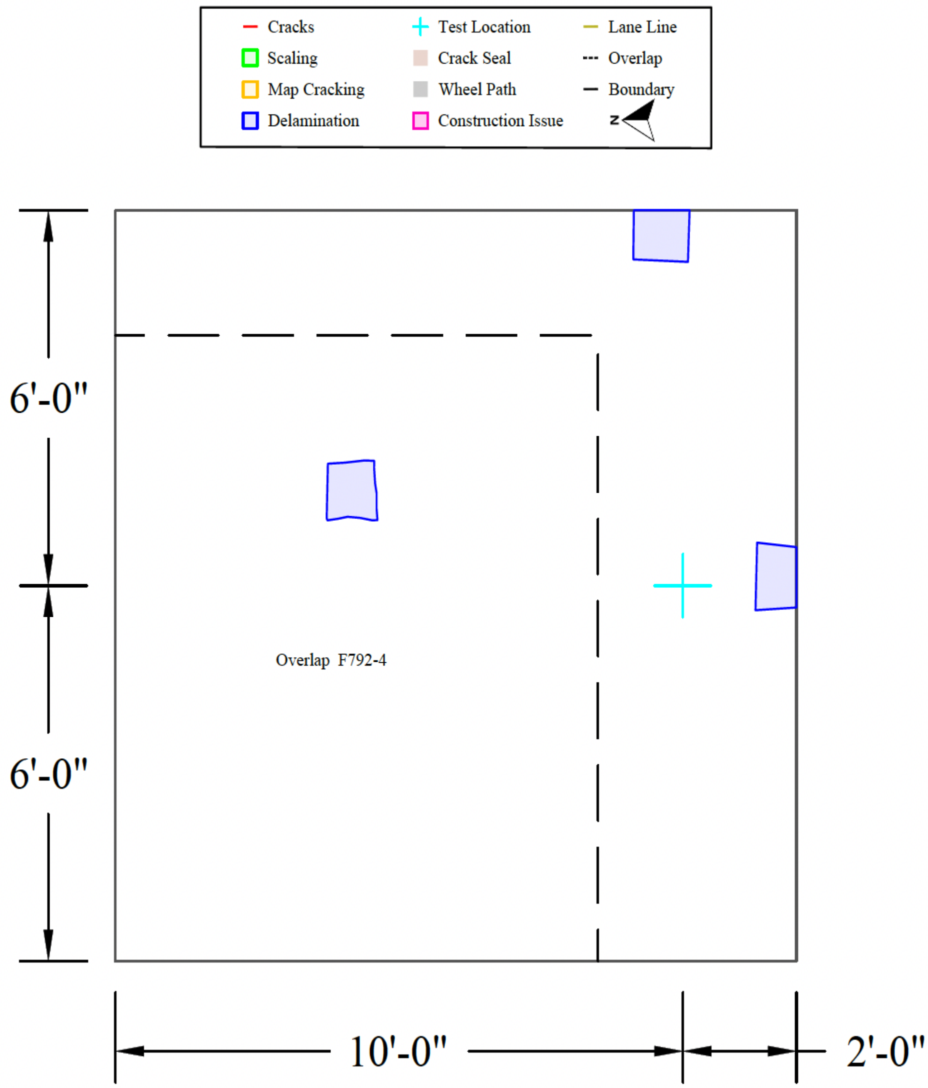

Figure C.14 Test location 5 of lightweight concrete deck at bridge F-792.

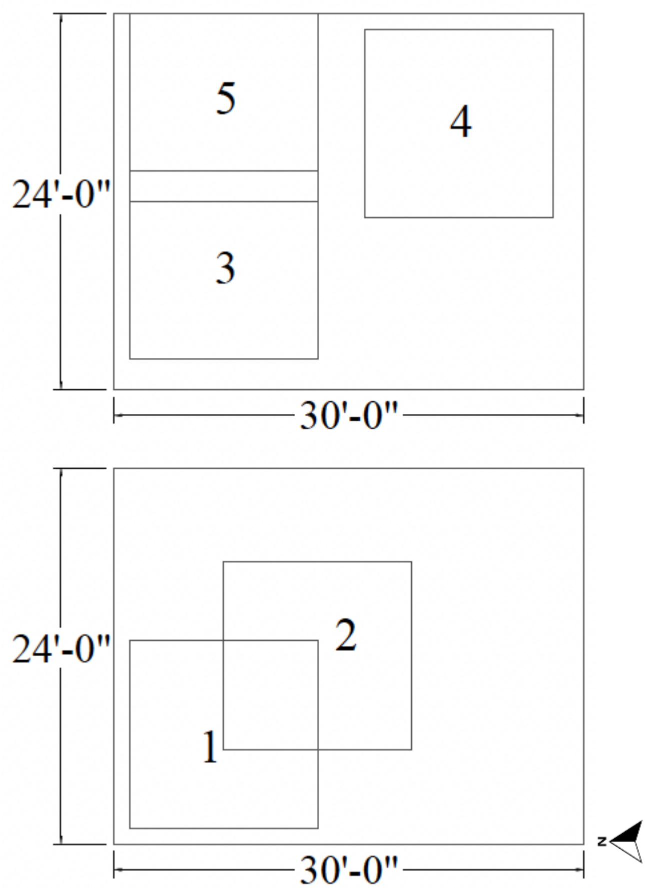

Figure C.15 Normal-weight concrete approach slabs at bridge C-989.

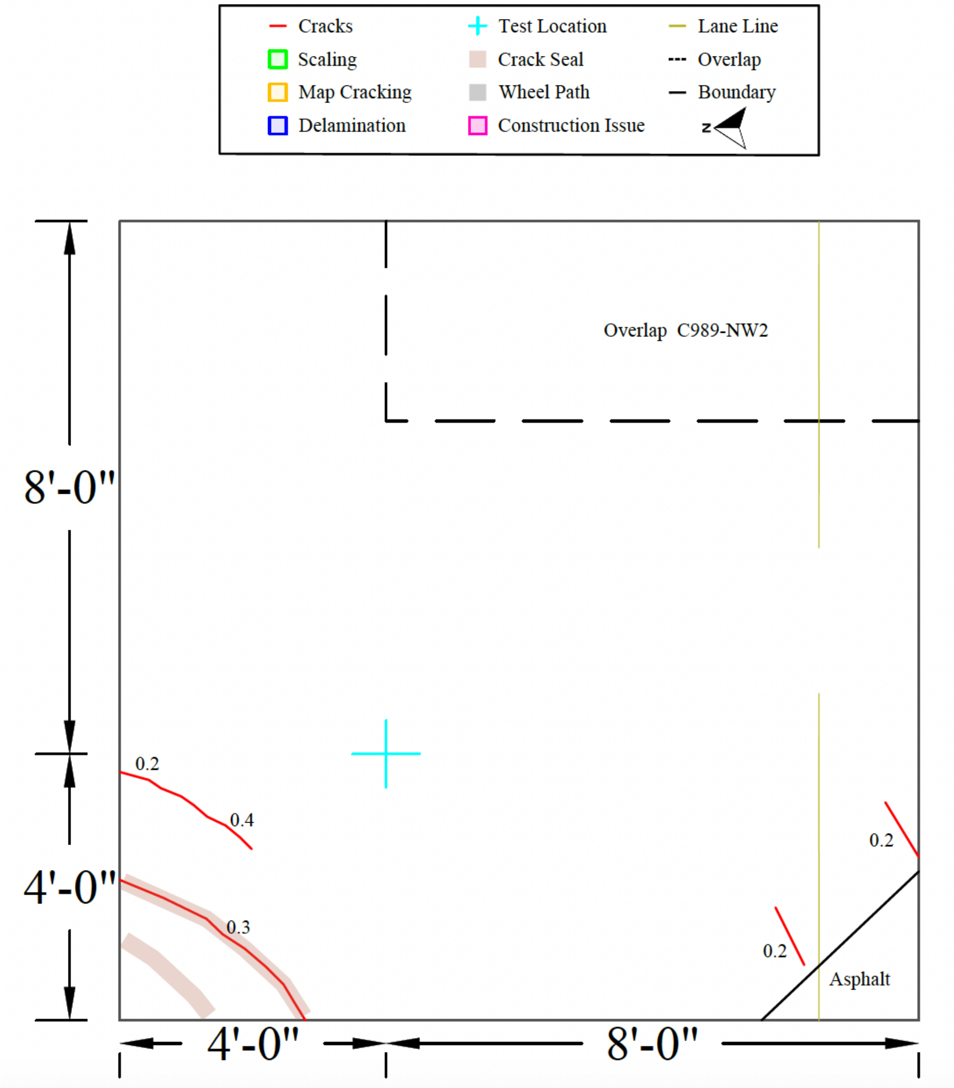

Figure C.16 Test location 1 of normal-weight concrete approach slabs at bridge C-989.

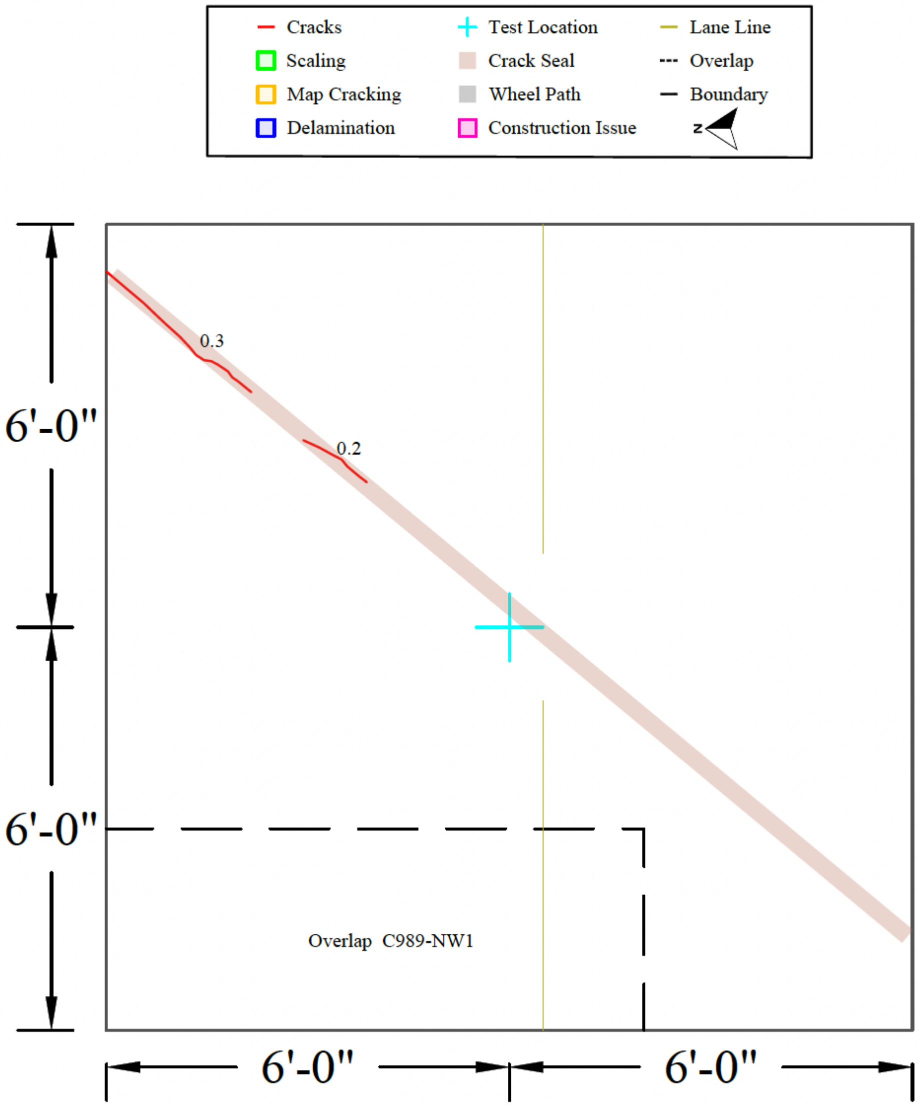

Figure C.17 Test location 2 of normal-weight concrete approach slabs at bridge C-989.

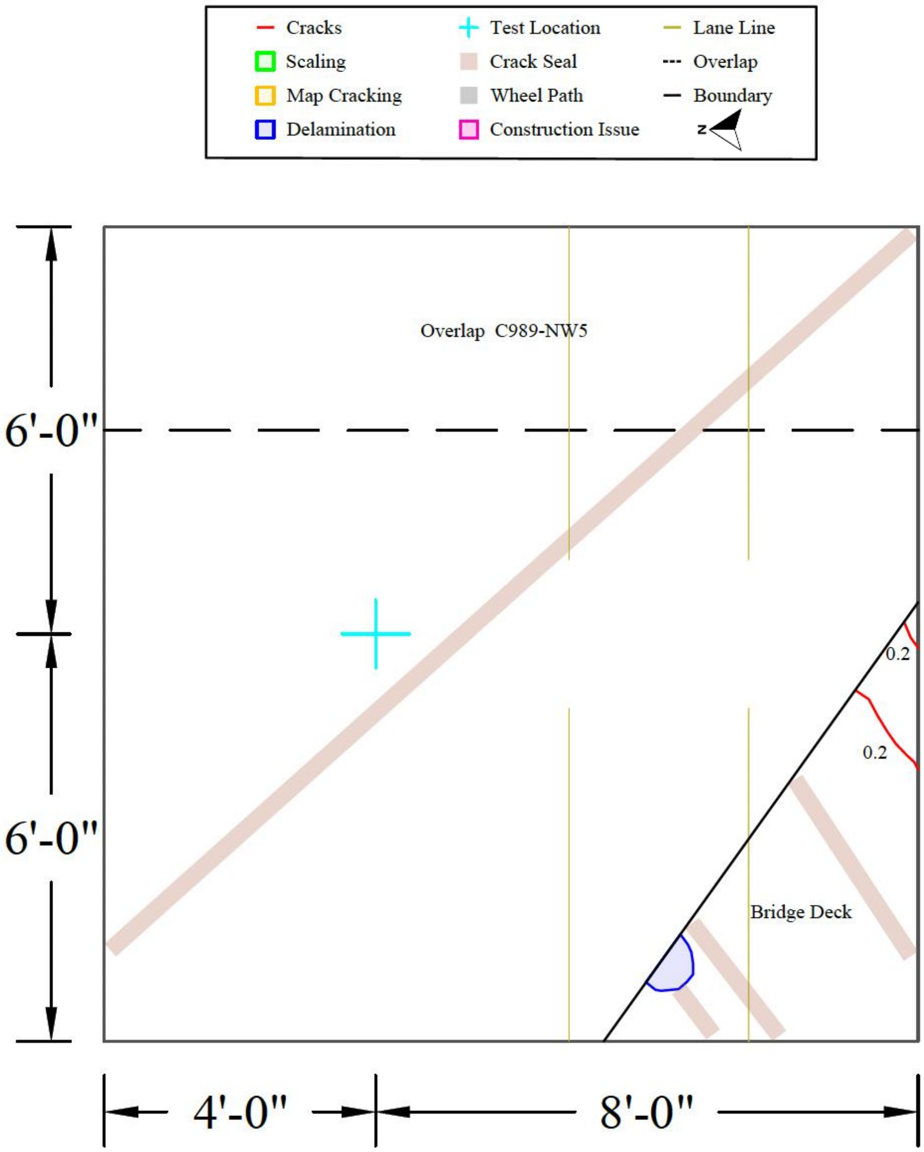

Figure C.18 Test location 3 of normal-weight concrete approach slabs at bridge C-989.

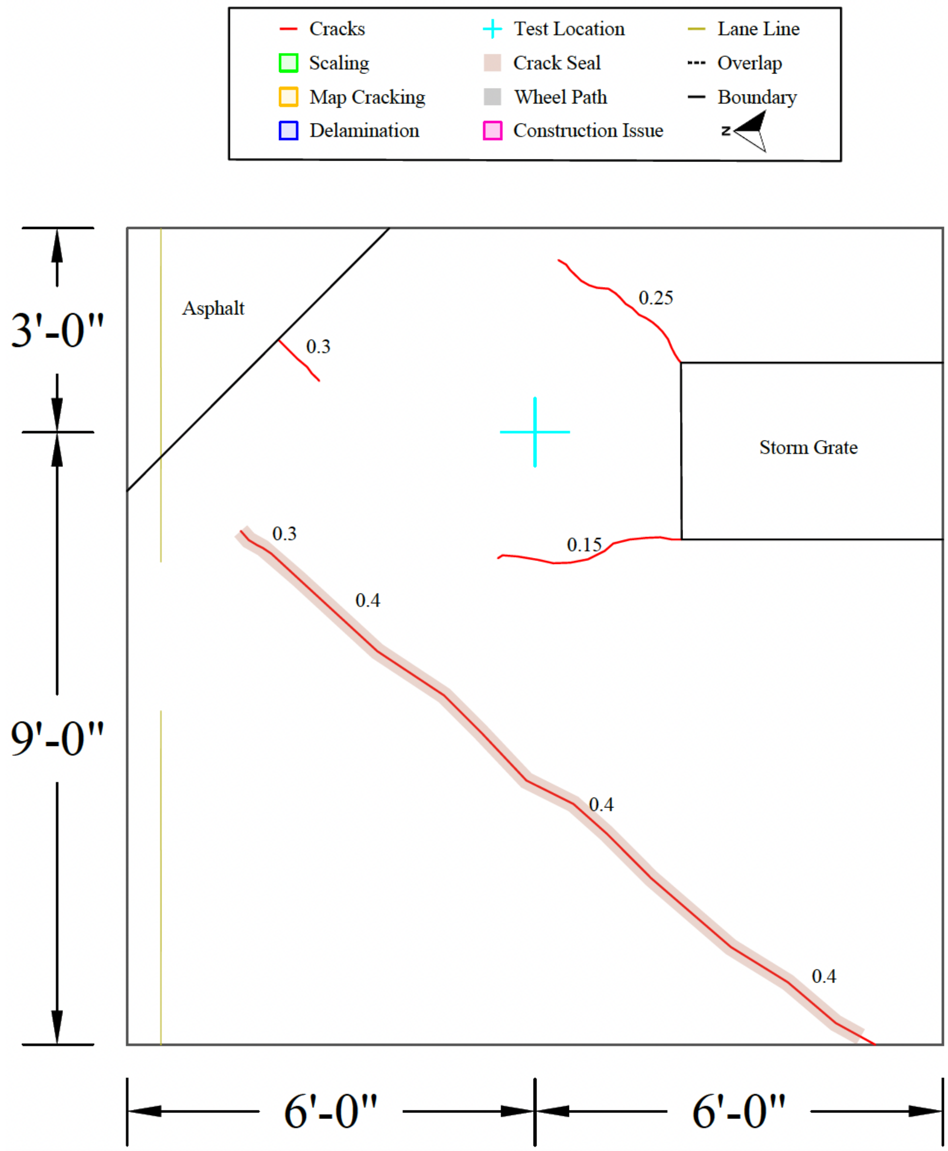

Figure C.19 Test location 4 of normal-weight concrete approach slabs at bridge C-989.

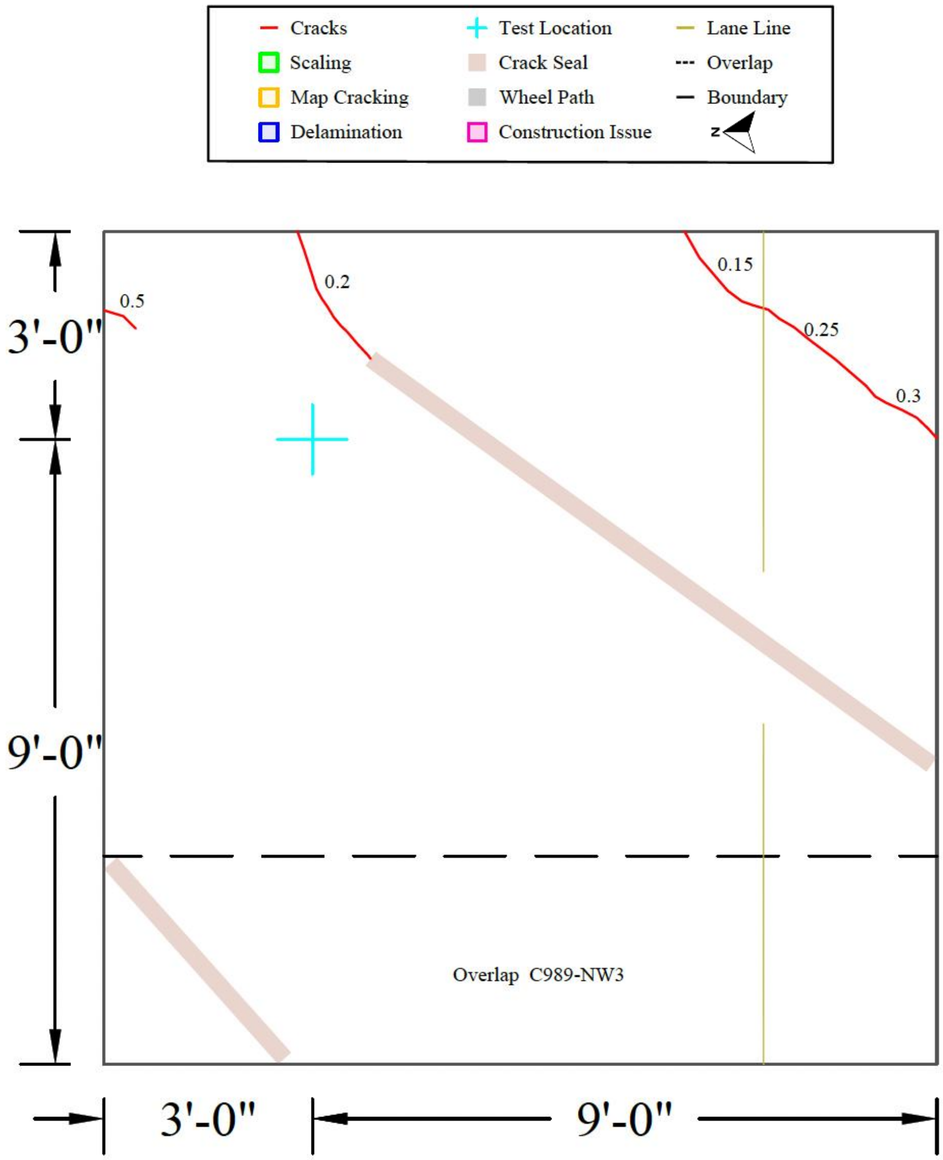

Figure C.20 Test location 5 of normal-weight concrete approach slabs at bridge C-989.

APPENDIX D: CORE AND CYLINDER PHOTOGRAPHS

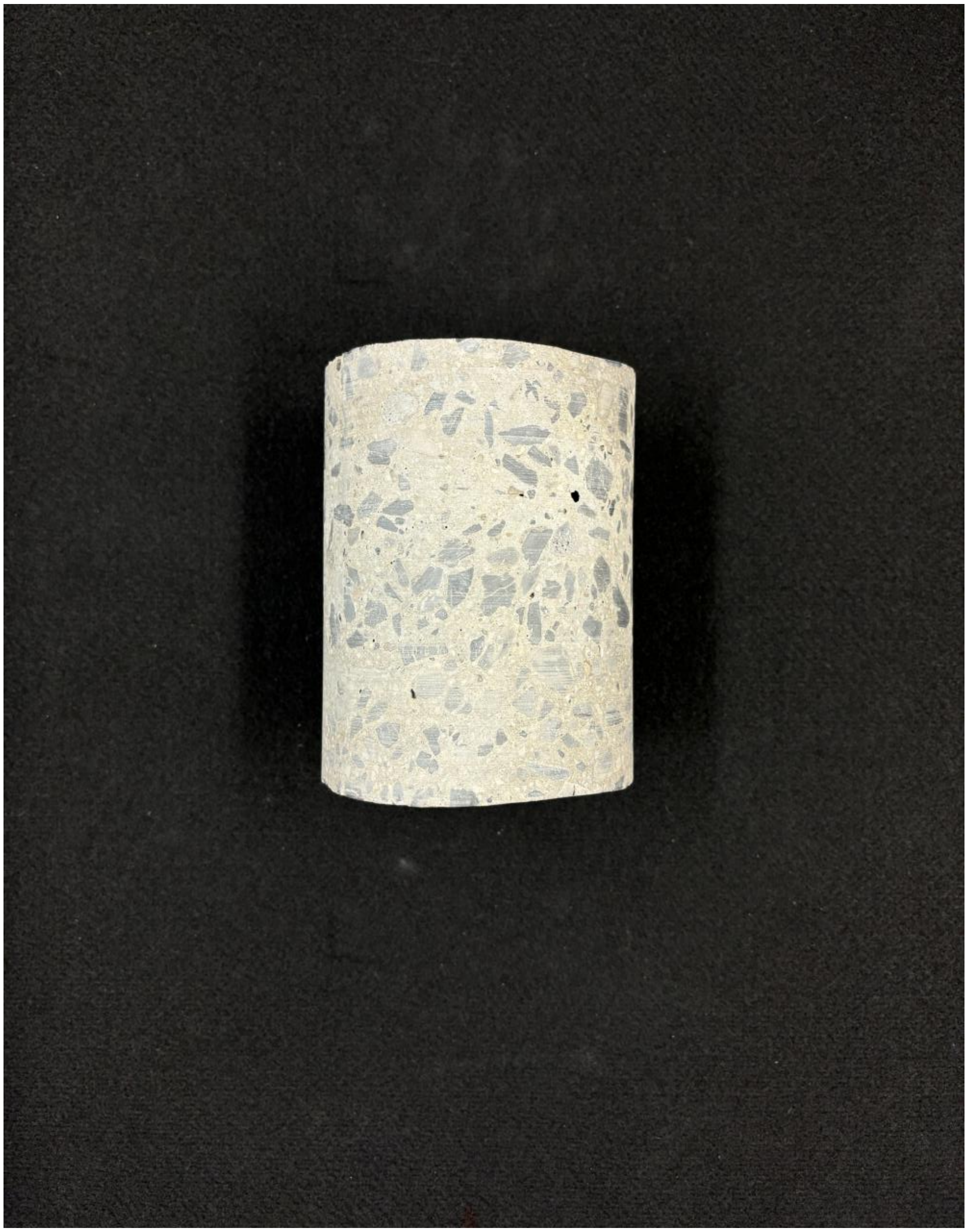

Figure D.1 Core 1 of lightweight concrete deck at bridge C-989.

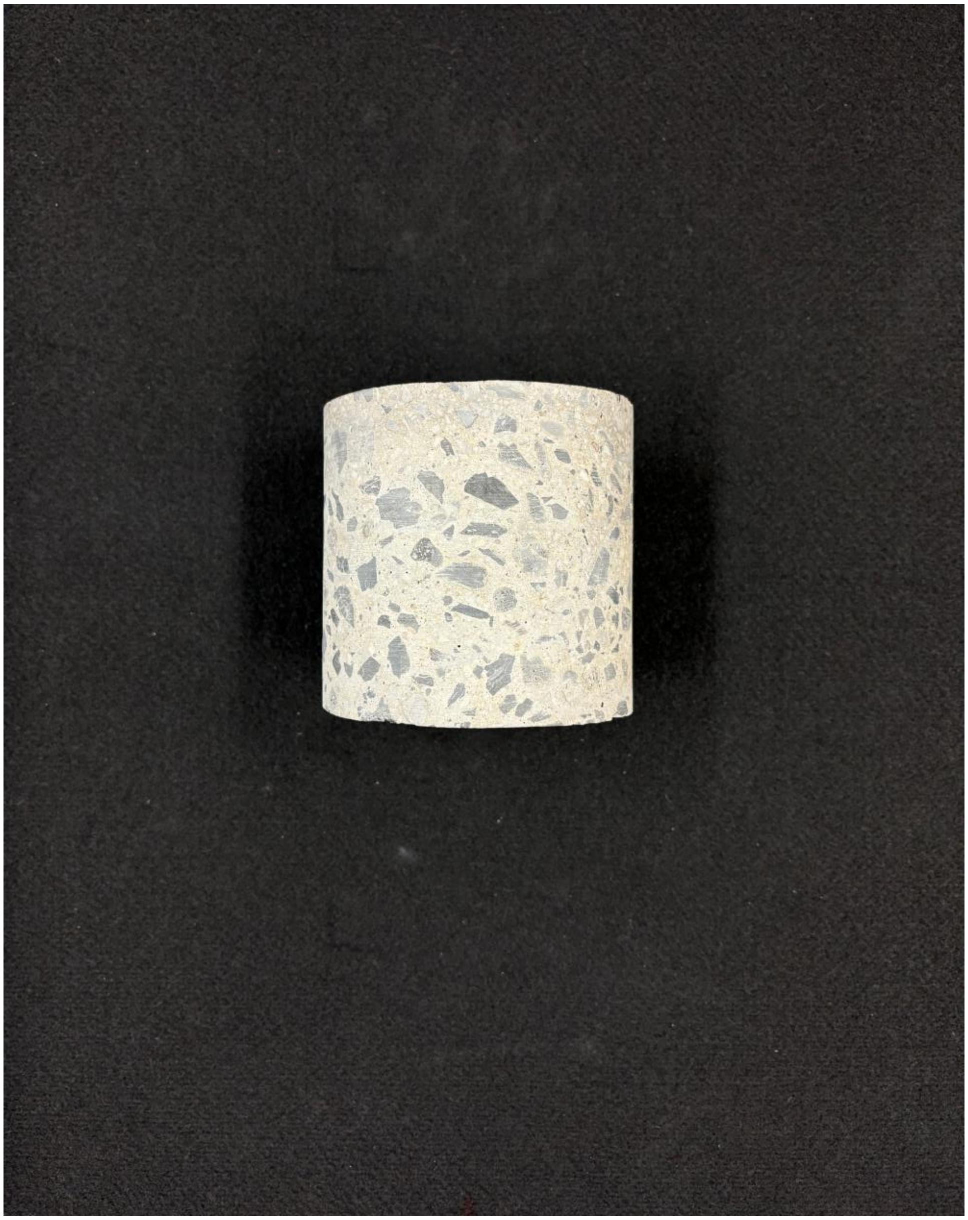

Figure D.2 Core 2 of lightweight concrete deck at bridge C-989.

Figure D.3 Core 3 of lightweight concrete deck at bridge C-989.

Figure D.4 Core 4 of lightweight concrete deck at bridge C-989.

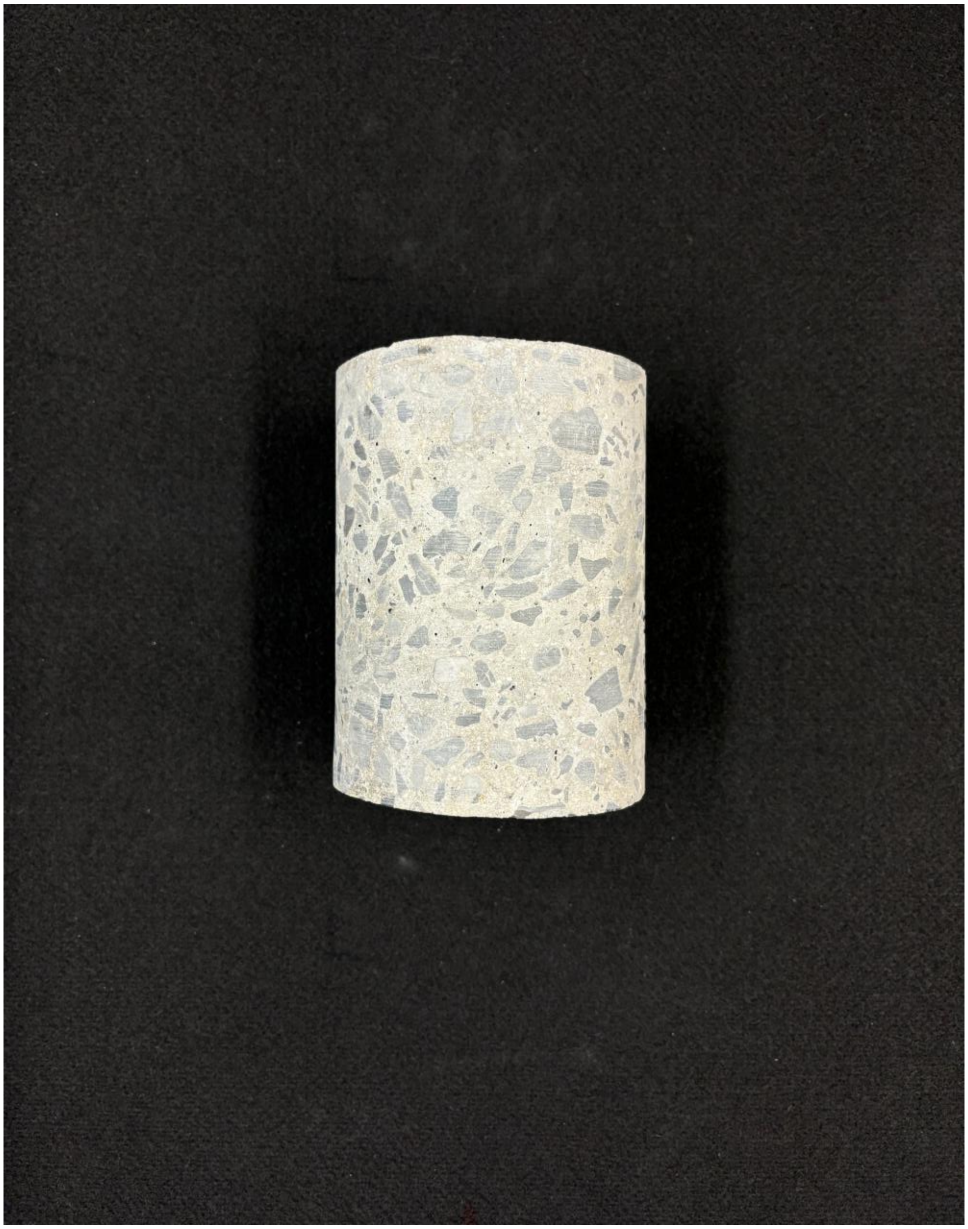

Figure D.5 Core 5 of lightweight concrete deck at bridge C-989.

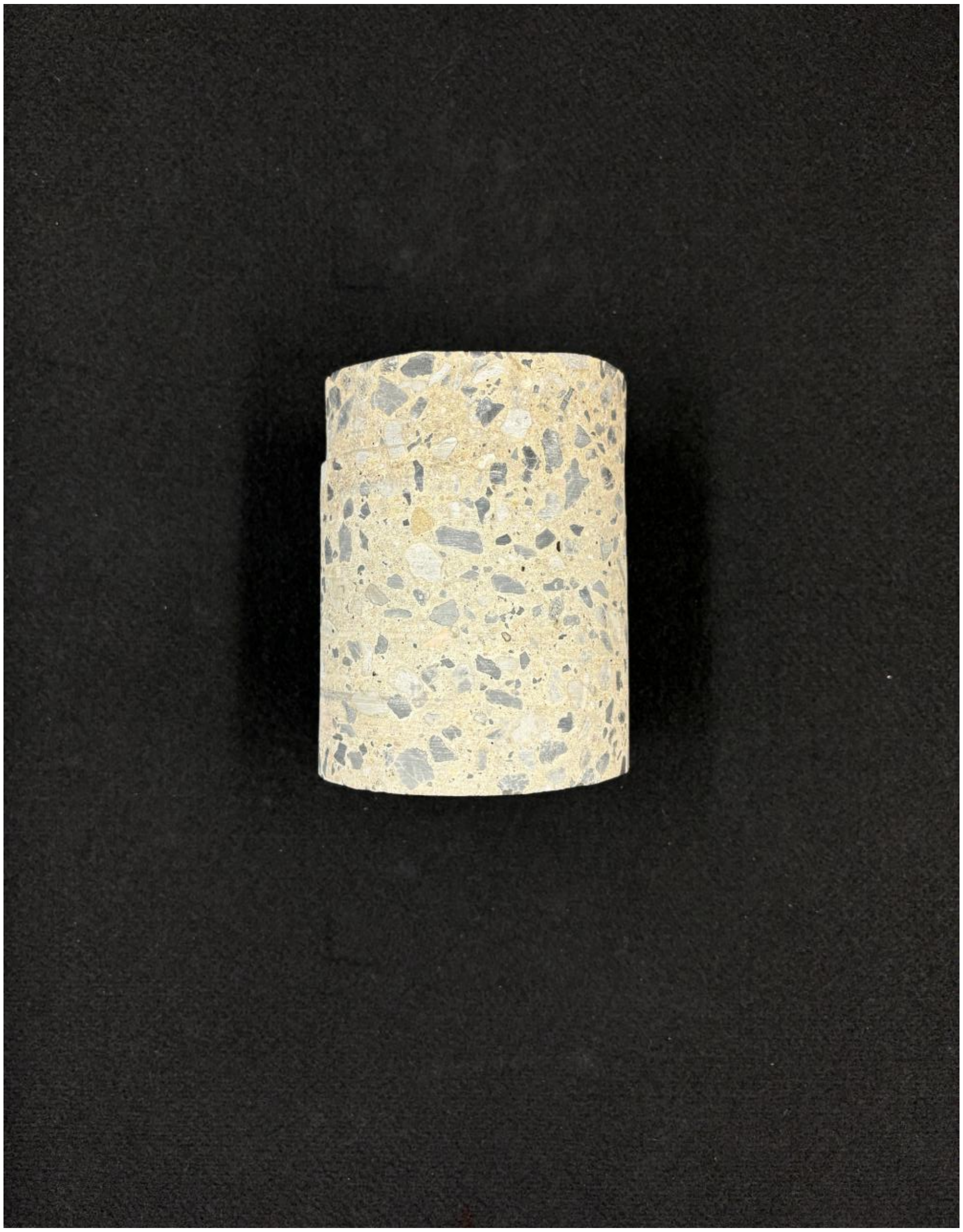

Figure D.6 Core 1 of lightweight concrete deck at bridge C-1011.

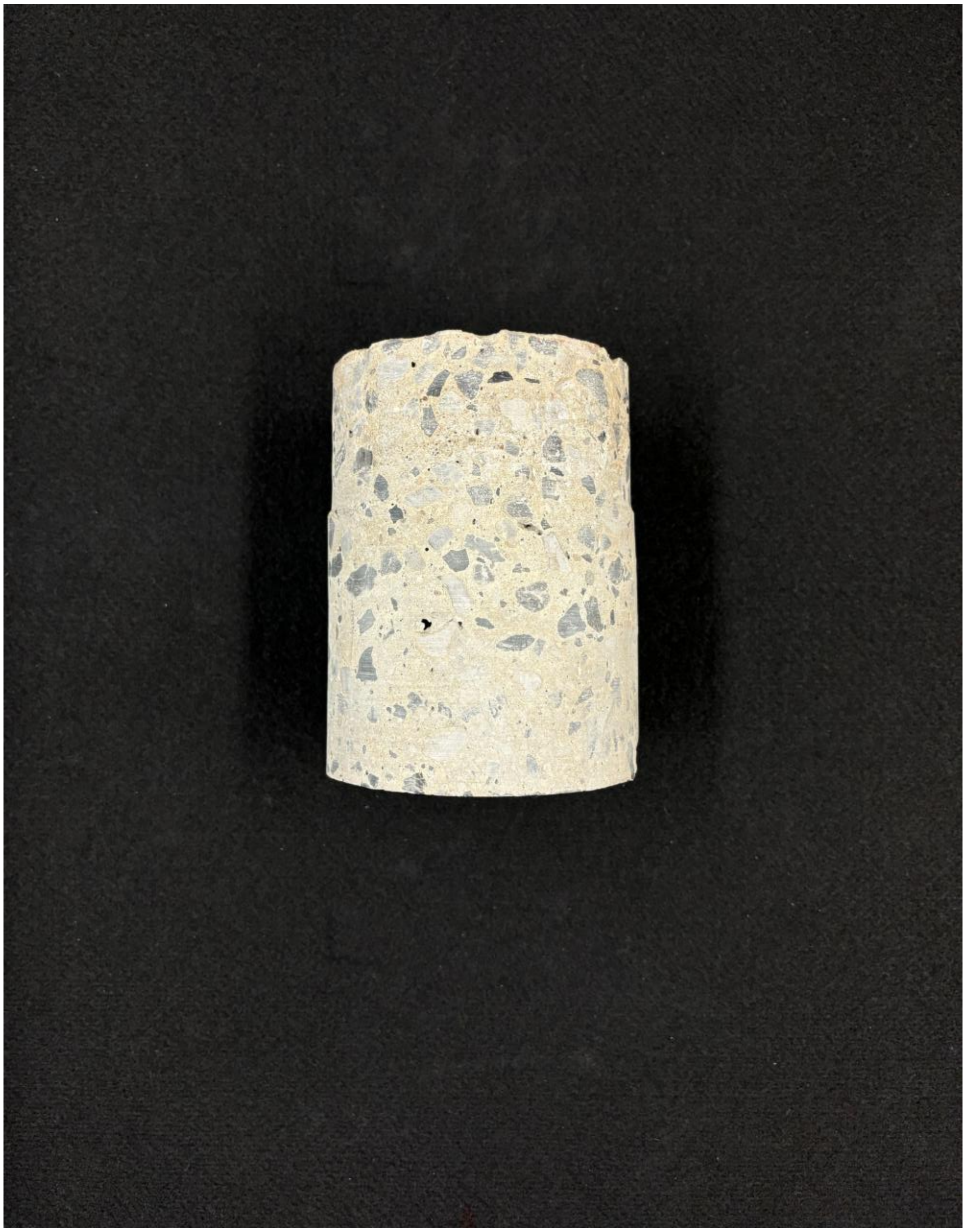

Figure D.7 Core 2 of lightweight concrete deck at bridge C-1011.

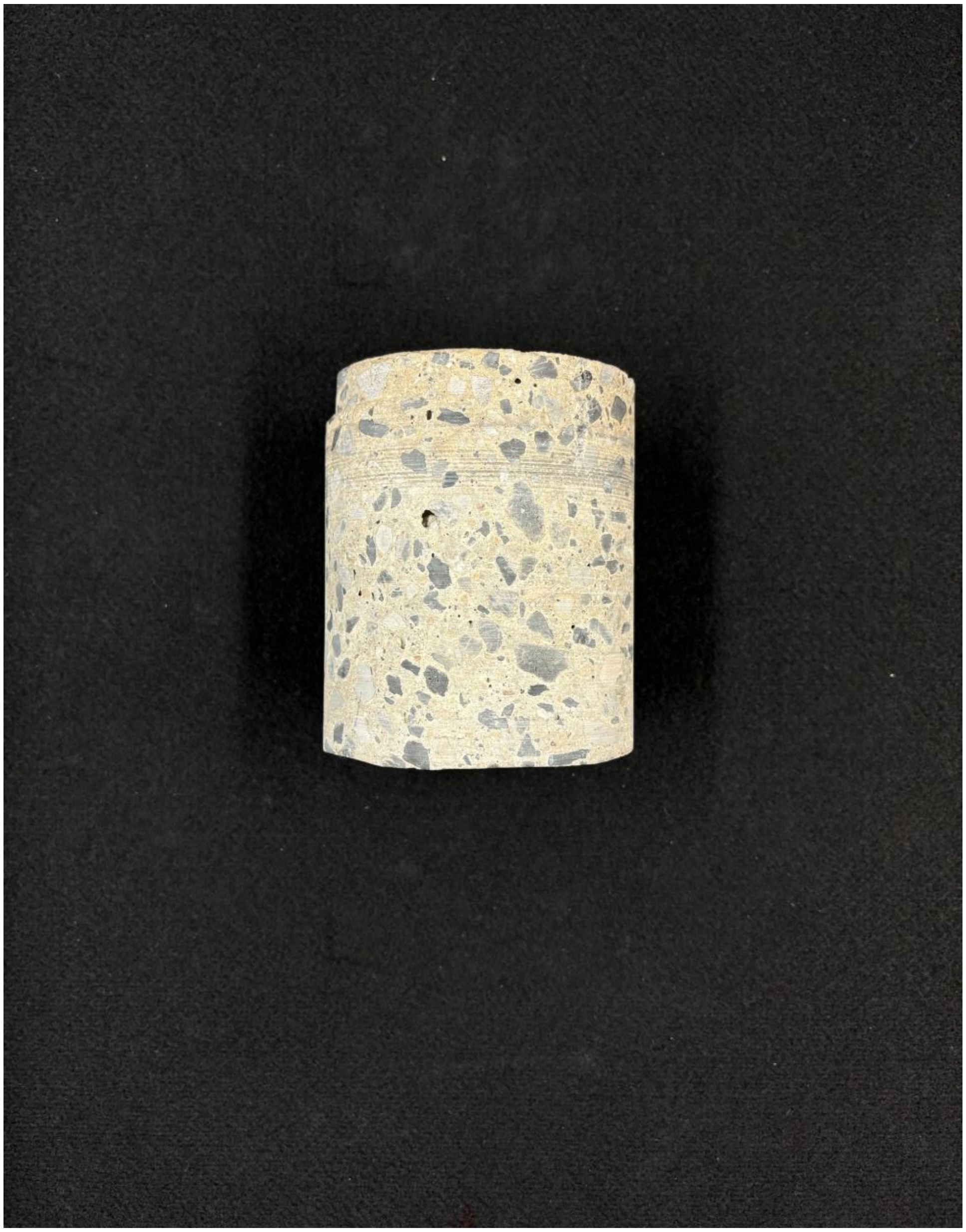

Figure D.8 Core 3 of lightweight concrete deck at bridge C-1011.

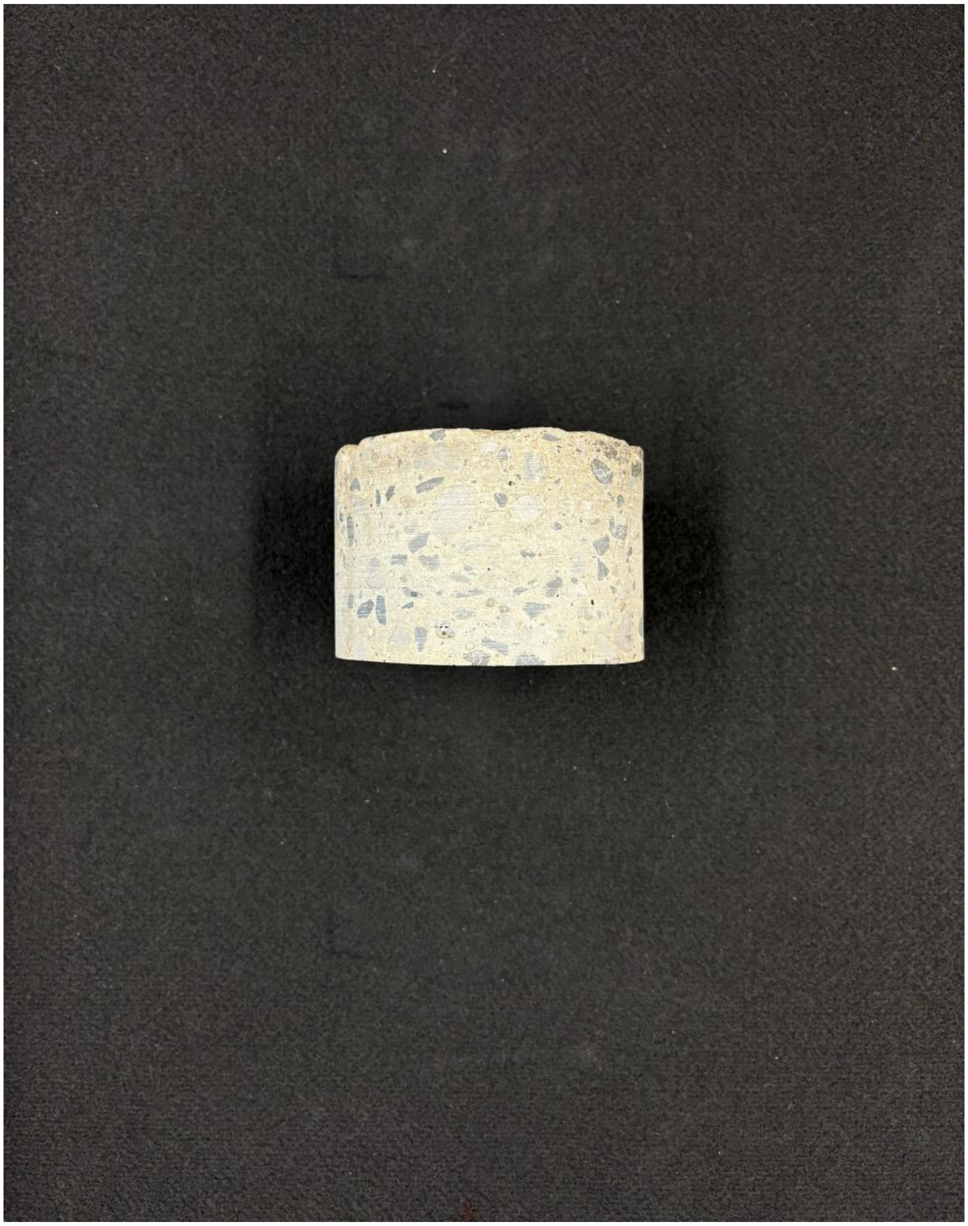

Figure D.9 Core 4 of lightweight concrete deck at bridge C-1011.

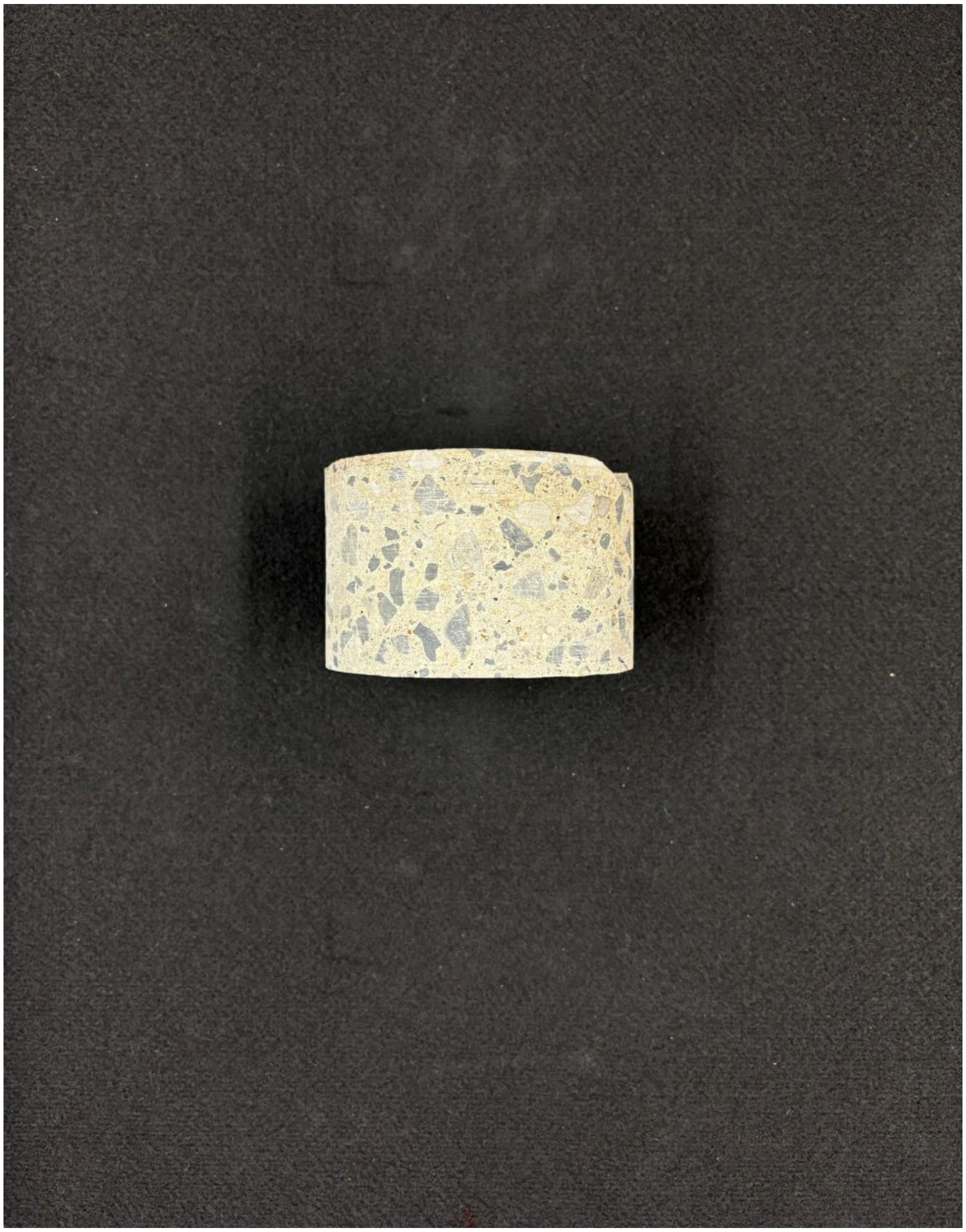

Figure D.10 Core 5 of lightweight concrete deck at bridge C-1011.

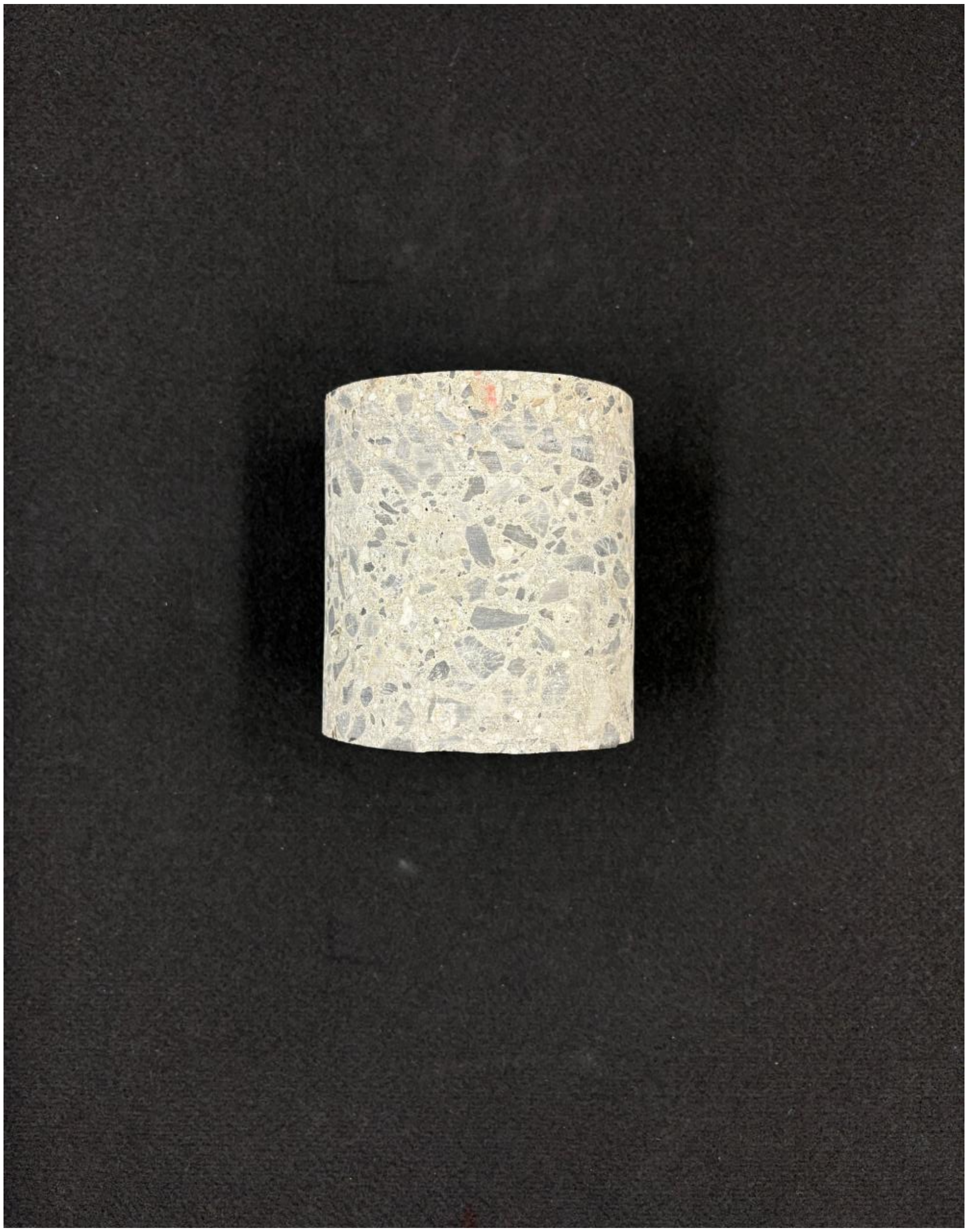

Figure D.11 Core 1 of lightweight concrete deck at bridge F-792.

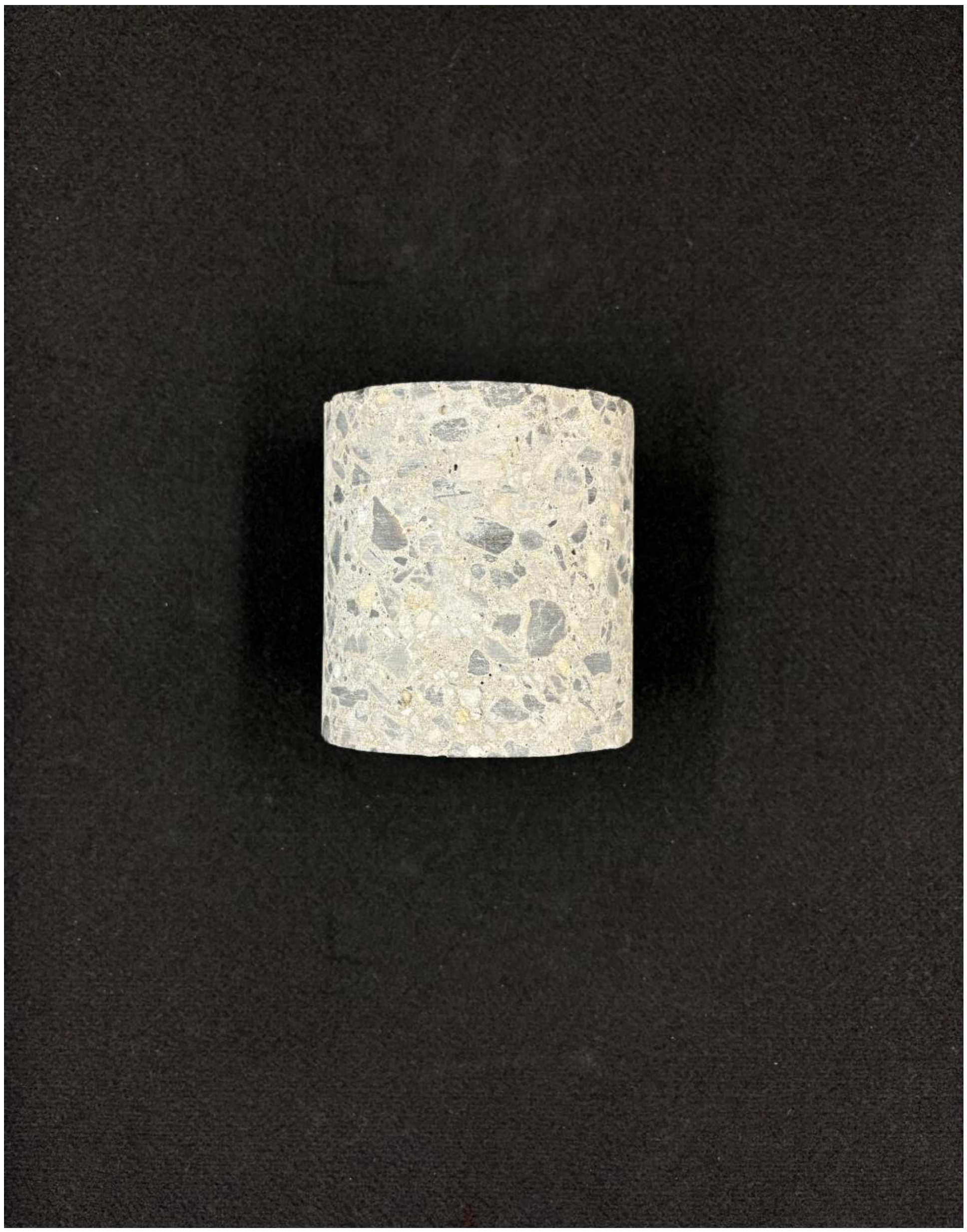

Figure D.12 Core 2 of lightweight concrete deck at bridge F-792.

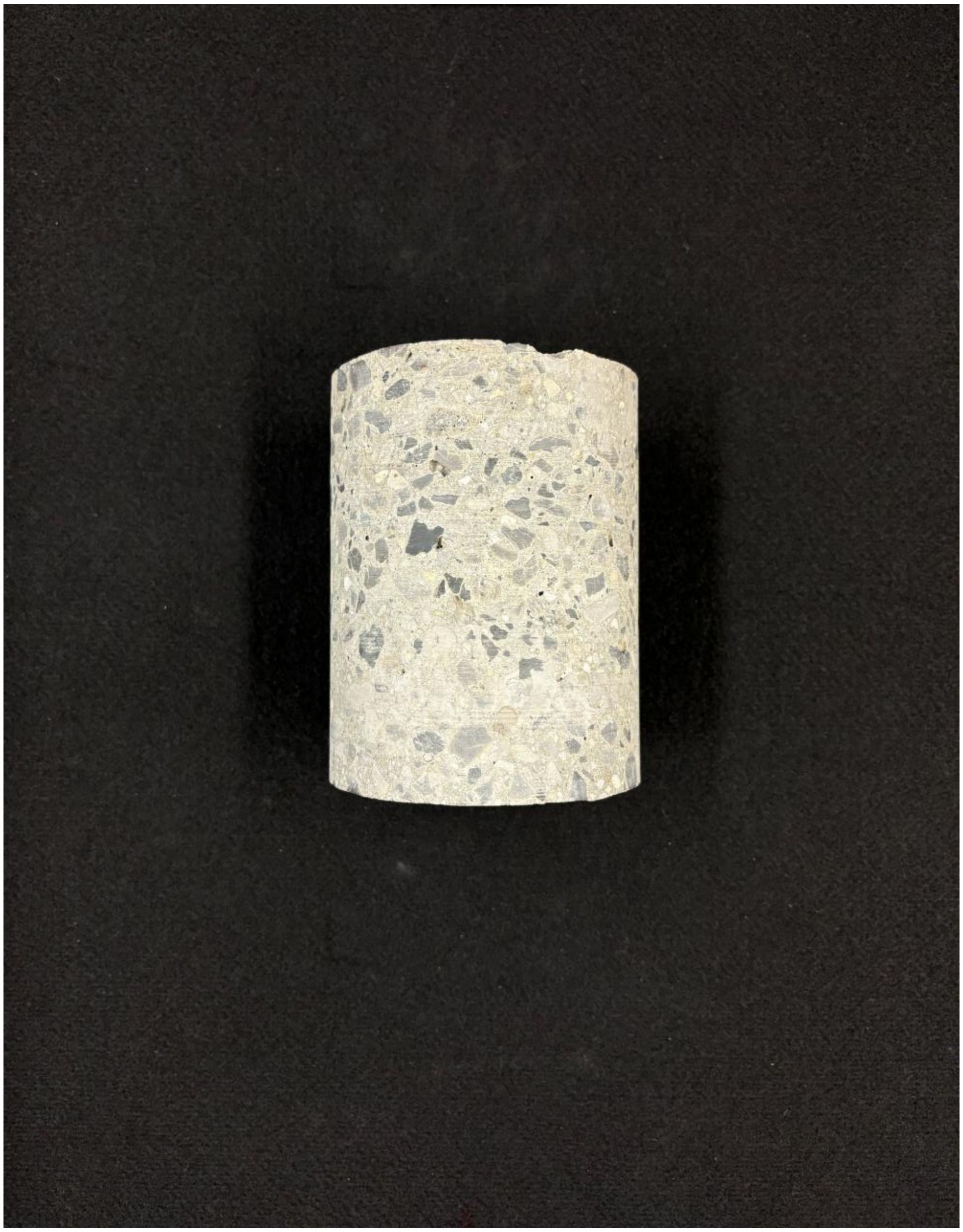

Figure D.13 Core 3 of lightweight concrete deck at bridge F-792.

Figure D.14 Core 4 of lightweight concrete deck at bridge F-792.

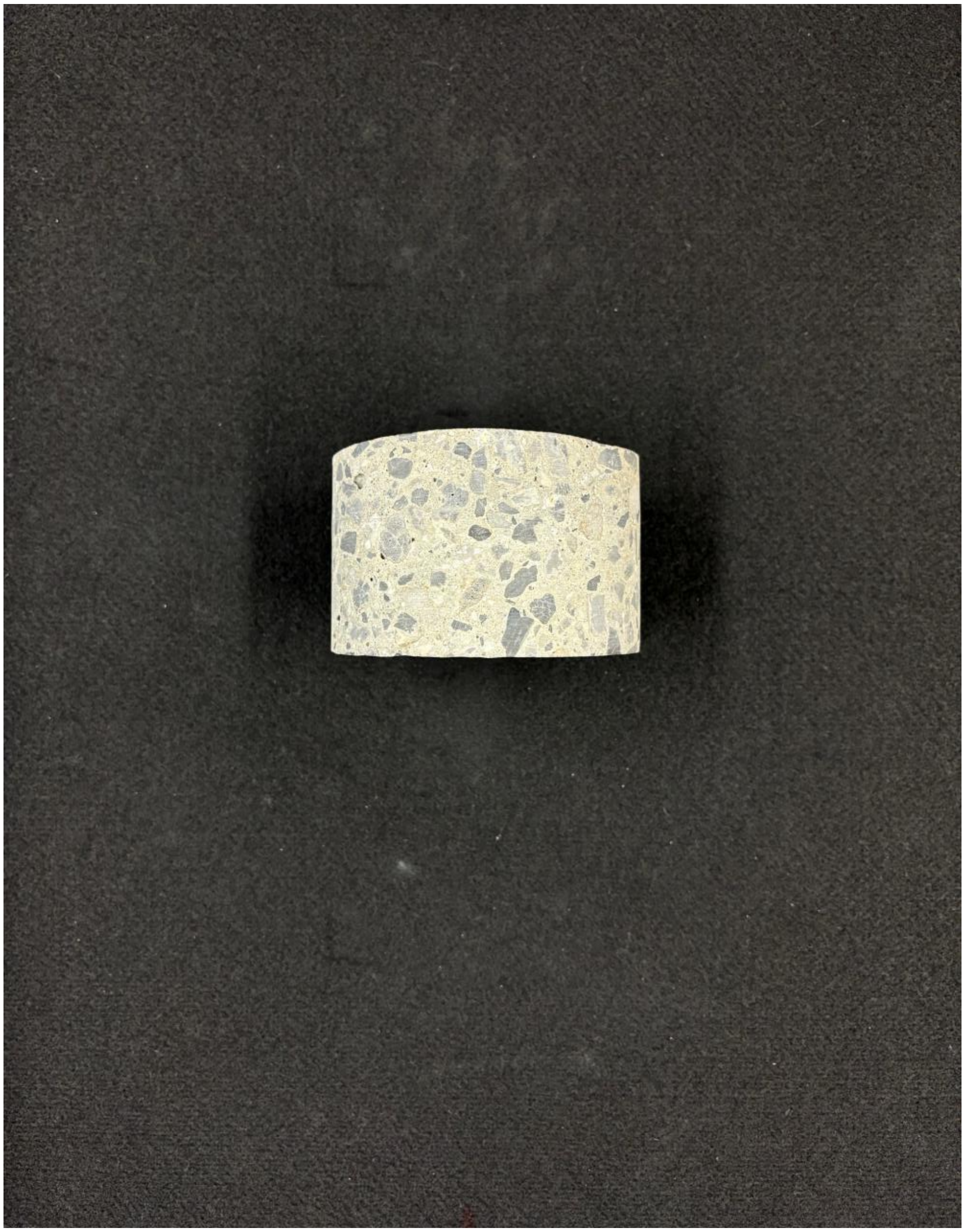

Figure D.15 Core 5 of lightweight concrete deck at bridge F-792.

Figure D.16 Core 1 of normal-weight concrete approach slabs at bridge C-989.

Figure D.17 Core 2 of normal-weight concrete approach slabs at bridge C-989.

Figure D.18 Core 3 of normal-weight concrete approach slabs at bridge C-989.

Figure D.19 Core 4 of normal-weight concrete approach slabs at bridge C-989.

Figure D.20 Core 5 of normal-weight concrete approach slabs at bridge C-989.

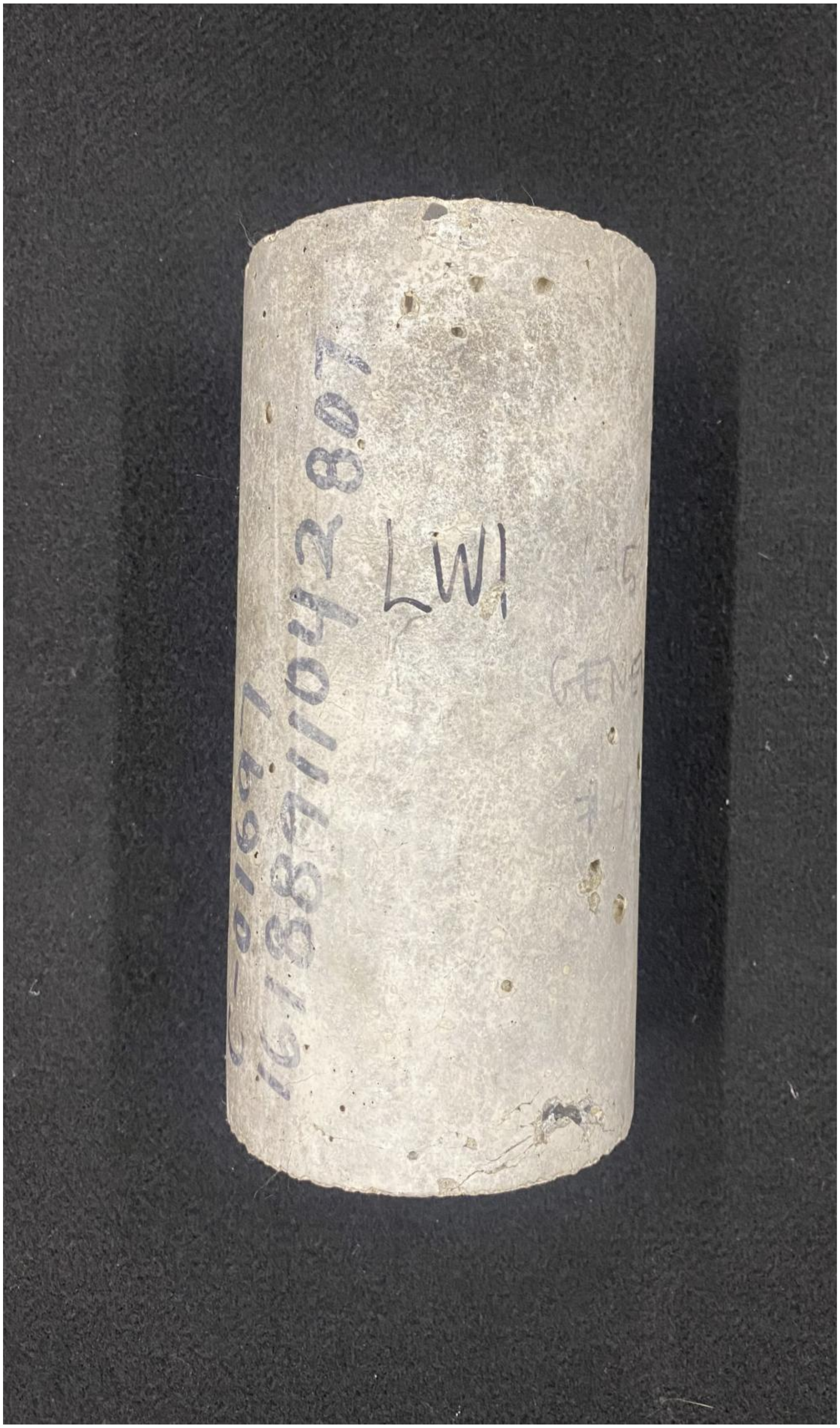

Figure D.21 Cylinder 1 of lightweight concrete deck at bridge C-993 (after testing).

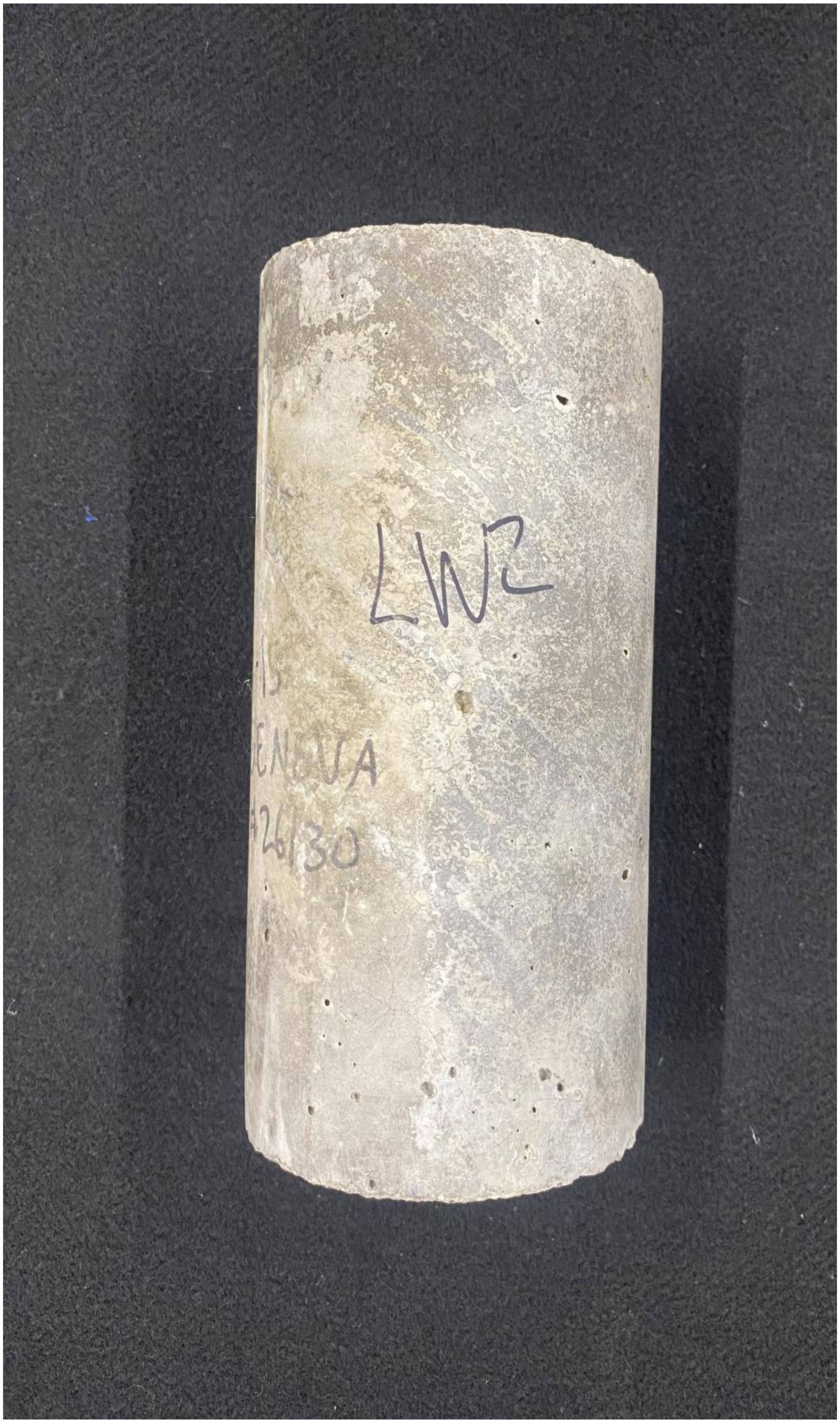

Figure D.22 Cylinder 2 of lightweight concrete deck at bridge C-993 (after testing).

Figure D.23 Cylinder 3 of lightweight concrete deck at bridge C-993 (after testing).

Figure D.24 Cylinder 1 of normal-weight concrete deck at bridge F-818 (after testing).

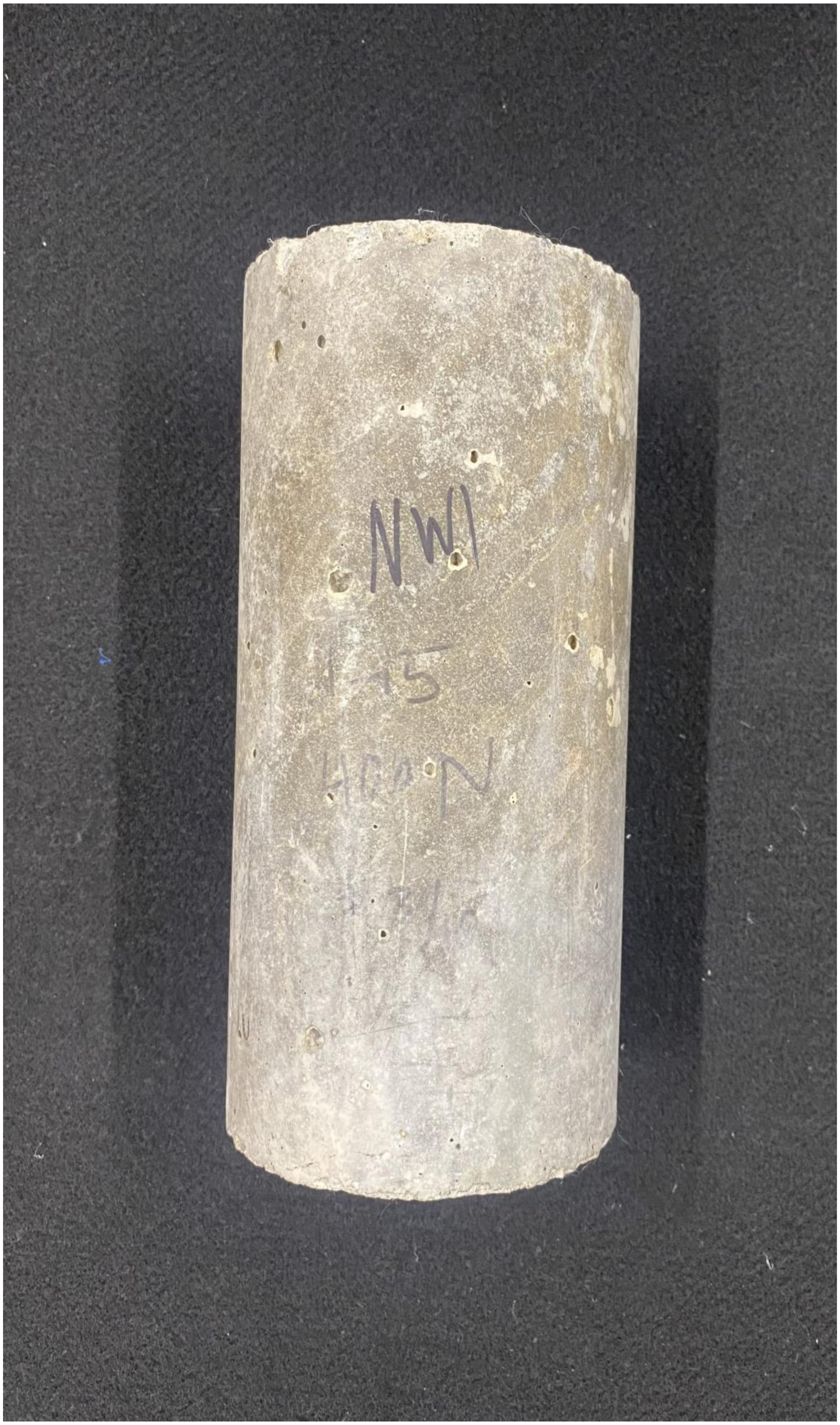

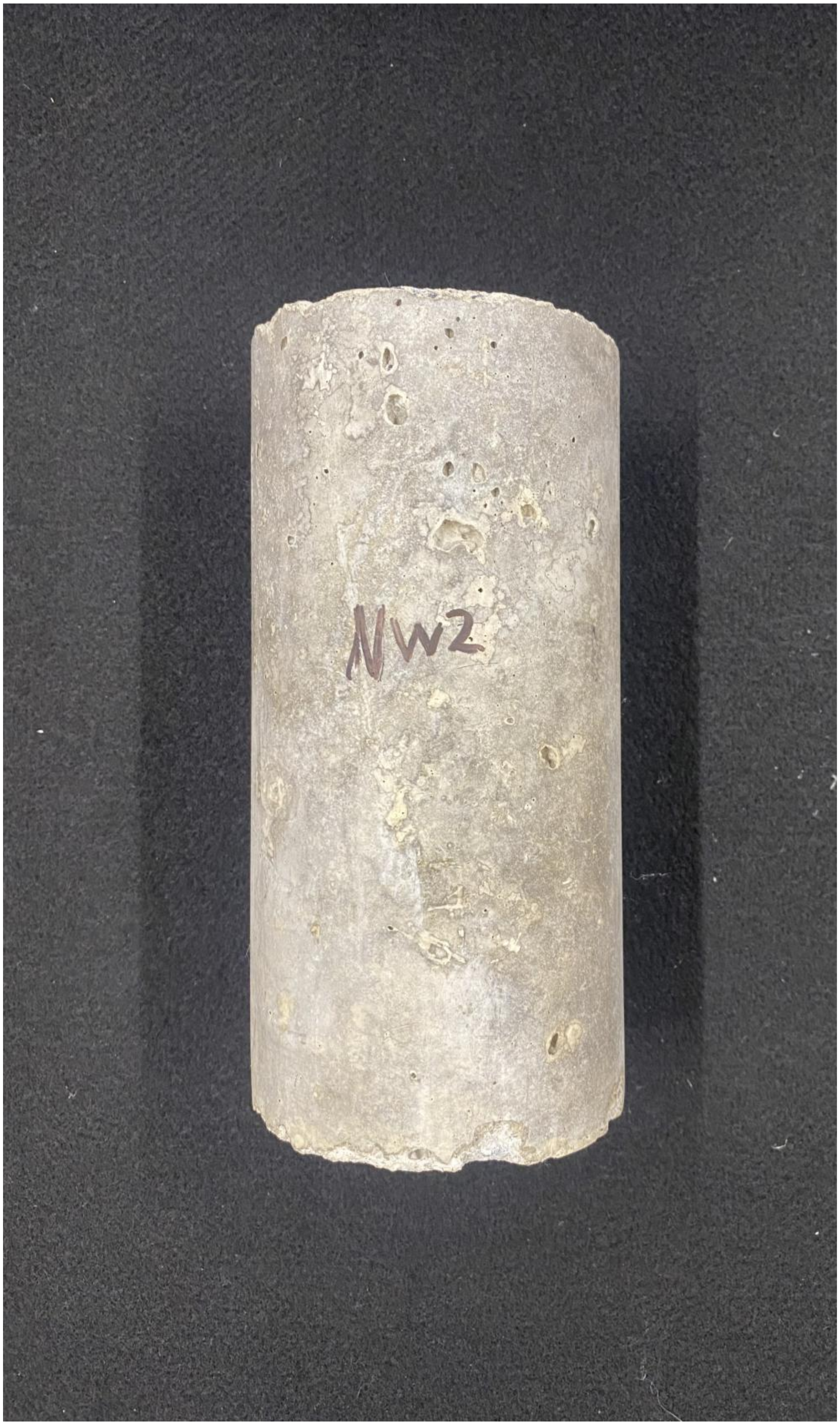

Figure D.25 Cylinder 2 of normal-weight concrete deck at bridge F-818 (after testing).

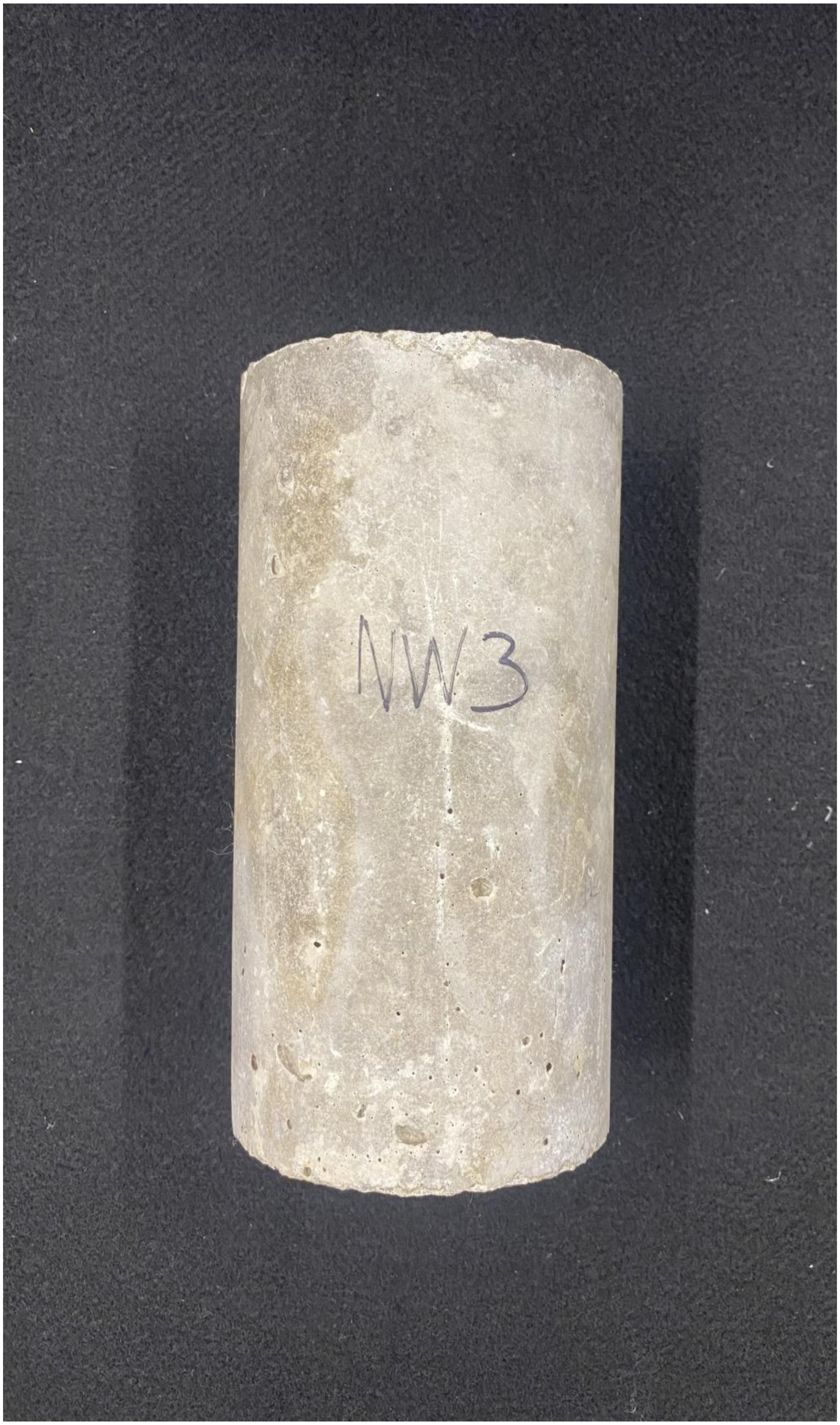

Figure D.26 Cylinder 3 of normal-weight concrete deck at bridge F-818 (after testing).

APPENDIX E: LIGHTWEIGHT COARSE AGGREGATE PHOTOGRAPHS

Figure E.1 Aggregate in core 1 of lightweight concrete deck at bridge C-989.

Figure E.2 Aggregate in core 2 of lightweight concrete deck at bridge C-989 (1).

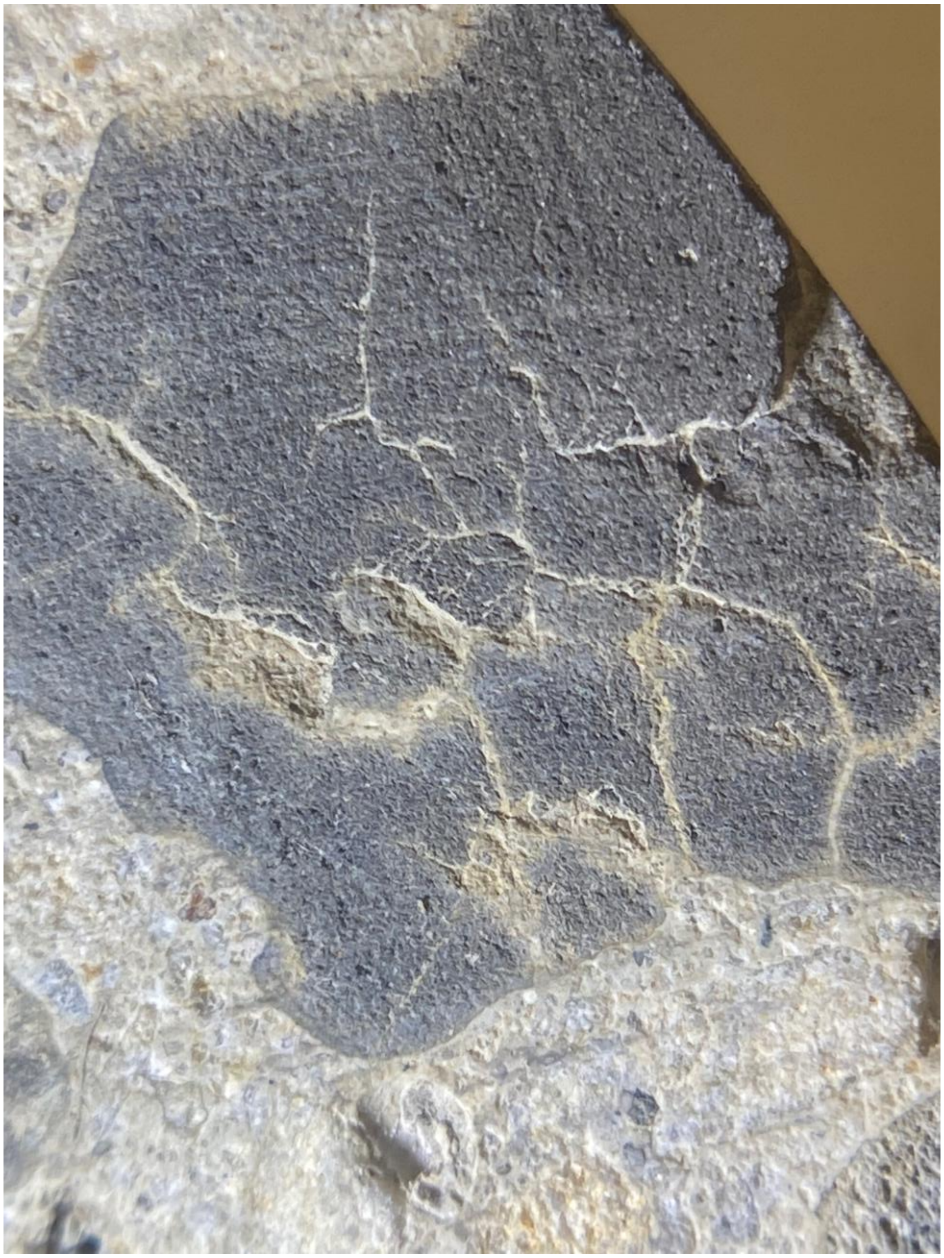

Figure E.3 Aggregate in core 2 of lightweight concrete deck at bridge C-989 (2).

Figure E.4 Aggregate in core 2 of lightweight concrete deck at bridge C-989 (3).

Figure E.5 Aggregate in core 3 of lightweight concrete deck at bridge C-989.

Figure E.6 Aggregate in core 4 of lightweight concrete deck at bridge C-989.

Figure E.7 Aggregate in core 5 of lightweight concrete deck at bridge C-989.

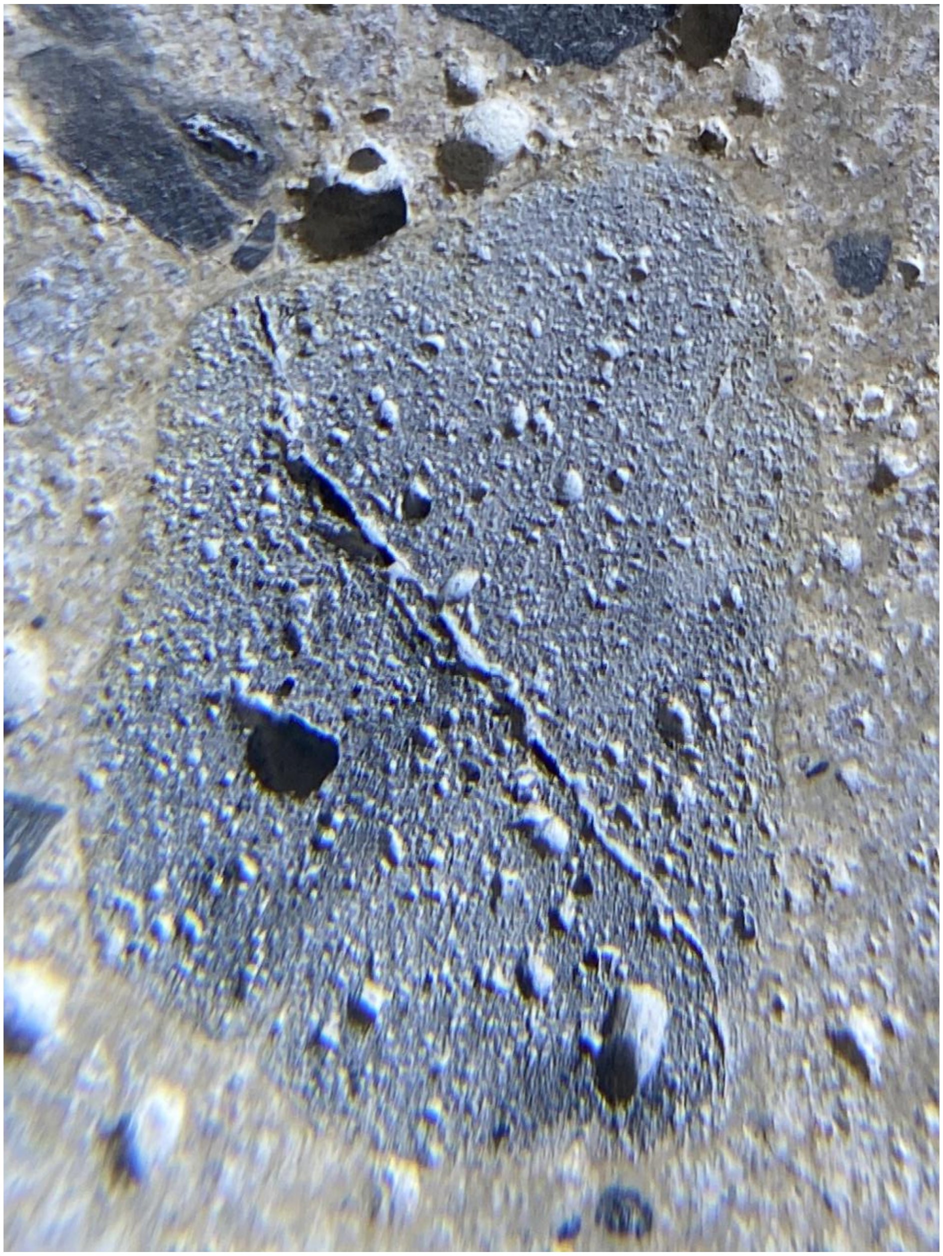

Figure E.8 Aggregate in core 1 of lightweight concrete deck at bridge C-1011 (1).

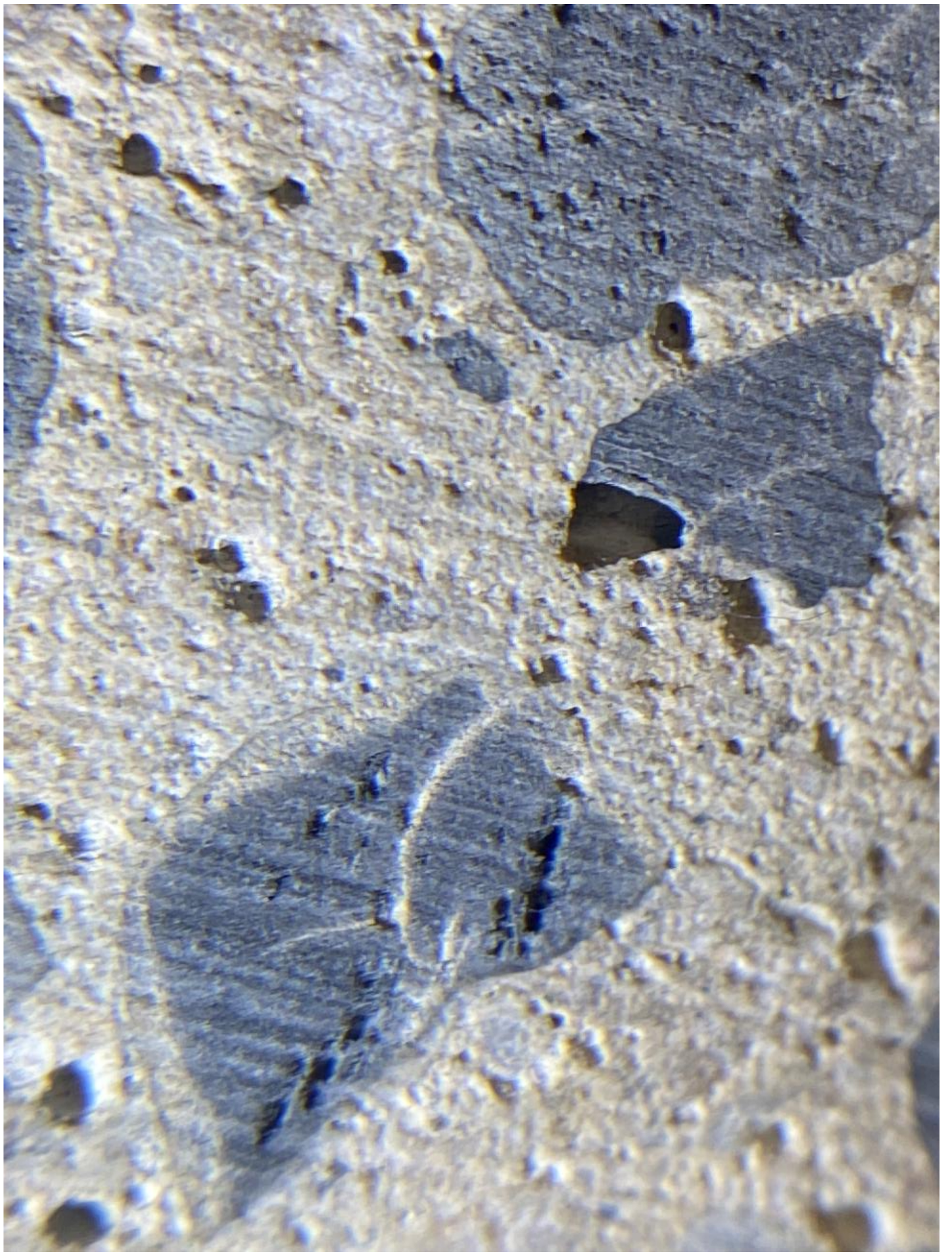

Figure E.9 Aggregate in core 1 of lightweight concrete deck at bridge C-1011 (2).

Figure E.10 Aggregate in core 2 of lightweight concrete deck at bridge C-1011 (1).

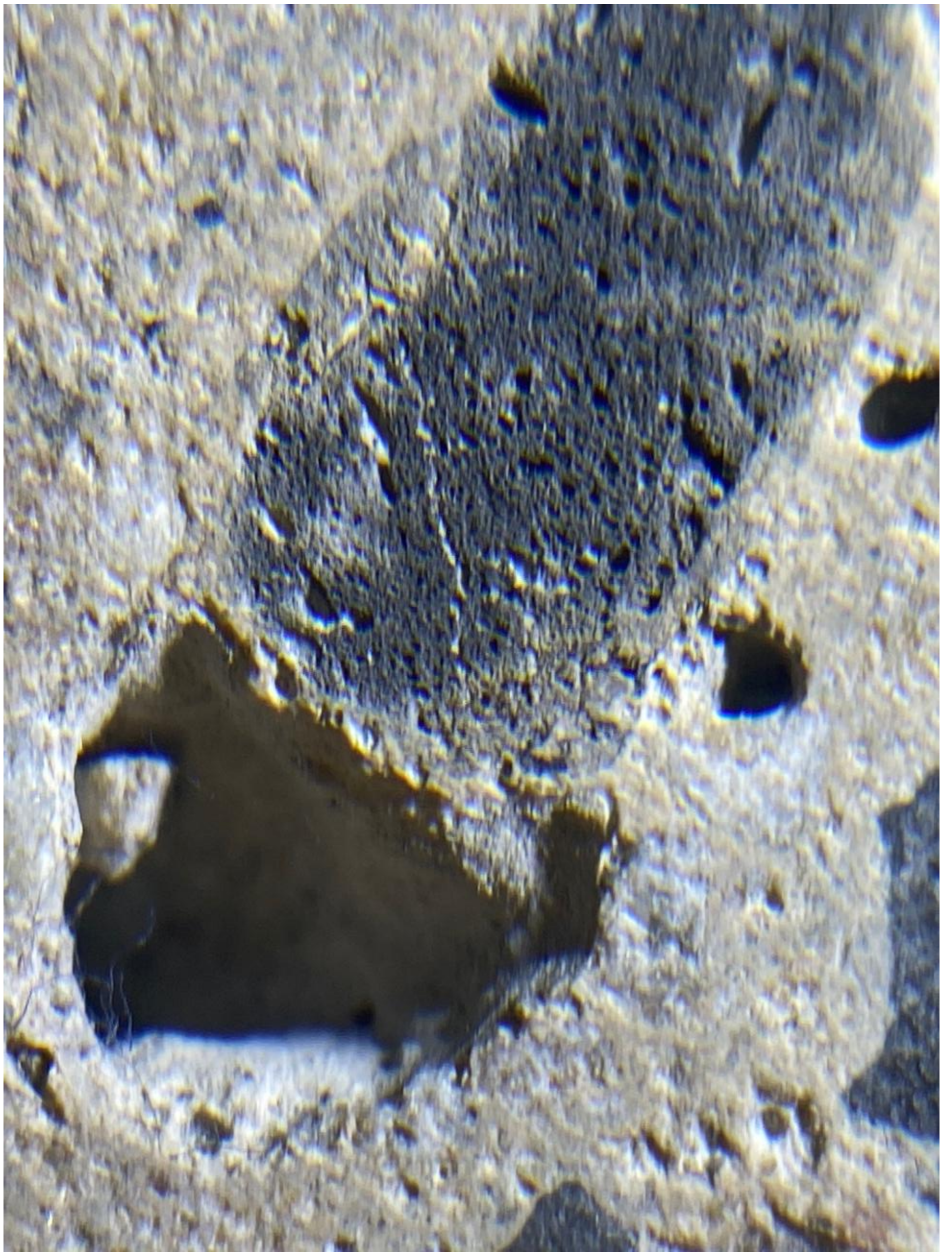

Figure E.11 Aggregate in core 2 of lightweight concrete deck at bridge C-1011 (2).

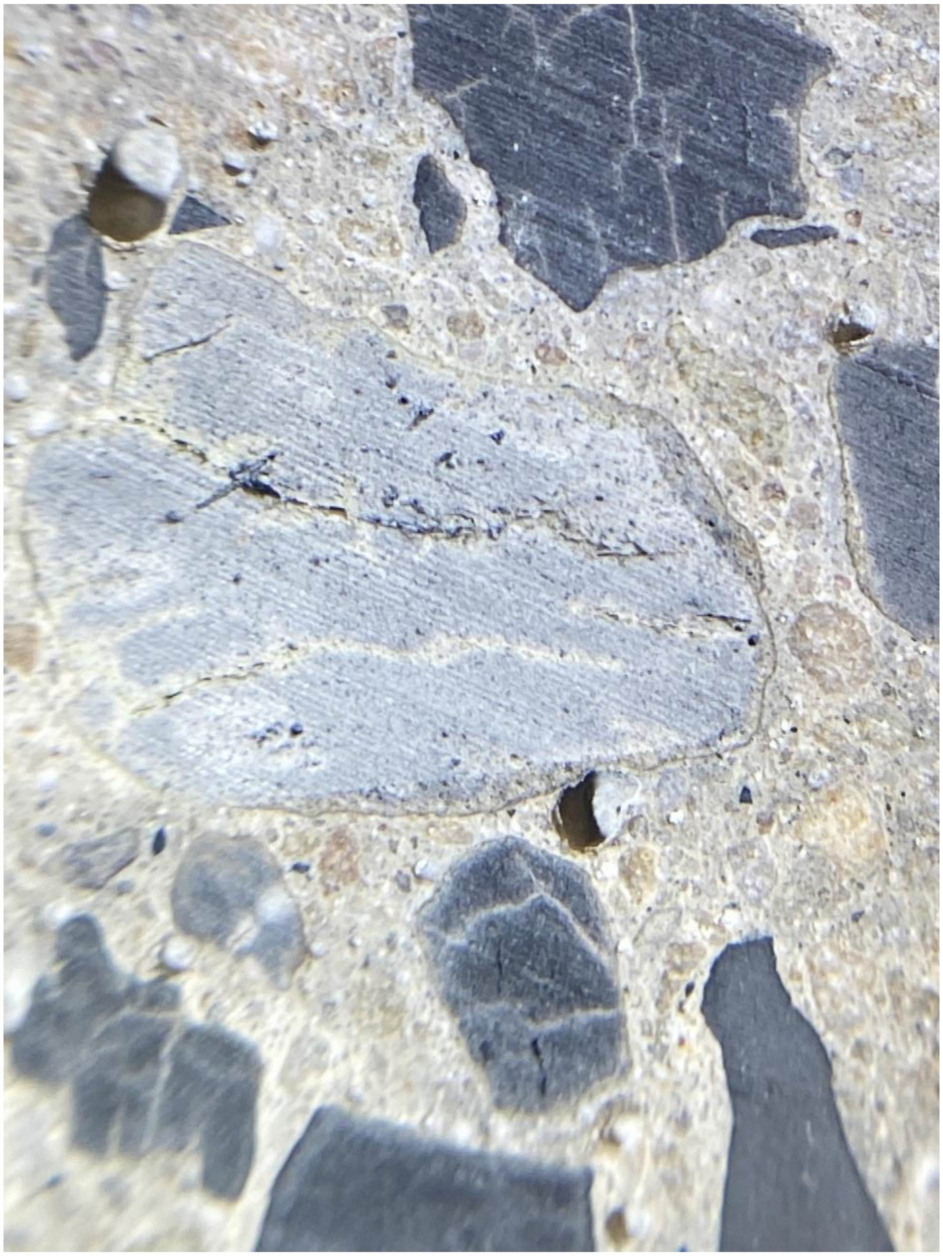

Figure E.12 Aggregate in core 3 of lightweight concrete deck at bridge C-1011 (1).

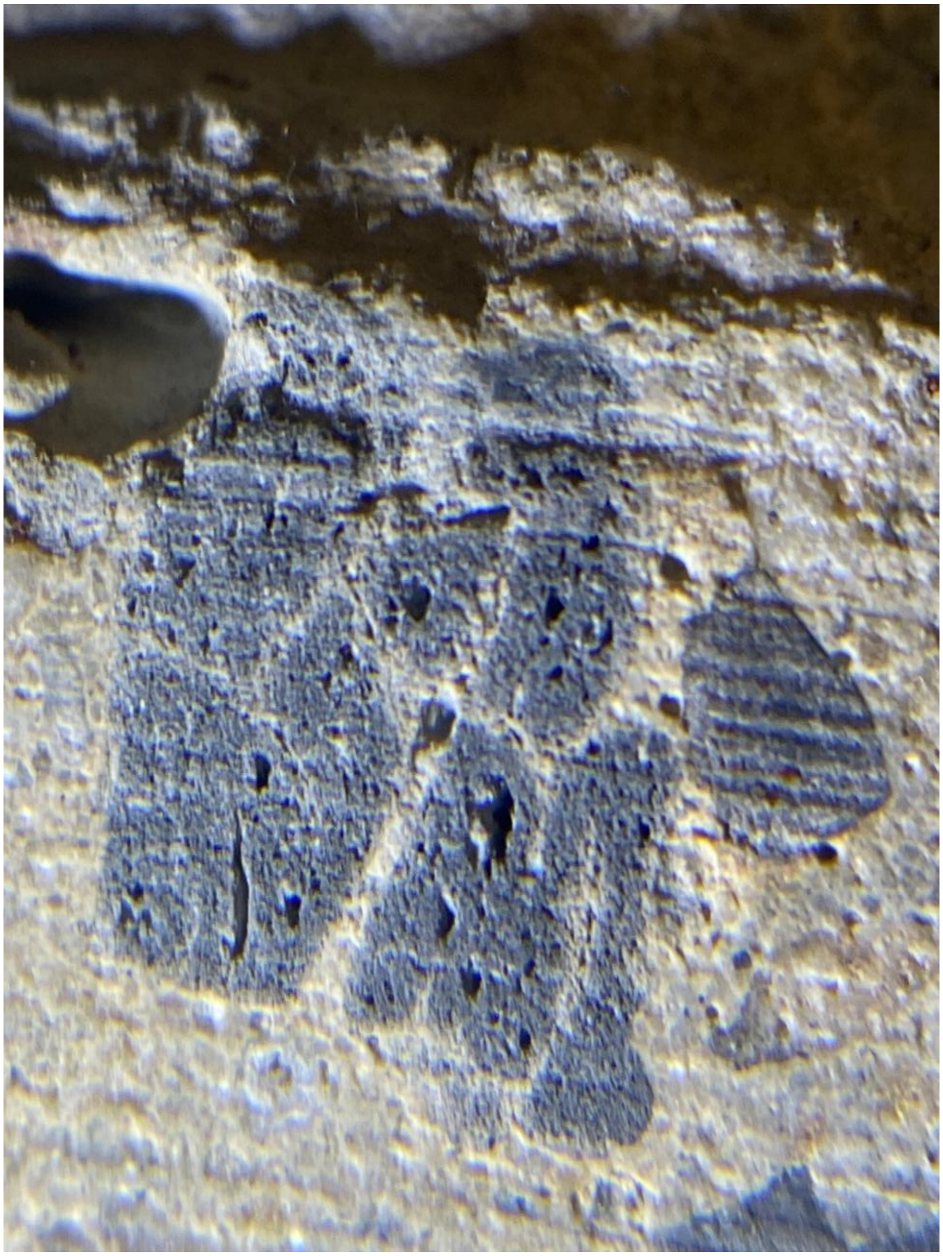

Figure E.13 Aggregate in core 3 of lightweight concrete deck at bridge C-1011 (2).

Figure E.14 Aggregate in core 4 of lightweight concrete deck at bridge C-1011.

Figure E.15 Aggregate in core 5 of lightweight concrete deck at bridge C-1011.

Figure E.16 Aggregate in core 1 of lightweight concrete deck at bridge F-792 (1).

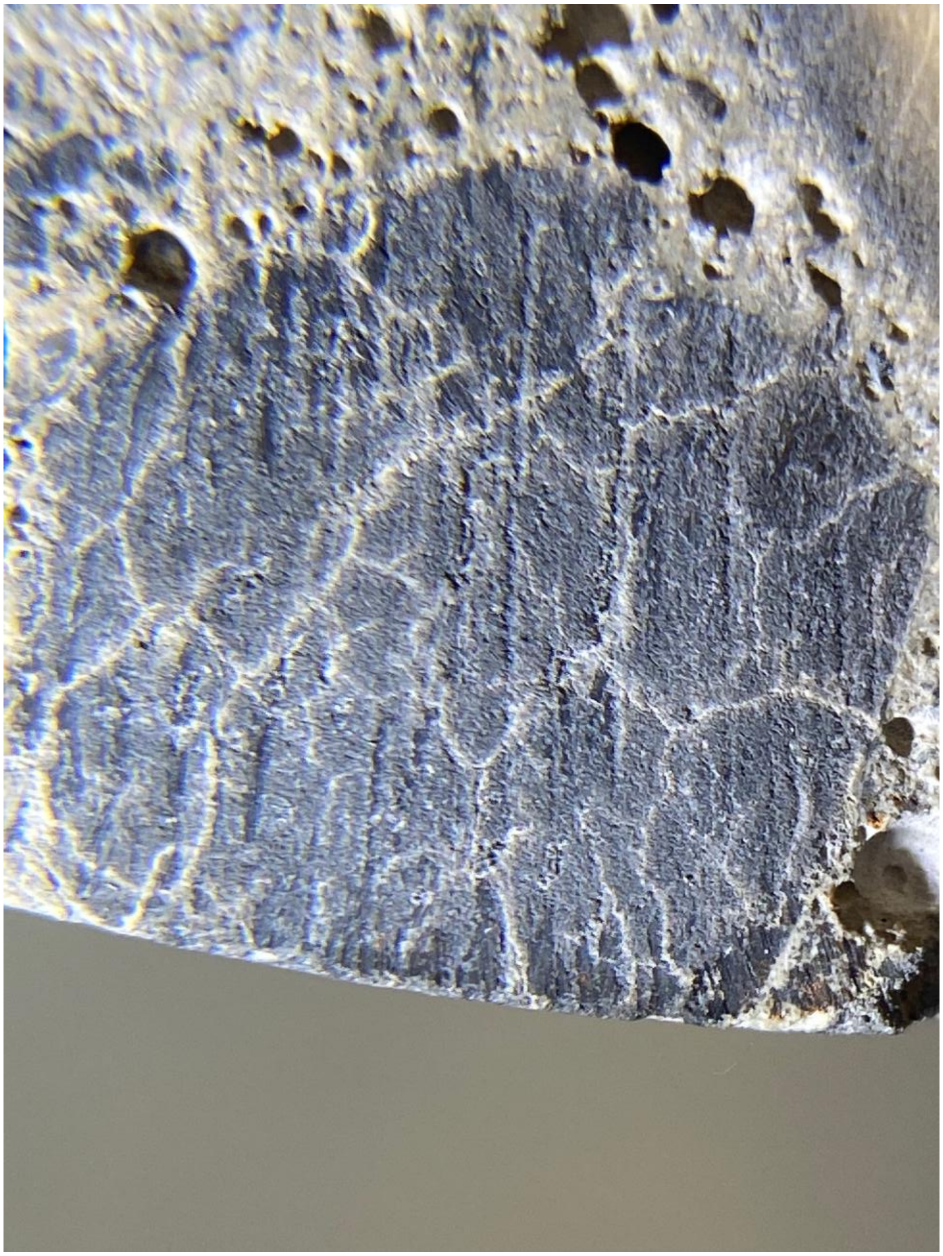

Figure E.17 Aggregate in core 1 of lightweight concrete deck at bridge F-792 (2).

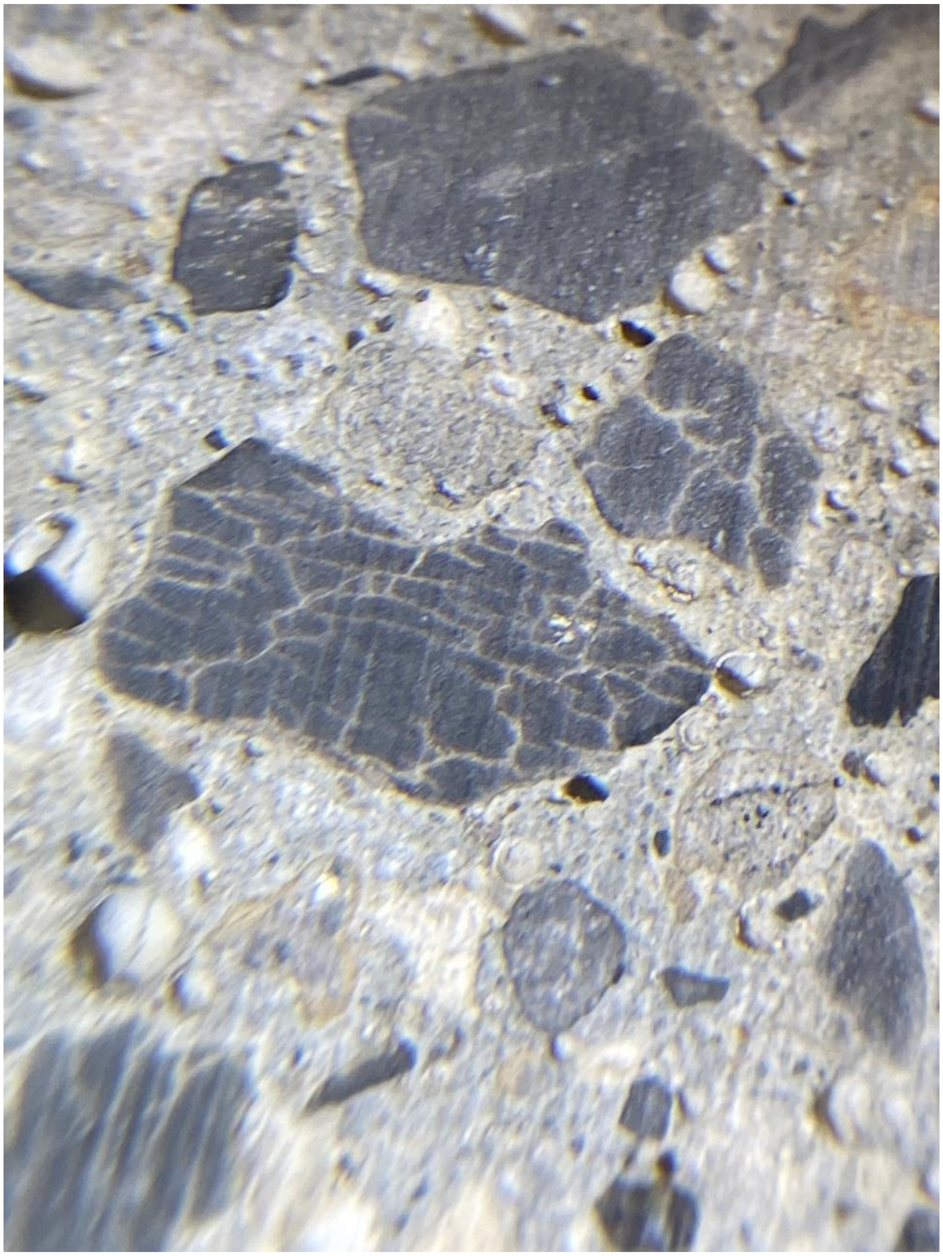

Figure E.18 Aggregate in core 2 of lightweight concrete deck at bridge F-792 (1).

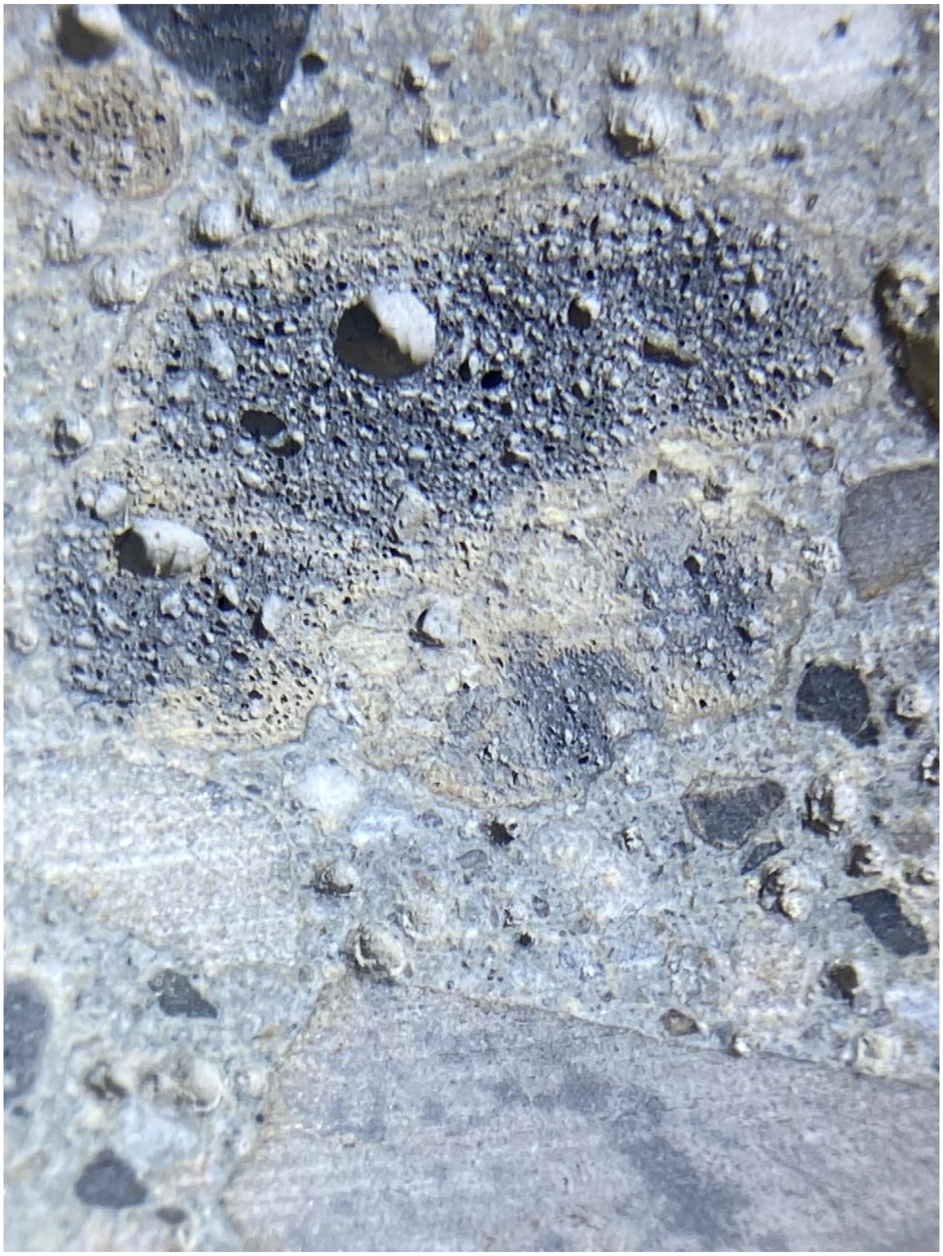

Figure E.19 Aggregate in core 2 of lightweight concrete deck at bridge F-792 (2).

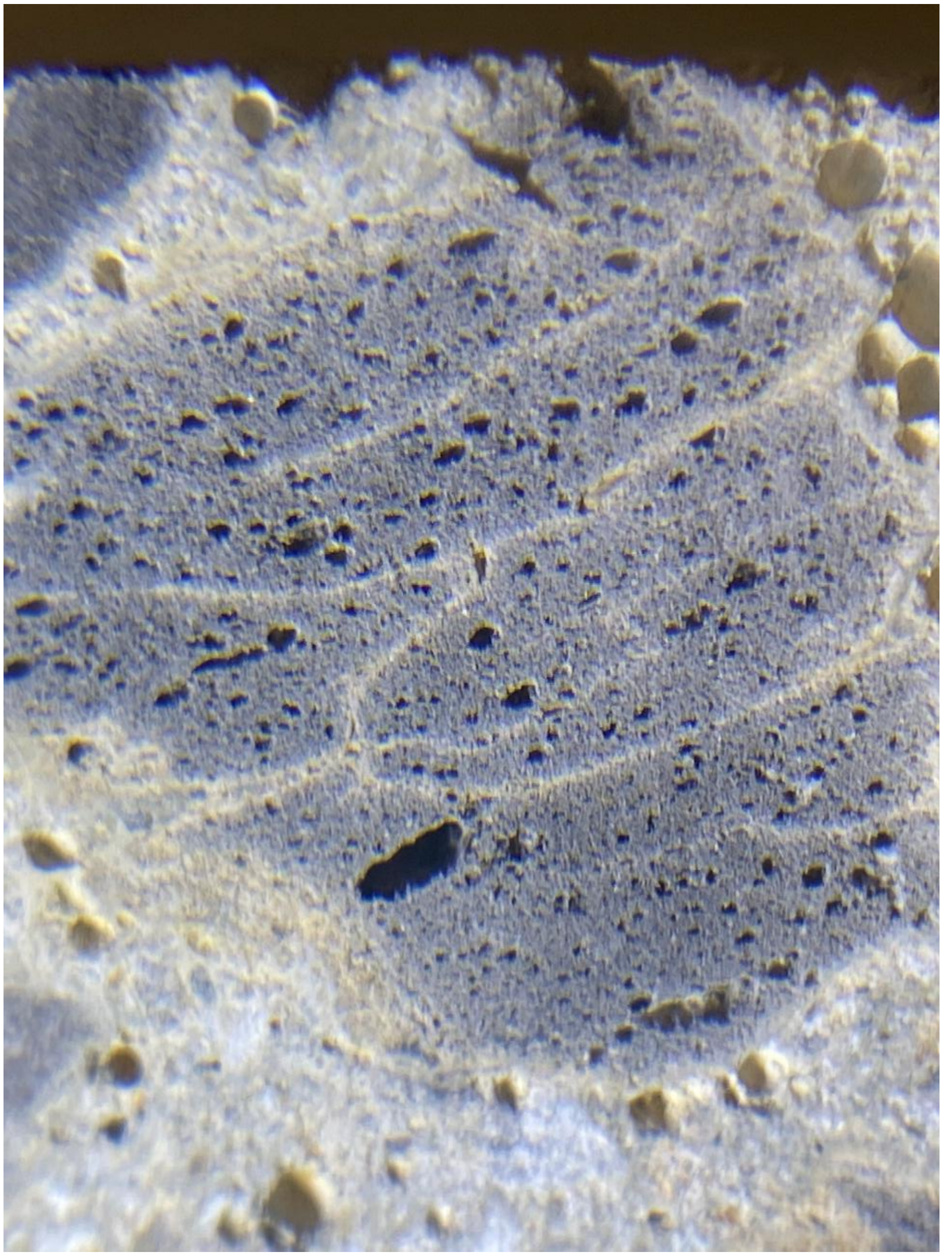

Figure E.20 Aggregate in core 3 of lightweight concrete deck at bridge F-792.

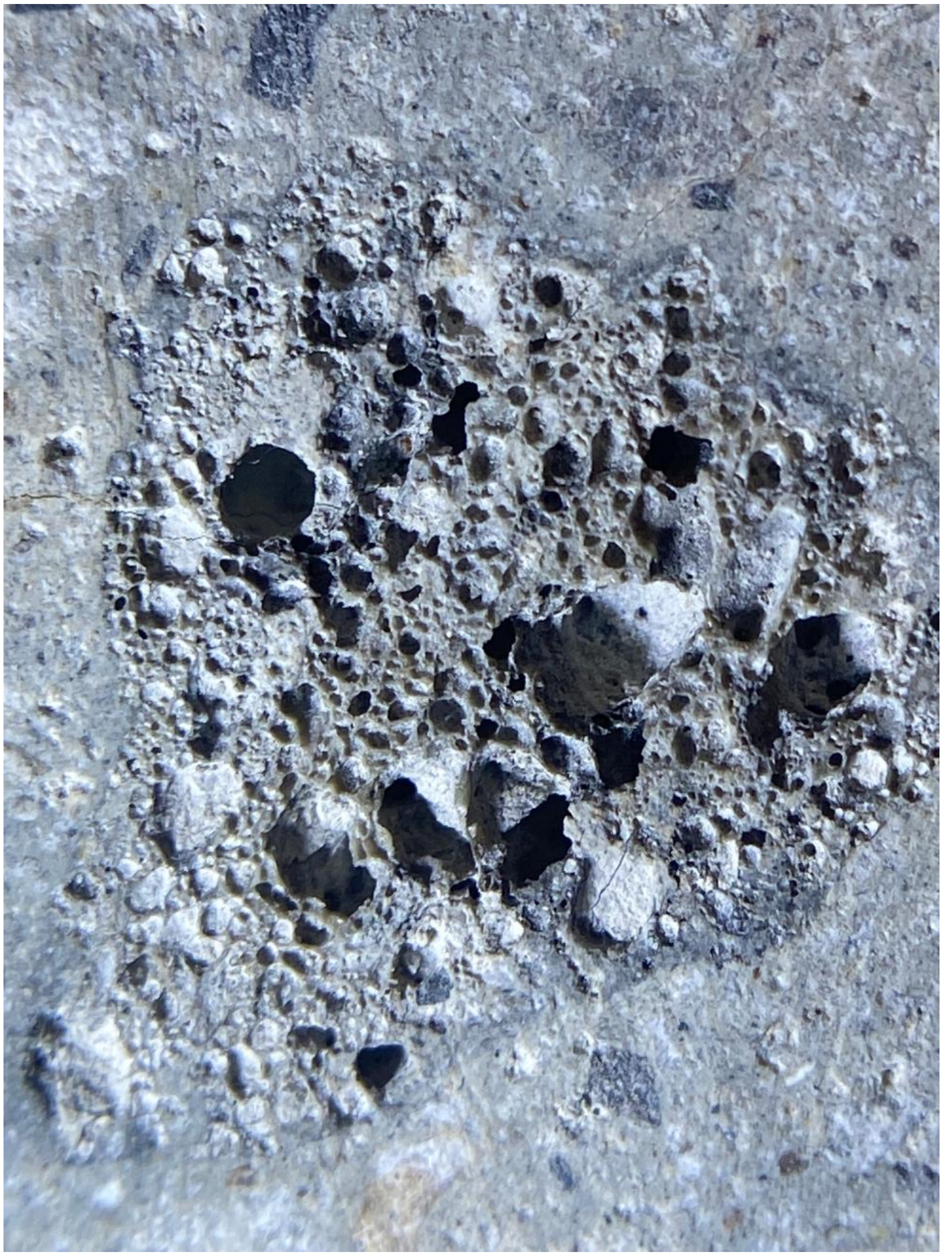

Figure E.21 Aggregate in core 4 of lightweight concrete deck at bridge F-792 (1).

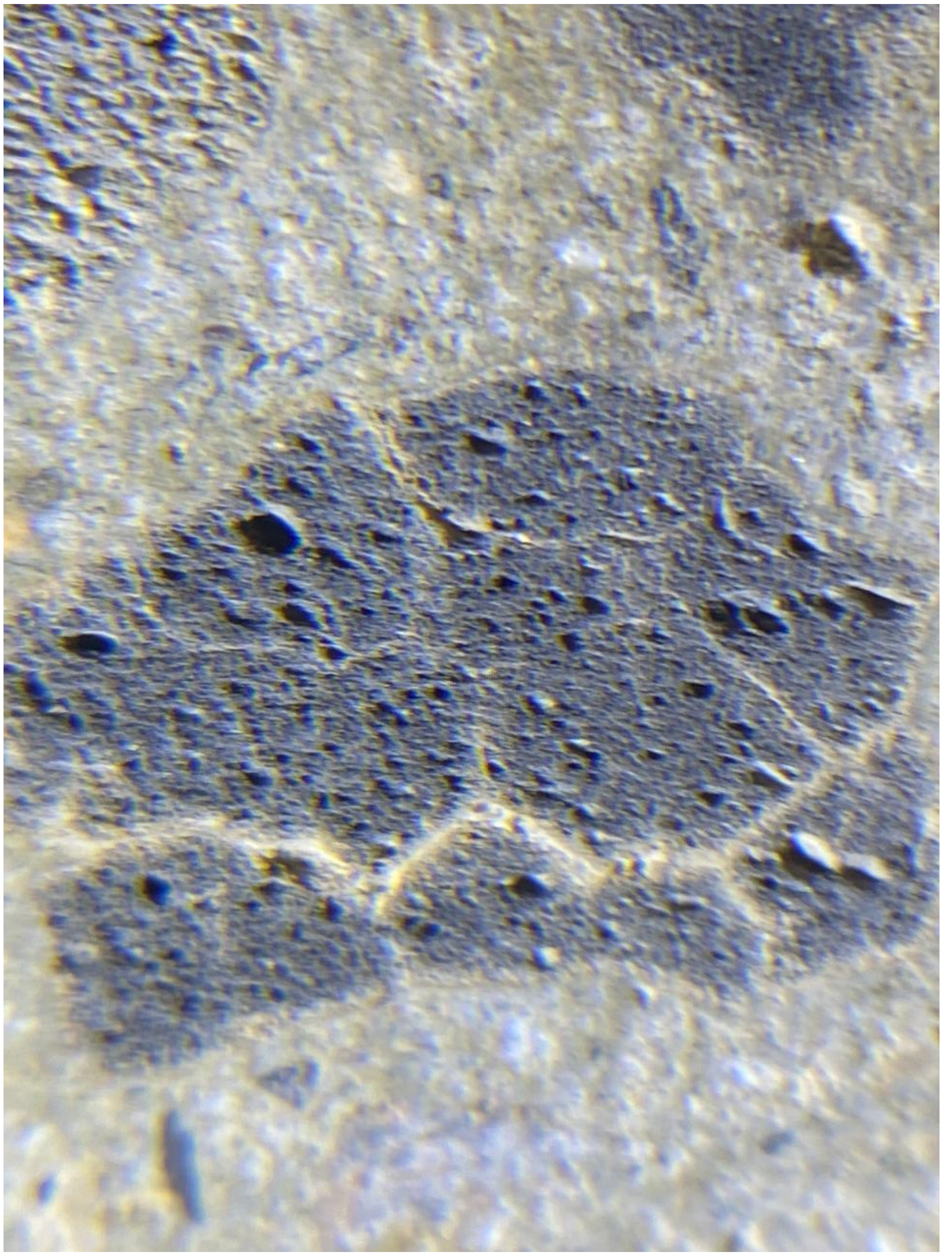

Figure E.22 Aggregate in core 4 of lightweight concrete deck at bridge F-792 (2).

Figure E.23 Aggregate in core 4 of lightweight concrete deck at bridge F-792 (3).

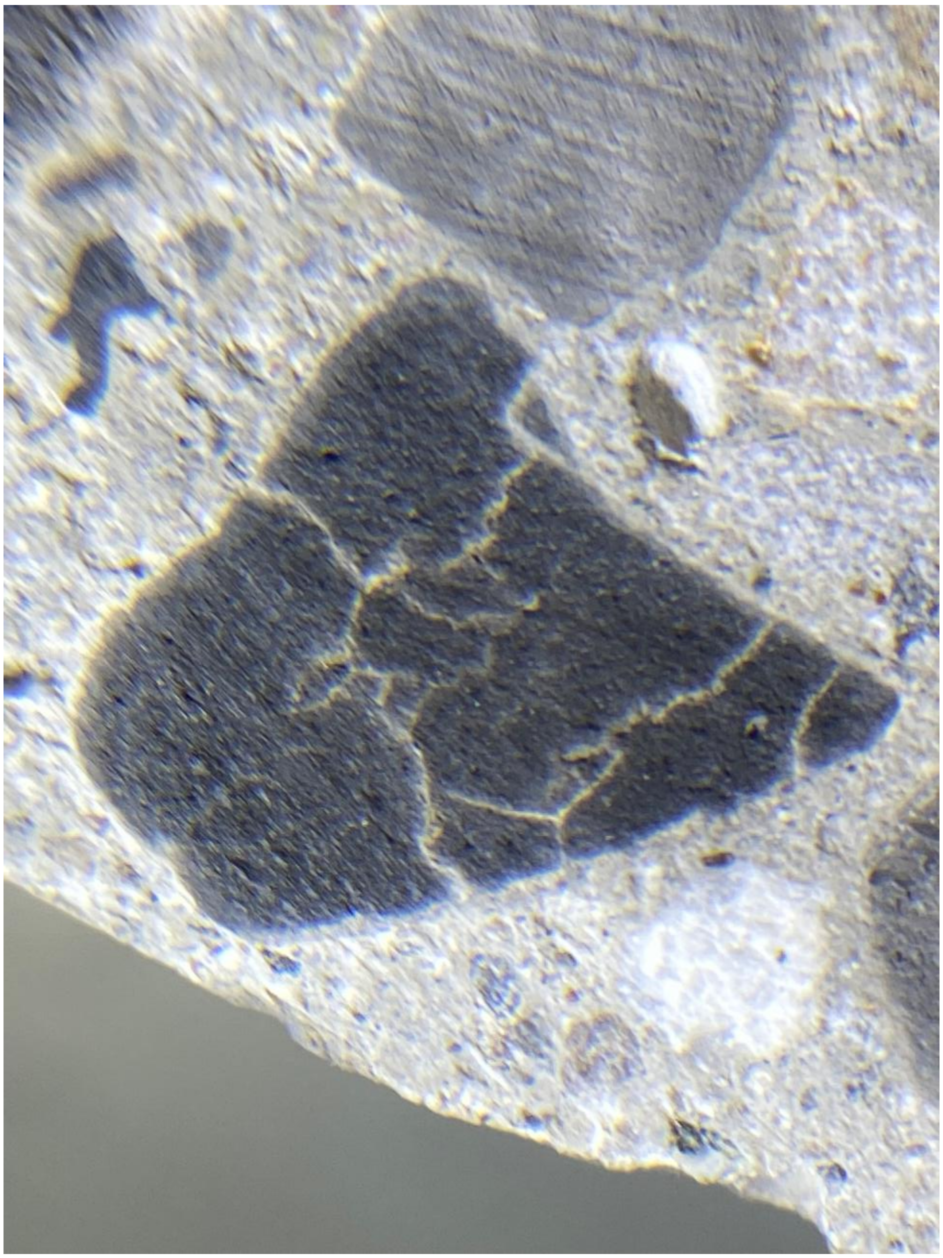

Figure E.24 Aggregate in core 5 of lightweight concrete deck at bridge F-792 (1).

Figure E.25 Aggregate in core 5 of lightweight concrete deck at bridge F-792 (2).

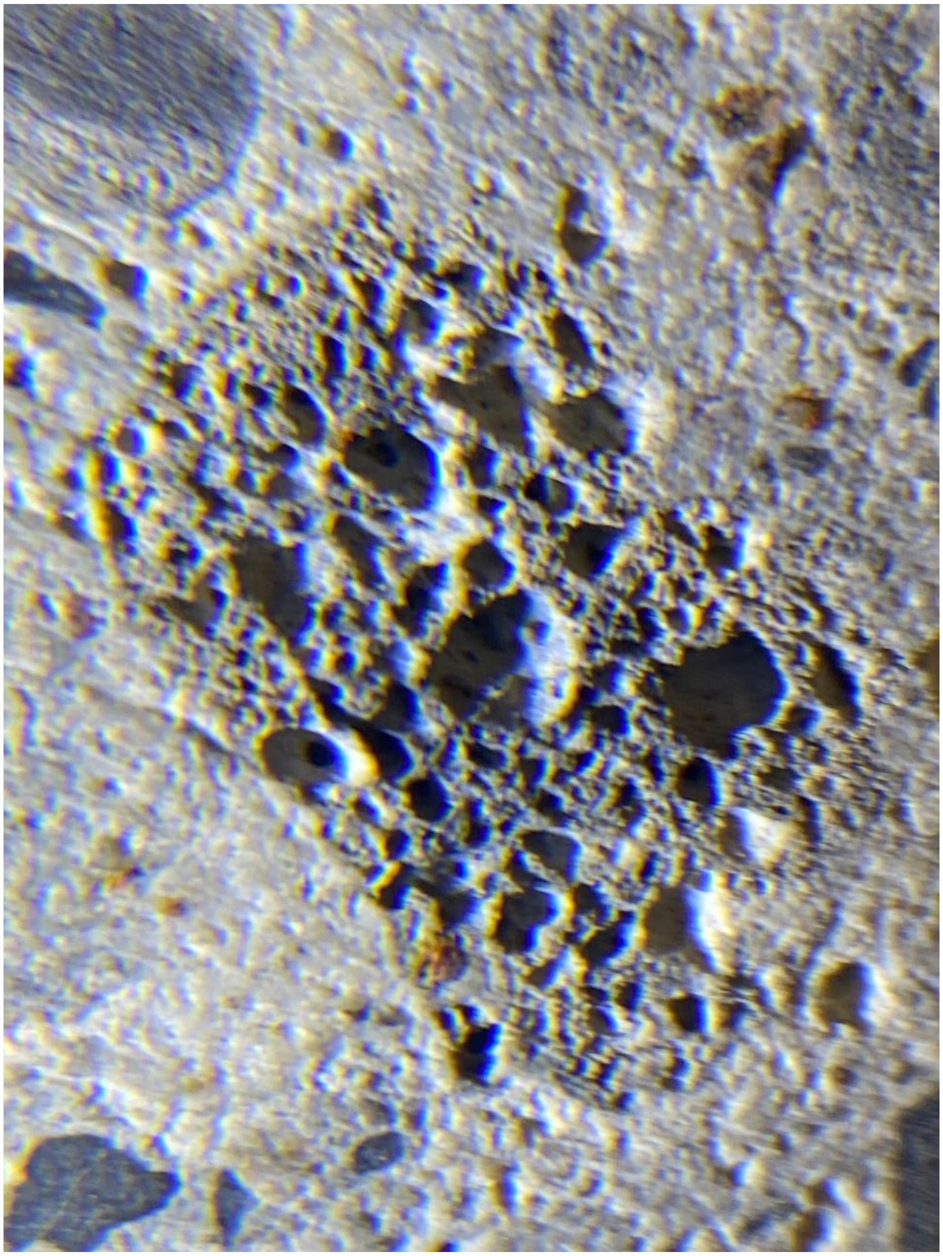

Figure E.26 Aggregate in core 5 of lightweight concrete deck at bridge F-792 (3).